UNIVERSITY OF NAIROBI

DEPARTMENT OF EARTH AND CLIMATE SCIENCES

ANALYSIS OF SUBTROPICAL ANTICYCLONES AS SYNOPTIC CONTROLS OF SEASONAL RAINFALL EXTREMES IN EAST AFRICA

KAREN CHERONO KIRUI

I56/38907/2020

Dissertation submitted in partial fulfilment of the requirement for the degree of Master of Science in Meteorology, of The University of Nairobi.

March 2023

DECLARATION

I declare that this dissertation is my original work and has not been submitted elsewhere for examination, award of a degree or publication. Where other people's work, or my own work has been used, this has properly been acknowledged and referenced in accordance with the University of Nairobi's requirements.

Signed Date

10th March 2023

Karen Cherono Kirui

This project has been done under our supervision and has been submitted to the University of Nairobi for examination with our approval as the candidate's supervisors.

Signed  Date 10th March 2023

…… ……

Prof. J.N. Mutemi

Signed 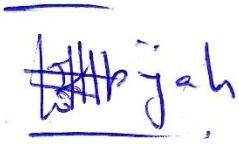 Date 10/03/2023

…… ……

Prof. F.J. Opijah

ABSTRACT

This study aims to investigate the influence of anticyclones adjacent to Africa on seasonal rainfall extremes over East Africa, focusing on the March to May (MAM) and October to December (OND) rainy seasons. Specific objectives for the study include identifying years with extreme rainfall, determining spatial distribution of rainfall for the identified years with rainfall extremes, comparing the pressure characteristics of the anticyclones during the extreme rainfall years with climatological patterns, and analysing moisture transport and circulation patterns during extreme rainfall years. Precipitation data and reanalysis datasets of mean sea level pressure (MSLP), zonal and meridional wind and specific humidity from 1981 to 2020 were used for analysis.

Four years of extremely high and extremely low rainfall were identified for each season using the tercile approach. Spatial distribution of rainfall anomalies depicted areas of concentration of ‘wetness’ and ‘dryness’ due to rainfall extremes. The pressure patterns and subsequently the moisture and circulation patterns were crucial in showing the impact of anticyclones on moisture flux during extreme rainfall years. During the MAM season, equatorward displacement of the Azores high and St. Helena high contributed to extremely high rainfall, while for dry years, the poleward displacement of these anticyclones resulted in less effective moisture influx.

In the OND season, the Mascarene and Siberian highs' eastward displacement with reference to the climatological evidence caused an influx of moist easterlies, contributing to wet years. Conversely, wet years experienced westward (compared to the climatology) displacement of these anticyclones, leading to converging easterlies and westerlies in the Indian Ocean, leaving East Africa devoid of moisture for rain formation.

The study highlights the significant role of subtropical anticyclones in influencing moisture patterns and controlling seasonal rainfall extremes in East Africa. The findings highlight the need for improved forecasting techniques, especially for extreme events like flooding and droughts. Furthermore, the study underscores the importance of developing and enhancing general circulation models for Africa to advance weather forecasting and analyse weather drivers and teleconnections effectively.

DEDICATION

This dissertation is dedicated to all my destiny helpers for their wise counsel, guidance, support and love. Their presence and encouragement cheered me on. It indeed takes a village.

ACKNOWLEDGEMENT

I would like to express my gratitude to the Almighty God for his guidance and for strengthening me. He truly makes everything beautiful in his time.

I am especially grateful to my supervisors Prof. Mutemi and Prof. Opijah. Thank you for your patience, guidance and support, pushing me to be concise in advocating the arguments presented in this study. Also grateful to GCRF African SWIFT where I have gotten to expand my knowledge in Meteorology.

I would like to express my deepest gratitude to my parents and siblings for their love. Their belief in me has motivated me through this process. Thank you for seeing me through to the completion of this work.

I am grateful to my fiancé Kelvin for being my biggest cheerleader, encouraging me to be the best version of myself as I tried to figure out much of this programme. We can now go for the full chicken!

I am grateful to Mike Anindo for wise counsel, patience and invaluable feedback in matters concerning growing in academia. Thank you for pushing me into constantly improving and finishing strong.

I am grateful to Emm and the Ahn family for hosting me throughout my studies. I am equally thankful to Miss P who has been an amazing support system, allowing me to lean on her faith and infectious charisma.

I am grateful to Mavuno church community, where I am taught and sharpened to be purposeful. To Reflectors, Discovered and the MDT community, who have inspired me to keep growing. I am especially grateful for the MDT staff for allowing me to commandeer their office space as I worked on this research. Special thanks to Dr. Kyama Mugambi for inspiring me into academia. Many thanks to the Ottos for their love and concern.

I am thankful to the Makerere-Bergen Research School facilitators for good feedback that affirmed this work and helped improve some of the concepts presented.

LIST OF TABLES

LIST OF FIGURES

LIST OF ABBREVIATIONS

CAB	Congo air boundary
CAMS_OPI	Climate Anomaly Monitoring System-Outgoing longwave radiation Precipitation Index
CDAS	Climate Data Assimilation System
CPC	Climate Prediction Center
DJFM	December, January, February and March
ENSO	El Niño Southern Oscillation
FAO	Food and Agriculture Organization of the United Nations
GrADS	Grid Analysis and Display System
GPCP	Global Precipitation Climatology Project
IOD	Indian Ocean dipole
ITCZ	Intertropical convergence zone
KMD	Kenya Meteorological Department
LTM	Long term mean
LVB	Lake Victoria basin
MAM	March, April, May
mb	Millibar
MJO	Madden-Julian Oscillation
MSLP	Mean Sea level pressure
NAO	North Atlantic Oscillation
NASA	National Aeronautics and Space Administration
NCAR	National Center for Atmospheric Research
NCEP	National Centers for Environmental Prediction
NOAA	National Oceanic and Atmospheric Administration
OND	October, November, December
ONI	Oceanic Niño Index
PGF	Pressure gradient force
SO	Southern Oscillation

SST	Sea surface temperature
TC	Tropical cyclone
TMA	Tanzania Meteorological Authority

CHAPTER ONE

INTRODUCTION

1.1 Background Information

East Africa is characterised by bimodal distribution of rainfall, the March to May (MAM) season known as the long rainy season and the October to December (OND) season known as the short rainy season (James *et al*.,2018). These rainfall seasons are controlled by various mechanisms including topography, influence of water bodies and the seasonal dynamics of tropical circulations (Nicholson, 2017). Therefore, a study on the characterisation of weather and climate systems is important to improve the skill of the predictions of weather (Mutemi *et al.*, 2006); during MAM and OND rainfall. Since the East Africa region is vulnerable to the effects of interannual fluctuations of rainfall (Nicholson, 2016), studying seasonal rainfall is important in ruling out uncertainties in the relationships between rainfall and the mechanisms associated with rainfall that have resulted from the use of other timescales (i.e. daily and monthly) apart from seasonal (Camberlin and Philippon, 2002).

Rainfall is the most important and active variable associated with atmospheric circulation (Sun *et al.*, 2018), and it is the most fundamental climatic element for East Africa (Ongoma *et al.*, 2015). For that reason, studies on the behaviour of rainfall in space and time and its variability in East Africa are essential. Since there are deficiencies in data from station gauges, other products like satellite estimates and models supplement gauge data for a more spatially homogeneous and temporally complete characterisation of weather and climate systems.

Escalation of drought occurrences in East Africa due to extremely low rainfall (Nicholson, 2016); and increased instances of flooding due to extremely high and more intense rainfall cause severe societal impacts (Kilavi *et al*., 2018). The characterisation of weather and climate systems is important for the extremes in seasonal rainfall in order to safeguard life and property through effective planning and implementation of protective action.

Seasonal rainfall and its extremes are linked to the properties of the subtropical anticyclones adjacent to the African continent: the Mascarene high in the south Indian Ocean, the St. Helena

high also known as the South Atlantic Subtropical high (SASH) (Sun *et al.*, 2017) in the south Atlantic Ocean, the Azores high in the north Atlantic Ocean and the Siberian high in Eurasia (Mutemi, 2003; Ongoma *et al.*, 2015). Some foundational studies on the role played by these subtropical anticyclones on the weather in East Africa were documented by Johnson and Morth (1960). These systems play an important role in short to extended range forecasting (Sun *et al.*, 1999). Moreover, the influence of anticyclones on seasonal rainfall in East Africa has not been studied exhaustively (Ongoma *et al.*, 2015).

1.2 Statement of the Problem

The features and systems that control weather and climate extremes have not been intensively investigated due to limited access of observational data. An example is the strong land-atmosphere interactions and influence from the Indian and Atlantic Oceans that increases the challenge of understanding the weather over East Africa and the factors that increase its complexity, posing a challenge to modelling of these teleconnection mechanisms especially on long timescales (James *et al*., 2018). There also has been an apparent conflict between climate projections of increased rainfall and the observed rainfall decline within a season, referred to as the 'Eastern Africa Climate Paradox' (Wainwright *et al.*, 2019a).

It is important to extensively study the drivers of seasonal rainfall, physical processes (James *et al.,* 2018); and the fluctuations observed when seasonal rainfall extremes occur. Results from studying the drivers of seasonal rainfall may offer significant input towards the development of general circulation models (GCMs) for Africa (James *et al*., 2018) especially with the use of reanalysis for higher resolution output (Sun *et al.*, 2018) to supplement the scarce and irregularly distributed station weather data (Nicholson and Klotter, 2021). Consequently, the output will be essential in strategically planning and implementing structures for protective action and mitigation given projections of more frequent events of seasonal rainfall extremes in the region and Africa (Dunning *et al.*, 2018), including the improvement of early warnings of extremely high rainfall that lead to flooding currently provided with short lead times (MacLeod *et al.*, 2021). Ergo, a study on the anticyclones that influence the weather over East Africa whilst influencing other synoptic controls of weather is a valid starting point. Hence, more reliable GCMs for Africa will be produced to improve forecasting and research. In addition, more reliable forecasts and warnings

provided to policy makers and the population will be important in preparing for and mitigating the effects of seasonal rainfall extremes.

1.3 Research Questions

The research questions this study sought to answer:

1. What are the specific years in the study period that exhibit extreme rainfall patterns during the MAM and OND seasons?
2. How does the spatial distribution of rainfall differ in the years with seasonal extremes compared to the climatological distribution during the MAM and OND seasons?
3. How do the location and orientation of anticyclones differ during the years of seasonal rainfall extremes compared to the climatological patterns?
4. What are the dominant patterns of moisture transport and circulation during the years of seasonal rainfall extremes?

1.4 Objectives

The overall objective of this study was to determine how the anticyclones adjacent to Africa influence seasonal rainfall extremes over East Africa.

To achieve the overall objective, the following specific objectives were undertaken:

1. To identify the years with seasonal rainfall extremes for the MAM and OND seasons.
2. To determine the spatial distribution of rainfall for the identified years with seasonal extremes versus the climatological distribution.
3. To compare the location, orientation and intensity of the anticyclones during the years of seasonal rainfall extremes with climatological patterns.
4. To investigate patterns and/or attributes of moisture transport and circulation for years of seasonal rainfall extremes.

1.5 Justification of the Study

With East Africa being prone to seasonal rainfall extremes, the population is exposed and vulnerable (Kilavi *et al*., 2018). Extremely high rainfall causes flooding that sweeps away people's livelihoods. Agricultural products are destroyed and swept away by floodwaters. Road networks may be demolished and power lines destroyed. Drainage systems, both in urban settings and river channels burst and threaten humanity. Floods can lead to water-borne diseases including Cholera.

On the other hand, extremely low rainfall may cause droughts and famines leading to crop failure and starvation of humans and animals, as well as reduction of generation of hydroelectric power (Finney *et al.*, 2020).

Disasters due to rainfall extremes lead to huge losses at individual, social and economic fronts and consequently, these parties suffer hefty costs to rebuild and recover from the losses. Yet, with climate change, future projections suggest that seasonal rainfall extremes could become more frequent (Wainwright *et al.*, 2021). Understanding seasonal rainfall extremes and the controls therein would be fundamental in generation of early warning information for safeguarding lives and property of the population. This would also allow for more effective planning in different sectors including agriculture, hydrology and water resources, energy and health. This will in turn aid in safeguarding life and property.

1.6 Significance of the Study

Rainfall extremes contribute to food insecurity and malnutrition among the African people, with the Eastern part of the continent having the highest population of undernourished people of more than 120 million. This reflects poorly on the efforts towards Zero Hunger pillar of the Sustainable Development Goals (SDGs) (FAO, 2021) given that the population of the countries in East Africa greatly depends on rain fed agriculture, despite frequent occurrence of droughts and floods (Nicholson, 2017) due to seasonal rainfall extremes. Nonetheless, it is an opportunity to put forward strategic management planning framework to safeguard the lives of the East African population from hunger and starvation.

East Africa is a hub for renewable energy resources to contribute to the livelihoods of the population. In addition, East African cities are becoming more cosmopolitan, playing host to people and businesses of all races and nationalities. With this, there is need to connect the science to humanity, safeguarding them and their property.

The information from more accurate and reliable seasonal forecasting can be very valuable in cushioning the people and the economy of East Africa. Spreading this knowledge throughout the African continent may be fundamental in helping subsistence, small-scale and large-scale economies navigate through rainfall variability. This sharing of knowledge can lead to collaborations and new inventions in urban planning, agriculture, technology and energy, as promoted by the African Union (2015).

1.7 Domain of Study

The region of study is East Africa, comprising of three countries: Kenya, Uganda and Tanzania (Hirons and Turner, 2018; Nicholson, 2017) as shown in Figure 1. The region of bimodal distribution of rainfall lies between longitudes 30°E and 43°E and latitudes 12°S and 5°N. However, the southern part of Tanzania from 10°S exhibits a unimodal rainfall regime from December to February (DJFM) (Ogallo, 1988) due to the southern migration of the ITCZ across the western Indian Ocean into Southern Tanzania (Ongoma *et al.*, 2015). Although it has two rainfall seasons, East Africa is drier than other equatorial tropical regions (Hirons and Turner, 2018).

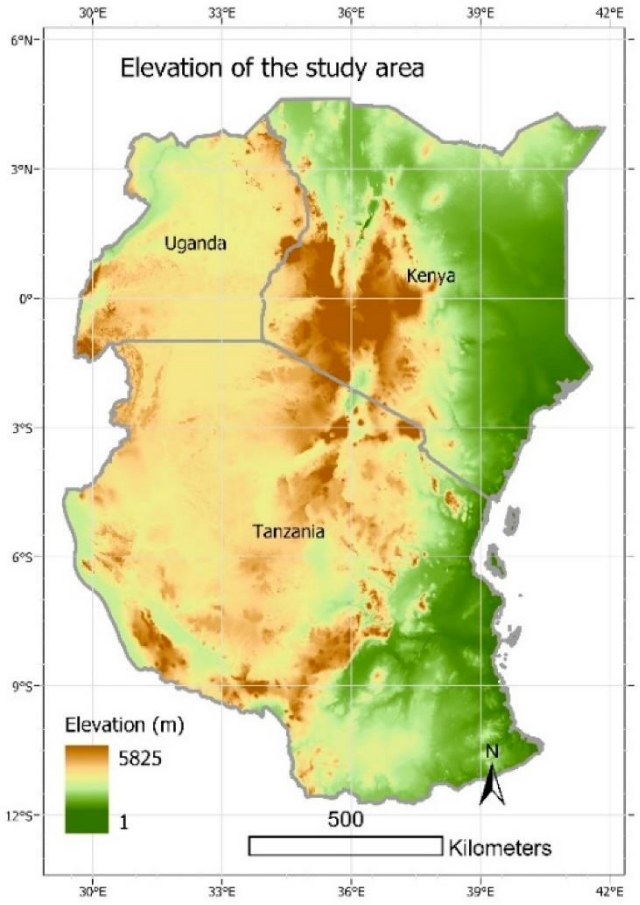

Figure 1: Map of East African countries showing varied elevation (source: Yengoh and Ardo, 2020)

MAM rainfall season is known as the long rainy season since it is heavier and lasts longer (Nicholson, 1996; Camberlin and Philippon, 2002) with the peak rainfall in April (Yang *et al.*,

2015). It is more difficult to predict the long rainy season. This is because the spatial structures of rainfall in MAM is more complex than at any other time of the year and is not well documented. Consequently, there is little knowledge on atmospheric and oceanic forcing for this rainfall season (Camberlin and Philippon, 2002). MAM season is weakly correlated with most large-scale drivers of rainfall like ENSO and IOD (Kilavi *et al.*, 2018).

The OND rainfall season is known as the short rainy season as it is brief and less intense compared to MAM (Nicholson, 2014) with peak rainfall in October (Yang *et al.*, 2015). The season exhibits strong associations with mechanisms of global circulation like ENSO and surface westerlies over equatorial western Indian Ocean (Nicholson, 2014), improving predictability of the season.

Rainfall in East Africa is highly variable in space due to topography and other physical features (Ongoma *et al.*, 2015) as depicted in Figure 1. East Africa has a complex topography with mountains such as Kilimanjaro (5898 m), Kenya (5919 m), Ruwenzori (5109 m) in close proximity to the equator yet they have snow caps. Other mountains include Mt Elgon (4321 m), Mt Meru (4556 m), Mt Longonot (2776 m), Menengai (2278 m), Ol Doinyo Lengai (2962 m). The Great Rift Valley and consequently the East African highlands have an almost north-south orientation, running through the region. The coastal plains are at the eastern part of the region (Yang *et al.*, 2015). These topographical features are important in low-level atmospheric circulations and moisture fluxes (Kinuthia and Asnani, 1982). There are inland lakes in East Africa including Lake Victoria which produces its own circulation and rainfall regime as it is a semi-permanent low-pressure region (Nicholson, 2014b) as well as lakes Turkana, Nakuru, Naivasha, Elementaita, Kivu, Albert, Edward. The Indian Ocean is an important source of moisture, circulation and other mechanisms modulate rainfall amounts over the region (Hastenrath *et al.*, 1993).

1.7.1 Controls of Seasonal Rainfall in East Africa

The controls of rainfall in East Africa are connected with fluxes of energy, momentum and matter. The subtropical highs strongly influence transport of moisture from the subtropical oceans (Cherchi *et al*., 2018). The interaction of the subtropical highs and other drivers are fundamental in moisture transport into and regional precipitation of East Africa. These drivers are briefly discussed below.

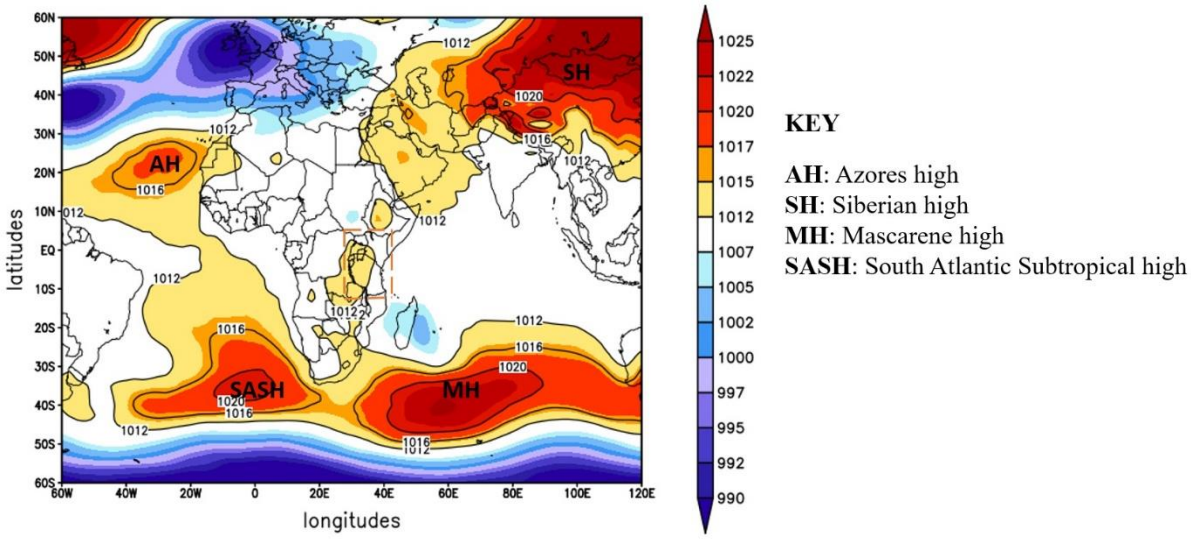

Figure 2: Map of Africa and the four anticyclones that influence East Africa weather depicted by sea level pressure in March 2018. East African region is enclosed in the dashed box.

The Intertropical convergence zone (ITCZ), a region of low pressure that encourages maximum convergence of surface northeasterly and southeasterly trade winds leading to formation of convective cells, cloudiness, high rainfall frequency and/or warmer sea surface temperatures (Souza and Cavalcanti, 2009). It is a major control of tropical rainfall on both land and ocean (Nicholson, 2018) as it crosses the region in its south-north then north-south migration between the months of March and May and October and December respectively, coinciding with the rainfall seasons in East Africa (Camberlin and Philippon, 2002).

The Congo air boundary (CAB) which is referred to as the region where low level westerlies (LLW) that originate from recurved southeasterlies in the Atlantic Ocean, and are moist and close to saturation due to transport over the Congo basin meet the dry easterly trade winds from the Indian Ocean at the surface, is associated with rainfall variability (Howard and Washington, 2019). The presence of CAB over parts of the East African region leads to enhanced rainfall conditions (Nyakwada *et al.*, 2009).

The Madden-Julian Oscillation (MJO) is an eastward propagating atmospheric wave that enhances or suppresses tropical convection (Finney *et al.*, 2020) with a typical oscillation period of between 30 and 90 days (Zhang, 2005). The MJO has been reported to enhance rainfall during certain

phases. For example, the second phase of the MJO favours the formation of tropical cyclones in the Indian Ocean. The fifth and sixth stages of the MJO are associated with drier conditions over the region (Omeny *et al.*, 2008). It has also been reported that different phases of the MJO can cause enhanced precipitation in some areas while suppressing it in other areas. For example, the third and fourth phases of the MJO resulted in high rainfall in the highlands while reduced rainfall was observed at the coast and the vice versa was true for the sixth and seventh phases of the MJO (Hogan *et al.*, 2015).

Tropical cyclones (TCs) developing in the Indian Ocean may indirectly affect parts of East Africa. However, the role of TCs in their influence of rainfall over East Africa is complex. For example, TCs Dumazile and Eliakim were associated with heavy rainfall. In contrast, cyclone Idai in March 2019 coincided with the late onset of MAM causing lower rainfall to be experienced in parts of East Africa especially in Kenya. During OND 2019, there were four TCs in the Indian Ocean that exacerbated the heavy rainfall experienced (Wainwright *et al.*, 2019b).

The Indian Ocean dipole (IOD) is a zonal anomaly in sea surface temperature (SST) (Webster *et al.*, 1999) that influences the East African rainfall majorly during OND season (Owiti *et al.*, 2008). The positive phase of the IOD causes higher than average SSTs which are associated with above average rainfall and floods while the negative phase of the IOD encourages cooling, leading to below normal rainfall and droughts (Ongoma *et al.*, 2015).

The El Niño Southern Oscillation (ENSO) and its evolutionary phases have been linked to rainfall in East Africa. During El Niño years, there is enhanced rainfall leading to flooding events in some areas. La Niña years on the other hand are characterised by extremely low rainfall leading to droughts (Mutemi, 2003). It has generally been believed that the OND rainfall increases during the warm phases and decreases during the cold phases of ENSO (Behera *et al.*, 2005). The Southern Oscillation (SO) contributes to anomalies in the OND season. During positive SO phase, pressure increases in the western Indian ocean and reduces in the eastern Indian Ocean, leading to lower rainfall. During the negative SO phase, pressure reduces in the western Indian Ocean and increases in the eastern Indian Ocean leading to enhanced rainfall over East Africa (Hastenrath *et al.*, 1993).

These large-scale controls of rainfall over East Africa described are complex and interact with each other. As a result, rainfall over the region is heterogeneous. Although there is strong coherence in patterns of interannual variability, the amount of and seasonality of rainfall may vary immensely over relatively short distances (Nicholson, 2017). This study aims to investigate one of the large-scale drivers of seasonal rainfall in order to quantify the large-scale dynamics and general circulation especially for cases of extreme weather.

CHAPTER TWO

LITERATURE REVIEW

2.1 Introduction

This chapter presents some of the previous research studies related to years with seasonal rainfall extremes for both MAM and OND seasons and how pressure and circulation patterns due to the anticyclones in the neighbourhood of Africa are linked to the seasonal rainfall extremes.

2.2 Recent Studies on Seasonal Rainfall Extreme Cases and their Drivers

Wainwright *et al*. (2021) noted that OND 2019 was one of the extremely high rainfall seasons in recent decades with severe flooding that led to destruction and loss of property. The research focussed on a strongly positive IOD event in the Indian Ocean and anomalously warm SSTs in the Indian Ocean in the neighbourhood of the East African coast. It was also noted that during OND, there is westerly transport of moisture from the East African coast into the central equatorial Indian Ocean. But for the case of strongly positive IOD events, the westerly flow is weakened by low level easterly wind anomalies present in the north Indian Ocean hence wetter conditions over East Africa.

Ngoma *et al.* (2021) did a study on Uganda and reported that 2001,2011, 2015 and 2019 OND seasons were wet while 1993, 2005, 2009 and 2018 were anomalously dry. The results of this study revealed that extremely high rainfall years for the OND season are linked to an ascending arm of the Walker circulation over the western Indian Ocean adjacent to the East African coast while dry years are linked to the descending arm of the Walker circulation over the western Indian Ocean. It was also noted that the weakening of the Mascarene high and strengthening of the high over north Africa encourages flow of westerlies from the Congo basin. The said westerlies converge with low level easterlies over from the Indian Ocean leading to enhanced rainfall over Uganda.

Uhe *et al.* (2018) attributed the extremely low rainfall of OND 2016 that led to droughts in parts of Kenya to La Niña, which is the negative phase of ENSO. Other recorded dry years of the OND due to La Niña included 2005 and 1998.

Kilavi *et al.* (2018) described the serious impacts of MAM 2018 rainfall as near 200 flood related deaths, approximately 300,000 people displaced due to flooding. The study linked the extremely high rainfall to MJO, tropical cyclones and anomalous westerlies.

Chang'a *et al*. (2020) noted that the most recent years of MAM seasonal rainfall extremes include: 2017, 2018,2019 and 2020. It was observed that the trend of rainfall between 2017 and 2020, which were characterised by extreme rainfall, is not homogenous across the region. However, station data revealed increasing rainfall trend. The results of the study found that MAM rainfall for the years between 2017 and 2020 exhibited spatial and temporal variability due to complex topography and multiple forcings associated with the rainfall regimes of the region. this study however focussed on the IOD, ENSO and the Walker circulation as the drivers of the extremely high rainfall. Nevertheless, the circulation patterns due to the Walker circulation can be linked to other studies like Ngoma *et al.* (2021) to understand how the anticyclones play a part.

Omondi and Lin (2023) noted that studies on spatial and temporal variability of extreme rainfall are few as most of the studies focus on the drivers of extreme events. In particular, this study highlighted the sparce network of station data as a limitation to adequately describe the spatial patterns of droughts. Gebremeskel *et al.* (2020) noted that the East African countries exhibited differences in drought trends, thus a challenge to describe the spatial distribution of extremely low rainfall for different years.

2.3 Anticyclones Influencing East African Rainfall

Manatsa *et al.* (2014) recognised that the position of the eastern ridge of the Mascarene high, defined by 1018 mb isobar, is important in rainfall variability during the OND season. It was noted that droughts are associated with westward displacement of the eastern ridge of the Mascarene high while enhanced rainfall was associated with eastward displacement of the eastern ridge of the Mascarene high. Studies by Ongoma *et al.* (2015) and Nkurunziza *et al.* (2019) corroborated this result. Ongoma *et al.* (2015) described that a less intense, zonal Mascarene high withdraws to have an eastward centre, which is associated with enhanced rainfall while a more intense, southeast-northwest oriented Mascarene high with a westward centre is associated with droughts. Yet, these studies did not focus on the behaviour of the Mascarene high during MAM season. Further, most studies on the Mascarene high, including Xulu *et al.* (2020) and Hermes and Reason (2009) have

made greater focus on the summer and winter months of both hemispheres, which do not reflect as the seasonal rainfall months for East Africa.

Nicholson (2014) recognised that the Azores high is a source of dry northwesterly winds. Convergence of the dry northwesterlies with maritime northeasterlies provide positive influence for convergence in the meridional arm of the ITCZ which enhances rainfall over the East African region. Studies on the North Atlantic Oscillation (NAO) which is due to the Azores high have been conducted by Shilenje *et al.* (2015) and McHugh and Rodgers (2001). However, the NAO correlation with rainfall over East Africa was found to be insignificant, except for the Lake Victoria basin for the OND season. This finding on the NAO presenting correlation with rainfall over the Lake Victoria basin is important in corroborating Nicholson (2014) findings that the Azores high is a precursor to the short rains.

Nicholson (2015) stipulated that the Arabian ridge, which is an extension of the Siberian high contributes to MAM rainfall especially in March when the low-level flow is easterly. However, in April, the anticyclonic flow weakens and becomes more contracted. The location of the Arabian ridge is important in determining dry and wet spells over East Africa as was advocated by Nyakwada (2009). When this ridge has a maritime component, it favours rainfall in East Africa whereas a continental component in the Arabian Peninsula results in diffluent flow, contributing to dry conditions in East Africa.

Nicholson (2017) noted that the St. Helena high is a driver of westerly wind anomalies from the Atlantic into the East African highlands, contributing to advection of moisture from the Congo basin for rain formation over the said highlands. This study also noted that one of the contributors to the late onset of MAM rainfall is the negative sea level pressure over South Atlantic Ocean. This is caused by a weakened St. Helena high and that the observation of these negative sea level pressure can be evident as early as January.

Thus, although not explicitly linked to the subtropical anticyclones, Johnson and Morth (1960) made the following remarks concerning easterly flow into the region leading to bimodal rainfall in East Africa: One, that winds for both rainfall seasons are predominantly easterly with northeasterlies being more productive of rainfall especially in November while southeasterlies (more than northeasterlies) are more often associated with rainfall during MAM. Enhanced rainfall would occur during MAM if westerlies occur within the region. More recent study by Finney *et*

al. (2020) expressed that convergence of low-level westerlies from the Congo basin and low-level easterlies from the Indian Ocean are paramount for rainfall in the East African region.

2.4 Teleconnections between the Anticyclones and Other Controls of East African Rainfall

Understanding that ENSO is an important factor to OND rainfall in East Africa and also provides spatial coherence rainfall, studies on the teleconnection between ENSO and the subtropical anticyclones have proven to be fundamental. Sun *et al.* (2017) found that St. Helena tends to be equatorward during El- Nino events and poleward during La Niña. Colberg *et al.* (2004) recognised that during El Niño, St. Helena was less intense and was more intense during La Niña.

Ongoma *et al.* (2015) found that the strength of the Mascarene high influences the ITCZ. Results showed that during OND, a weaker, zonally oriented Mascarene high with its centre to the East encourages wet conditions. In such cases, there was convergence in the lower troposphere causing moist air to rise, leading to extremely high rainfall leading to flooding events. On the other hand, a stronger Mascarene high which was oriented from South east to Northwest and even stretching inland inhibited moisture influx into the region. There was divergence in the lower troposphere signalling sinking motion and lower rainfall was received leading to drought conditions. These results were similar to previous findings by Sun *et al.* (1999) where weakening of the Mascarene high leads to an eastward shift of the meridional arm of the ITCZ resulting in moisture influx into East Africa leading to enhanced rainfall.

Howard and Washington (2019) recognised that low-level westerlies recurved from Atlantic Ocean trade winds contribute to convergence and rainfall over East Africa. These low-level westerlies had been previously researched by Sun *et.al,* (1999) noting that St. Helena plays an important role in rainfall over East Africa as it interacts with other drivers, that is ITCZ and CAB. When the St. Helena high intensifies and the Mascarene high weakens, strong westerlies flow into the East African region, strengthening the meridional arm of the ITCZ. This encourages moisture influx into the Congo Basin and influencing the position of CAB resulting in rainfall over Uganda and the western parts of Kenya and Tanzania. Howard and Washington (2019) also recognised that CAB disintegrates during the short rainy season, evident in October and November. Howard and Washington (2019) also recognised that CAB disintegrates during the short rainy season, evident in October and November.

Finney *et al.* (2020) described that direction of moisture flux across the East African region affects the intensity of rainfall at different times of the year. In addition, this study noted that westerlies from the CAB that may lead to enhanced rainfall are a consequence of lower pressure in Madagascar, which may be due to a weakened Mascarene high and/or occurrence of more frequent or intense tropical cyclones. This finding validated that the drivers of westerlies over East Africa can be on a large scale.

Nicholson (2014) noted that changes in the Azores high is an important precursor to ENSO and suggested that the correlation between the Azores high and ENSO could be used in improving the degree of predictability of OND rainfall. In addition, Fu *et al.* (2022) noted that the supressed Siberian high is a precursor to an El Niño event while an enhanced Siberian high in the previous boreal winter may contribute to a La Niña event. However, this may not reflect on the pressure patterns and subsequent circulation during an ENSO active year during the OND season.

Ongoma *et al.* (2015) studied the influence of the Mascarene high and IOD on the OND season over East Africa. Although it was realised that eastward (westward) shift of the centre of Mascarene high correlated with wet (dry) extremes of OND rainfall, it was not strongly correlated with positive (negative) IOD events. However, it was concluded that low-level convergence over western Indian Ocean and upper-level divergence resulted in wetter conditions whereas low-level divergence over western Indian Ocean and upper-level convergence resulted in drier OND season.

Morioka *et al.* (2015) found that variations of Mascarene high in southern hemisphere summer influence the SSTs of the Southern Indian Ocean which then influences anomalies of wind. It was found that stronger poleward meridional SST gradients offer favourable conditions for the strengthening of the Mascarene high. However, these results focused on the Southern African rainfall during austral summer.

Barimalala *et al.* (2020) noted that a trough in the Mozambique Channel is a feature due to the migration of the Mascarene High and is present between December and beginning of May. It depends on moisture from easterlies from MH and the North East monsoon. In the study, it was recognised that when this trough is strong, there is significant decrease of rainfall over LVB and Northern Tanzania which may be linked to weak North East monsoon penetrating the continent due to anomalous transport of moisture from mainland, leading to moisture deficit in Kenya and Tanzania. from the as well as cooling of SSTs along the eastern African coast hence unfavourable

for rain formation inland. This is evidence that a strong trough can contribute to extremely low rainfall over East Africa.

It has widely been expressed by researches such as Chang'a *et al*. (2020) and James *et al*., (2018) that it is important to investigate the evolution, dynamics and predictability of occurrences of extreme rainfall over the East African region especially because of projections of more frequent extreme rainfall events (Dunning *et al.*, 2018). Given that the anticyclones are centres of action on tropical circulation leading to equatorward advection of moisture (Sun *et al.*,2017), it is important to undertake further research on the influence of the four anticyclones and their teleconnection with other drivers that control seasonal rainfall extremes.

CHAPTER THREE

DATA AND METHODOLOGY

3.1 Introduction

This chapter describes the datasets used and the methods applied to realise the specific objectives of this study.

3.2 Datasets

Although surface weather data is important in forecasting and analysis of rainfall and other weather and climatic parameters, weather stations are sparsely distributed. The relatively few and irregularly distributed weather stations contribute to coarse resolution of data available for analysis, which is a challenge to data gridding. This is especially true for Africa where assessment of rainfall trends across the continent may prove difficult (Wainwright *et al.*, 2019a). Moreover, accurate and reliable records are essential in the study of climatic trends and variability as well as management of resources for socio-economic growth (Sun *et al.*, 2018). Reanalysis is important in reducing deficiencies due to sparsely distributed stations and incomplete areal coverage as it involves merging the said irregular observations and satellite estimates with models that encompass physical and dynamic processes. Yet, the satellite estimates may contain biases due to the indirect nature of the relationship between observations and precipitation (Sun *et al.*, 2018); missed detection of precipitation events and/or 'mismatch' in magnitude of correctly detected precipitation events (Serrat-Capdevila *et al.*, 2016). Nevertheless, the result of reanalysis is the generation of a synthesised estimate across a uniform grid (Sun *et al.*, 2018).

Reanalysed mean sea level pressure (MSLP) as well as zonal (u) and meridional (v) wind components at the 1000 mb level and specific humidity (q) at the 1000 mb level were obtained from NCEP/NCAR reanalysis datasets which are globally gridded monthly datasets with spatial resolution of 2.5° longitude by 2.5° latitude on the global grids (Kalnay *et al.*,1996) for a 40-year period spanning from 1981 to 2020. The 1000 mb level was chosen as it is important in observing convergence since convergence very near the surface prevails (Yang *et al.*, 2015) in addition to the fact that flows between the 1000 mb and the 850 mb are quite similar (Nicholson, 2014). However, NCEP/NCAR reanalysis datasets tend to overestimate the precipitation data over Africa (Manatsa *et al.*, 2014). For this reason, for precipitation, CAMS_OPI which is combined gauge

and satellite dataset for monthly precipitation estimates with spatial resolution of 2.5° x 2.5° on the global grids (Janowiak and Xie, 1999) and GPCP that uses merged gauge and satellite data with spatial resolution of 2.5°x 2.5° on the global grids with monthly temporal scale (Adler *et al.*, 2018) were used. In order to ascertain the validity of these datasets for the East African region, six representative stations in Kenya were chosen depicting different topographical and climatic conditions. These include Kisumu and Mombasa for stations near water bodies, Garissa and Marsabit which are arid, Dagoretti and Narok which are highland stations.

Table 1: Summary of Datasets Used in the Study

Parameter	**Dataset/Product**	**Resolution**		**Coverage**
		Spatial	**Temporal**	
Rainfall	CAMS_OPI	2.5°	Monthly	Global
	GPCP	2.5°	Monthly	Global
	Six representative stations		Monthly	Kenya
MSLP	NCEP/NCAR reanalysis	2.5°	Monthly	Global
Wind (u and v components)				
Specific humidity				

3.3 Methods

In order to achieve the objectives of the study, scripts were written using the scripting language and user-defined functions in order to perform multiple and complex computations on the datasets as well as visualising the meteorological parameters. The global merged rainfall datasets were scaled down to the East African domain so as to delineate rainfall coverage over the region. Similarly, NCEP/NCAR datasets were scaled down to longitudes 60°W to 120°E and latitudes 60°N to 60°S to delineate pressure distribution and moisture flow into East Africa.

3.3.1 Identification of Years with Seasonal Rainfall Extremes

For all datasets used, a 30-year baseline period from 1981 to 2010 defined the climatology. The monthly climatology was derived from monthly averages for the said baseline period as in Equation (1). The MAM and OND seasonal climatology were defined as the mean of the three, monthly climatology for each season as shown in Equation (2).

$$\overline{X_a} = \frac{\sum x_{a_i}}{n} \quad \ldots (1)$$

$$\bar{\bar{X}} = \frac{\overline{X_a}+\overline{X_b}+\overline{X_c}}{3} \quad \ldots (2)$$

Where $\overline{X_a}$, $\overline{X_b}$ and $\overline{X_c}$ are the climatology for the months denoted as *a*, *b* and *c*, x_{a_i} is the data value of month *a* for year *i*, n is the number of years (i.e 30 years). $\bar{\bar{X}}$ represents the seasonal climatology. If the variable is precipitation, the seasonal value is the sum of the values for the individual 3-months, and for variables like pressure and wind, the season value is the average of the three months (i.e. equation 2).

Seasonal composites for each season of each year were obtained by taking the mean for the months of each season. The various precipitation datasets were standardized using Equation (3):

$$Z = \frac{Y_i - \mu}{\sigma} \quad \ldots (3)$$

In Equation (3), Z is the standardised precipitation, *Y* is the precipitation value for a year *i*, μ and σ are the climatology and the standard deviation of the data from 1981 to 2010. Standardised data were organised in terciles. The four highest values from the first tercile were chosen as the years of extremely high rainfall (wet years) and the four lowest values from the third tercile were chosen as the years of extremely low rainfall (dry years). Time series were plotted for the MAM and OND seasons to graphically exhibit the years with seasonal rainfall extremes, as well as validate the tercile approach.

3.3.2 Determination of the Spatial Distribution of Extreme Rainfall in East Africa

The MAM and OND precipitation climatology were plotted. Seasonal precipitation was defined as the accumulated/ sum total of monthly rainfall averaged between 1981 to 2010. For the identified years with seasonal extremes, rainfall anomalies were calculated using Equation (4)

$$AY_i = Y_i - \mu \quad \ldots (4)$$

In Equation (4), AX_i is the precipitation anomaly for year *i*, Y_i is the precipitation for year *i*, and μ is the climatology. The rainfall anomalies were then plotted to observe the extent and regions of concentration of wetness or dryness for the extreme years.

3.3.3 Identification of Properties of the Anticyclones for Years of Seasonal Rainfall Extremes from the Climatology

The monthly climatological distribution of pressure was plotted using monthly MSLP data. Climatological pattern of pressure systems was plotted, having taken the average of MSLP of each month of each season. The same process was applied for the individual years with seasonal rainfall extremes for both the MAM and OND seasons.

3.3.4 Determination of Attributes of Circulation and Moisture for Years with Seasonal Rainfall Extremes

Generation of wind equatorward of the anticyclones was considered important in moisture transport and facilitating seasonal rainfall for the region. The moisture transport was determined by multiplying specific humidity, q with wind.

$$\vec{Q} = q\vec{V}_h \quad \ldots (5)$$

From Equation (5) above, $\vec{Q}$ is the overall moisture transport and $\vec{V}_h$ is the horizontal wind vector.

The Helmholtz theory was then applied in the decomposition of the wind field into divergent and rotational (non-divergent) components, on the global domain (Li *et al*., 2006, Hammond and Lewis, 2021).

$$\vec{V}_h = \vec{V}_\lambda + \vec{V}_\psi \quad \ldots (6)$$

From Equation (6) $\vec{V}_\lambda$ is the divergent wind component and $\vec{V}_\psi$ is the rotational wind component. Equation (7) and Equation (8) apply for moisture transport based on decomposed wind defined in Equation (6).

$$\vec{Q}_\lambda = q\vec{V}_\lambda \quad \ldots (7)$$

$$\vec{Q}_\psi = q\vec{V}_\psi \quad \ldots (8)$$

In Equations (7) and (8), $\vec{Q}_\lambda$ represents divergent moisture flux and $\vec{Q}_\psi$ represents rotational moisture flux.

These moisture flux components were superimposed on MSLP plots in order to adequately determine moisture flows into the region. Further, divergent moisture flux given in Equation (7) was relied on in this study as it deals with low-level circulation from cooling to heating regions which explains divergent circulation and differential heating (Pokam *et al.*, 2014) given that the physics of subtropical high pressure systems is related to atmospheric heating (Sun *et al.*, 2017). This is important because of meridional pressure gradient due to the subtropical high pressure systems is equatorward and results to easterly flow (Hastenrath, 1991), influencing moisture flux and rain formation in the East African region.

CHAPTER FOUR

RESULTS AND DISCUSSION

4.1 Introduction

This chapter presents results from the various methods employed to achieve the objectives of the study. The behaviour of the anticyclones for the extremely high rainfall years (wet cases) and the extremely low rainfall years (dry cases) and the consequential moisture attributes and/patterns are discussed.

4.2 Identification of Years of Seasonal Rainfall Extremes

Time series graphically represented the results of the terciles of standardised precipitation data used to identify four extremely high and four extremely low seasonal rainfall for both the MAM and the OND rainfall seasons in Sections 4.2.1 and 4.2.2 respectively.

4.2.1 Years with Rainfall Extremes for MAM Season

Figure 3 displays a time series of MAM precipitation obtained from merged datasets (CAMS_OPI and GPCP) and the 6-selected representative stations. From Figure 3, CAMS_OPI which was the main dataset identified 2020 as the wettest year for the MAM season followed by 2018, 1981 then 1986 while the driest year was 2000 followed by 2004, 1998 and finally 2009. The merged datasets were quite similar for the wet cases, except that GPCP recorded the highest precipitation in 2018. For the dry cases, the merged datasets recorded similar values in 2000 and 2004 while they varied for 1998 and 2009. The consistency observed on the merged datasets can be attributed to averaging of the datasets across East Africa. Nevertheless, for the selected stations, the time series in Figure 3 showed a lot of spatial incoherence as was described by Camberlin and Philippon (2002).

KMD (2021), TMA (2021) and Gacheru *et al.* (2020) recognised that the long rainy season of 2020 was exceptionally wet, with several meteorological stations in Kenya recording 75% more than their long-term means (LTMs) while some stations in Tanzania recorded 175% excess of the LTMs. Kilavi *et al*. (2018) pointed out that MAM 2018 was one of the wettest on record with exceptionally high rainfall in the months of March and April.

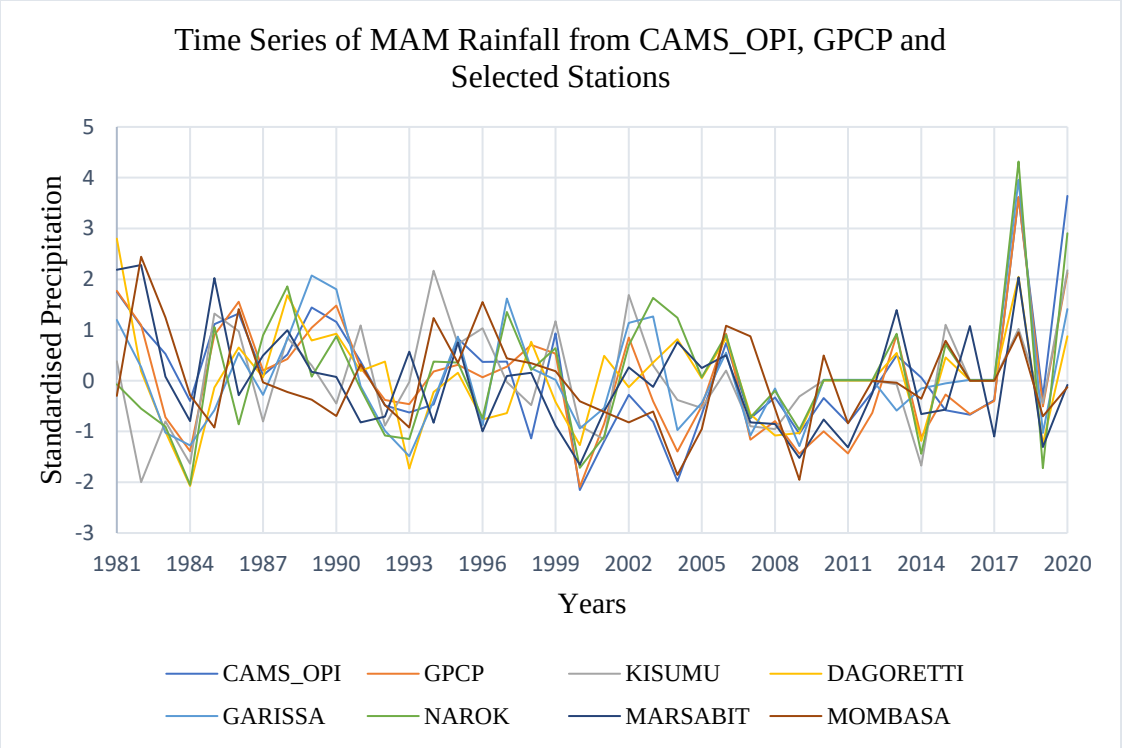

Figure 3:Time series of standardised MAM precipitation obtained from CAMS_OPI, GPCP and 6-selected stations in Kenya from 1981 to 2020

Nicholson (2016) acknowledged that 1998, 2000 and 2009 were characterised by well below average rainfall in East Africa and beyond. Nicholson (2017) listed 2004 as a year of extremely low rainfall during MAM season. Lyon and DeWitt (2012) indicated an abrupt decline of MAM rainfall after 1999, with rainfall for period 1999-2009 being 15% less than that of the previous decade. The results obtained affirm these results since 2000, 2004 and 2009 are listed as years of extremely low rainfall.

4.2.2 Years with Rainfall Extremes for OND Season

Figure 4 indicates a time series of OND precipitation obtained from merged datasets and the 6-selected representative stations. From Figure 4, the highest peak of rainfall was observed in the year 1997, followed by 2019, then 2006 and finally 1982. The lowest precipitation amounts observed were in the years 2005, 1998, 1993 and finally 2016. Similar to MAM cases, the merged datasets presented similar results for both wet and dry years.

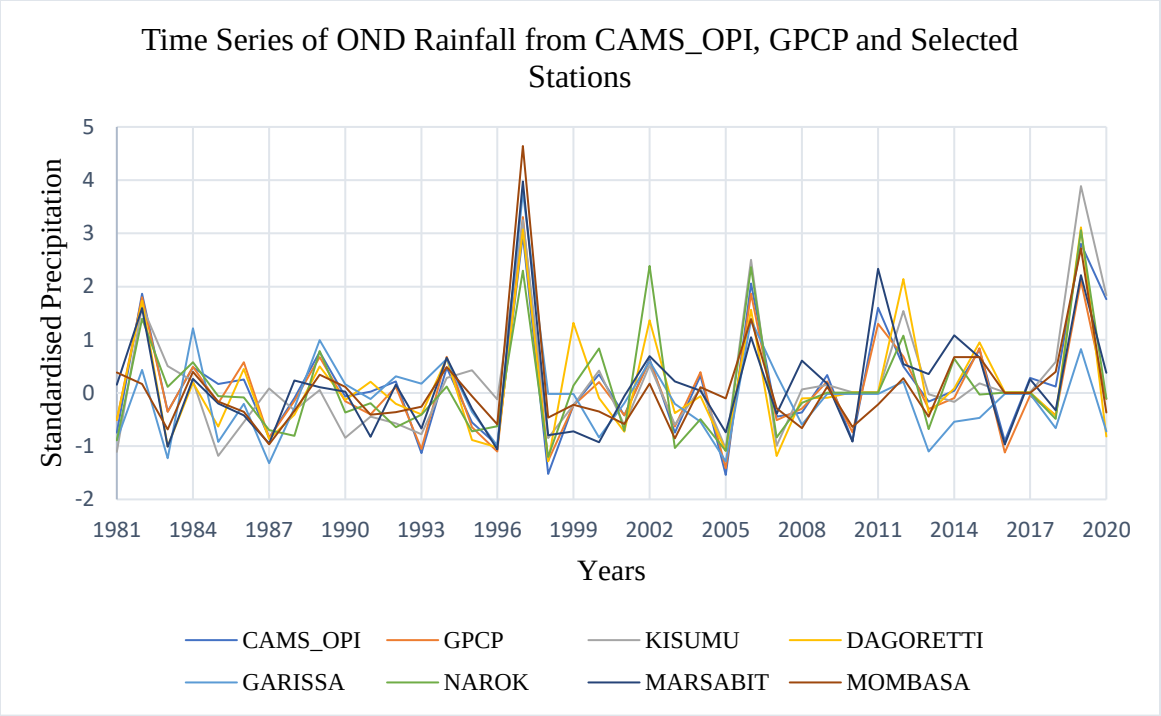

Figure 4:Time series of standardised OND precipitation obtained from CAMS_OPI, GPCP and 6-selected stations in Kenya from 1981 to 2020

Based on the six representative stations, OND rainfall as in the time series in Figure 4 showed more spatial coherence as compared to MAM rainfall in the time series shown in Figure 3, validating findings by Camberlin and Philippon (2002) that OND rainfall in East Africa exhibits more spatial coherence as compared to MAM.

All the years of extremely high rainfall of the OND season had positive Oceanic Niño Index (ONI) (https://origin.cpc.ncep.noaa.gov/products/analysis_monitoring/ensostuff/ONI_v5.php). ONI is a primary indicator by NOAA obtained by tracking three-month average SSTs in tropical Pacific Ocean between 120° and170°W, used for tracking the ocean part of ENSO (Lindsey, 2009). The year 1997, which had the highest rainfall for the OND season was associated with a strong El Niño event (Black, 2005). The same is true for 1982 which had a strong El Niño (Nicholson, 1996). Nevertheless, although there was no significant El Niño event in 2019, Kenya alone recorded above 125% of OND long term averages (Wainwright *et al.*, 2021). Some of these years of extremely high rainfall were characterized by floods, for example, 1982, 1997 and 2006 (Nicholson, 2014). In contrast, the year 1998 had a strong La Niña and was characterised by drought while 2005 and 2016 were weak La Niña years (Uhe *et al.*, 2018).

Therefore, based on the time series in Figures 3 and 4, the years with extreme rainfall were summarized in Table 2 below.

Table 2: Identified Years of Seasonal Rainfall Extremes for Both MAM and OND Seasons

	Extremely low rainfall years	**Extremely high rainfall years**
MAM	2000, 2004, 1998, 2009	2020, 2018, 1981, 1986
OND	2005, 1998, 1993, 2016	1997, 2019, 2006, 1982

4.3 Spatial Distribution of Rainfall

The monthly and seasonal distribution of rainfall is described below. The climatology of both MAM and OND rainfall are discussed in Sections 4.3.1 and 4.3.2 respectively. Thereafter, the spatial distribution for the years of extreme rainfall is discussed in Section 4.3.3. For Section 4.3.3, rainfall anomalies are utilised to depict the extreme amounts of rainfall observed for the years listed in Table 2. Although regions of rainfall concentration were noted, they are not discussed extensively as they may reflect mesoscale and small-scale factors, which is beyond the scope of synoptic control of anticyclones.

4.3.1 Rainfall Climatology of MAM Season

Figure 5 shows the spatial distribution of rainfall for March, April and May and the seasonal cumulative rainfall using both merged datasets. In Figure 5 CAMS_OPI and GPCP datasets revealed similar spatial distribution of precipitation for the MAM season. However, GPCP depicted higher rainfall as compared to CAMS_OPI.

In Figure 5, rainfall was confined in the South, particularly in Tanzania in March. It moved northward in April, where the rainfall band was within the equatorial region. In May, rainfall was much less than in March or April and was more northward as compared to April. This is consistent with the findings of Asnani (1993) where the rainfall band moves from the southern hemisphere to the northern hemisphere during MAM season. It is evident that peak rainfall is experienced in April (Camberlin and Philippon, 2002) which marks the highest rainfall for the entire year (Yang *et al.* 2015).

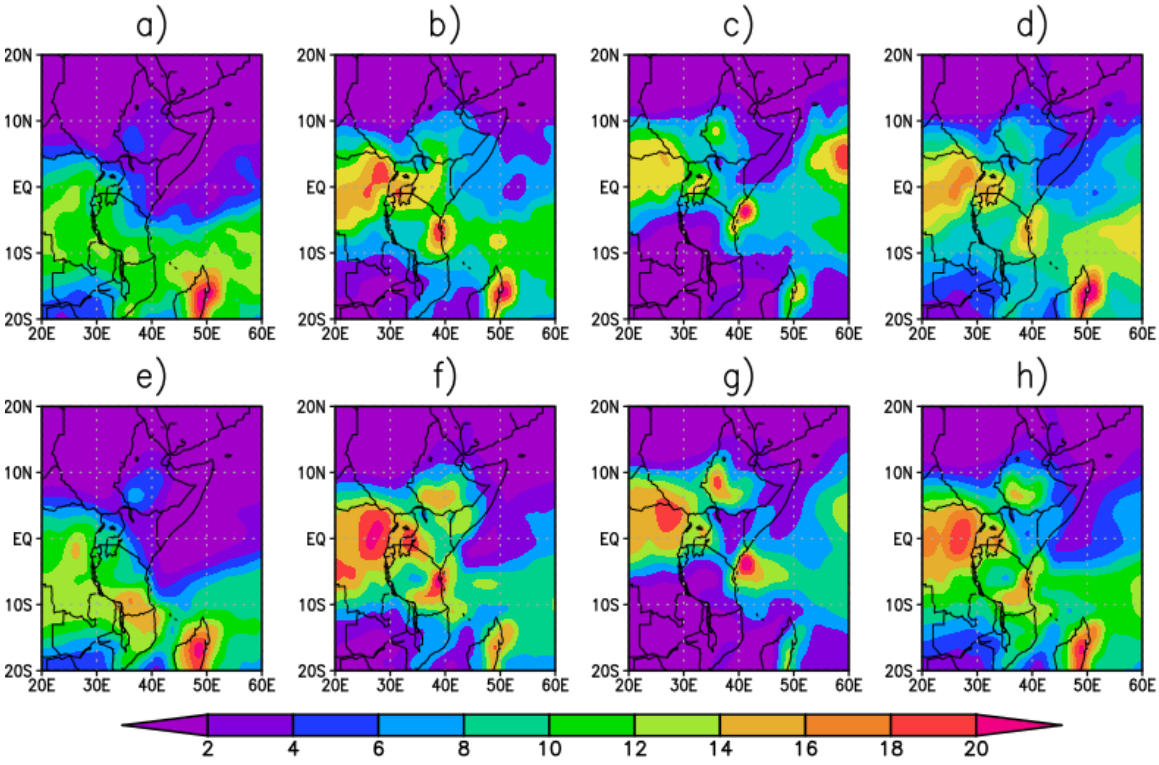

Figure 5:The spatial distribution of rainfall (mm/day) for MAM season using the merged datasets. a) to d) were from CAMS_OPI dataset where a) is March climatology, b) is April climatology, c) is May climatology and d) is cumulative rainfall from March to May. e) to h) were obtained from GPCP dataset where e) is March climatology, f) is April climatology, g) is May climatology and h) is cumulative rainfall from March to May.

4.3.2 Rainfall Climatology of OND Season

Figure 6 shows the spatial distribution of rainfall for October to December and the seasonal cumulative rainfall using both merged datasets. In Figure 6, CAMS_OPI and GPCP datasets revealed similar distribution of precipitation for the OND season. However, the precipitation amounts differed in that CAMS_OPI recorded higher precipitation for the East African region. Nevertheless, in October, rainfall was mostly confined in the northern hemisphere and partly the equatorial region. In November, rainfall was confined to the equatorial region. In December, rainfall was concentrated in the southern hemisphere, over the southern part of the region and more southward. This is consistent with the findings of Gudoshava *et al.* (2022) and Asnani (1993) that the rainfall band migrates from the northern hemisphere to the southern hemisphere between October and December.

The short rainy (OND) season showed a similar pattern of precipitation to the long rainy season (MAM). However, based on Figures 5 and 6, the short rainy season recorded lesser rainfall as compared to MAM, corroborating the evidence by Yang *et al.* (2015).

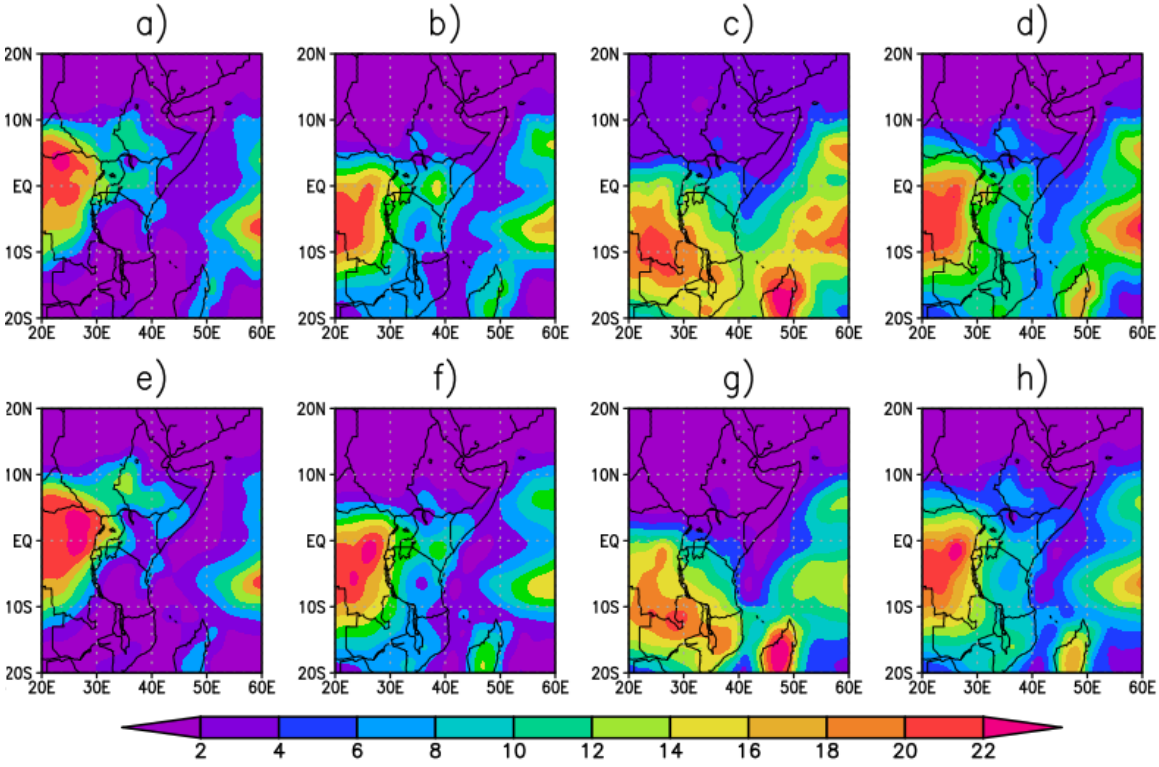

Figure 6:The spatial distribution of rainfall (mm/day) for OND season using the merged datasets. a) to d) were from CAMS_OPI dataset where a) is October climatology, b) is November climatology, c) is December climatology and d) is cumulative rainfall from October to December. e) to h) were obtained from GPCP dataset where e) is October climatology, f) is November climatology, g) is December climatology and h) is cumulative rainfall from October to December.

Based on Figures 5 and 6, CAMS_OPI and GPCP datasets depicted similar results, proving that CAMS_OPI is valid for monitoring of rainfall in East Africa. This is concurrent with Janowiak and Xie (1999) findings that CAMS_OPI lent itself well to the task of real-time monitoring of global precipitation and was suggested as a better option as compared to GPCP for real-time monitoring of precipitation on climatic spatial scales.

4.3.3 Spatial Distribution of Rainfall during Years of Extreme Rainfall

Rainfall anomalies were utilised in observing the spatial distribution of rainfall for the years of extreme rainfall for both the MAM and OND seasons as discussed in Sections 4.3.3.1 and 4.3.3.2.

4.3.3.1 Spatial Distribution for Years of Extreme Rainfall During MAM Season

Figure 7 shows the comparison of 2020 which was the wettest observed MAM season using CAMS_OPI dataset and 2000 which was the driest on the CAMS_OPI dataset for MAM rainfall. In March 2020, positive precipitation anomalies were observed particularly in Uganda and Tanzania and the western parts of Kenya as in Figure 7a). In April, high positive precipitation anomalies were observed particularly in coastal Tanzania as in Figure 7b). In May, positive rainfall anomalies were observed in some parts of Tanzania.

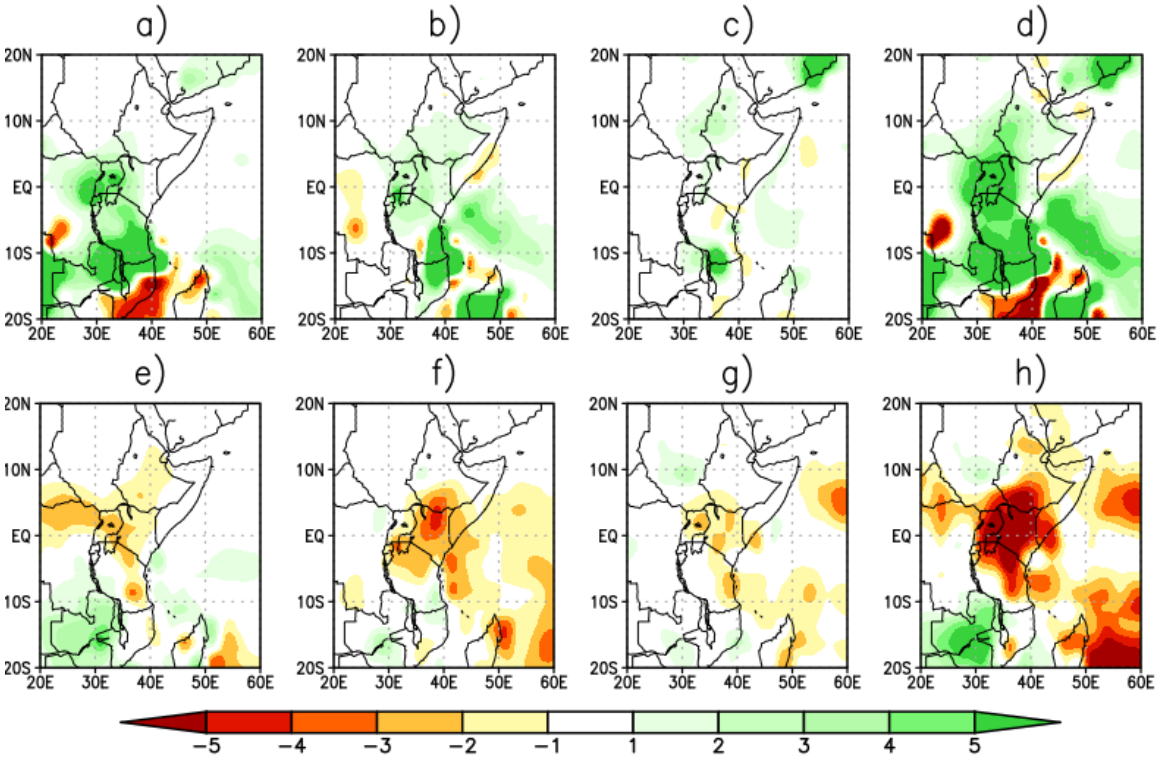

Figure 7: The MAM rainfall anomalies for select wet and dry years using CAMS_OPI dataset. Top is 2020 (extremely high rainfall) where a) is March, b) is April, c) is May and d) is the sum total of precipitation anomalies observed in a), b) and c). Bottom row is 2000 (extremely low rainfall) where e) is March, f) is April, g) is May and h) is the sum total of precipitation anomalies observed in e), f) and g).

From the MAM totals in Figure 7d), it was evident that the region experienced very high rainfall. Narok and Kisumu stations from the time series in Figure 3 confirm the observation on Figure 7d) as they are located in the western part of Kenya, which experienced very high positive rainfall anomalies.

The case of 2000 revealed a contrasting case with below average rainfall. In March 2000 as in Figure 7e), most of the region was dry, except the western part of Tanzania, which can be broadly attributed to a spill-over from the wetter Zambia and Democratic Republic of Congo (DRC). In April, very dry conditions were observed particularly in Northern Kenya and the western part of the Lake Victoria Basin (LVB) in Figure 7f). In May, most parts of the region remained dry as in Figure 7g). As from the MAM totals of 2000 in Figure 7h), it was evident that most parts of the region (Kenya, Uganda and Northern Tanzania) were extremely dry. This is evident from the time series in Figure 3, where all stations recorded very low rainfall.

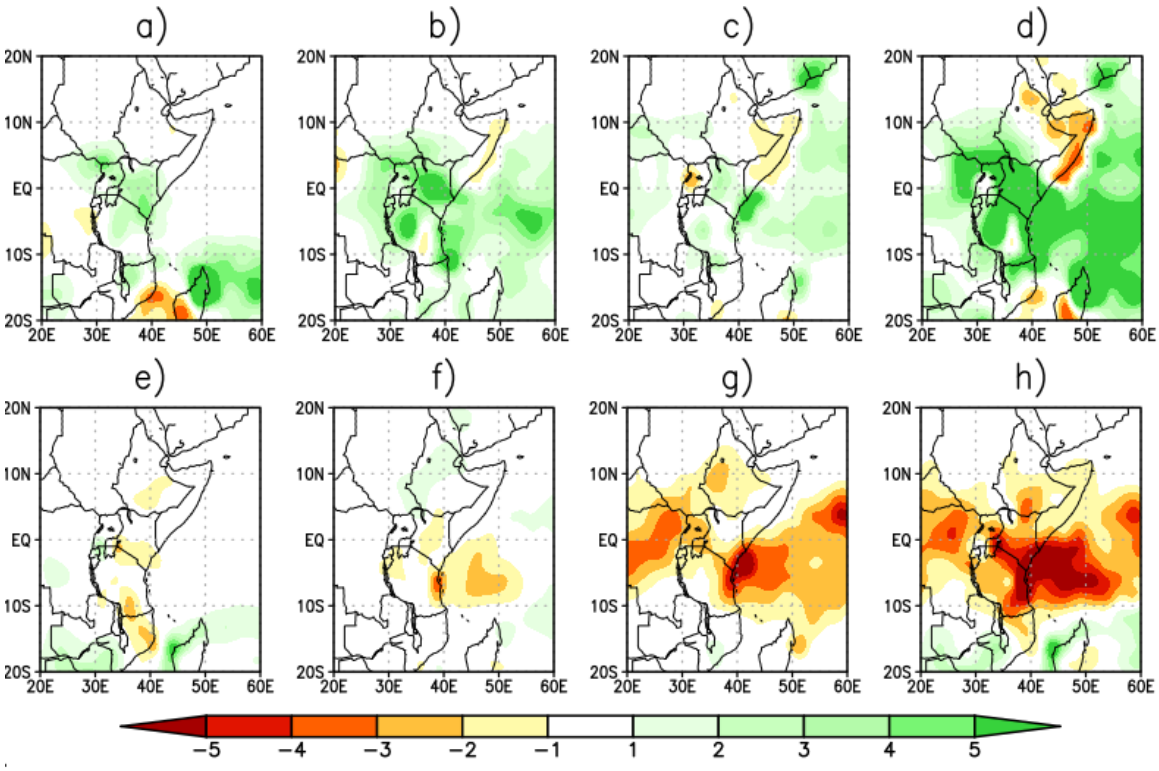

Figure 8: MAM rainfall anomalies for 2018 which was a wet case and 2004 which was a dry case using CAMS_OPI dataset. Top row is 2018 where a) is March, b) is April, c) is May and d) is the sum total of precipitation observed in a), b) and c). Bottom row is 2004 where e) is March, f) is April, g) is May and h) is the sum total of precipitation observed in e), f) and g).

Figure 8 depicts the extremely high rainfall of MAM 2018 and extremely low rainfall of MAM 2000. In March 2018 shown in Figure 8a), positive precipitation anomalies were observed particularly in Northern Uganda and some parts of Northern Tanzania and most parts of Kenya, especially the south eastern part of Kenya, close to the Tanzanian border. In April, high positive precipitation anomalies were observed in most parts of the region as in Figure 8b). In May, positive

rainfall anomalies were observed in some parts of Kenya and Tanzania, with the highest anomalies off the Kenyan coast. In general, most parts of the region were extremely wet during MAM season of 2018 as evidenced in Figure 8d). On the other hand, the year 2004 was dry, with the lowest rainfall anomalies experienced in coastal Kenya in May, as in Figure 8g). Figure 8h) shows that most parts of East Africa were dry, which is evident in the time series in Figure 3 which indicated Mombasa, on the Kenyan coast was exceptionally dry as well as Garissa and Kisumu, all within the very negative rainfall anomalies indicated by dark red in Figure 8h).

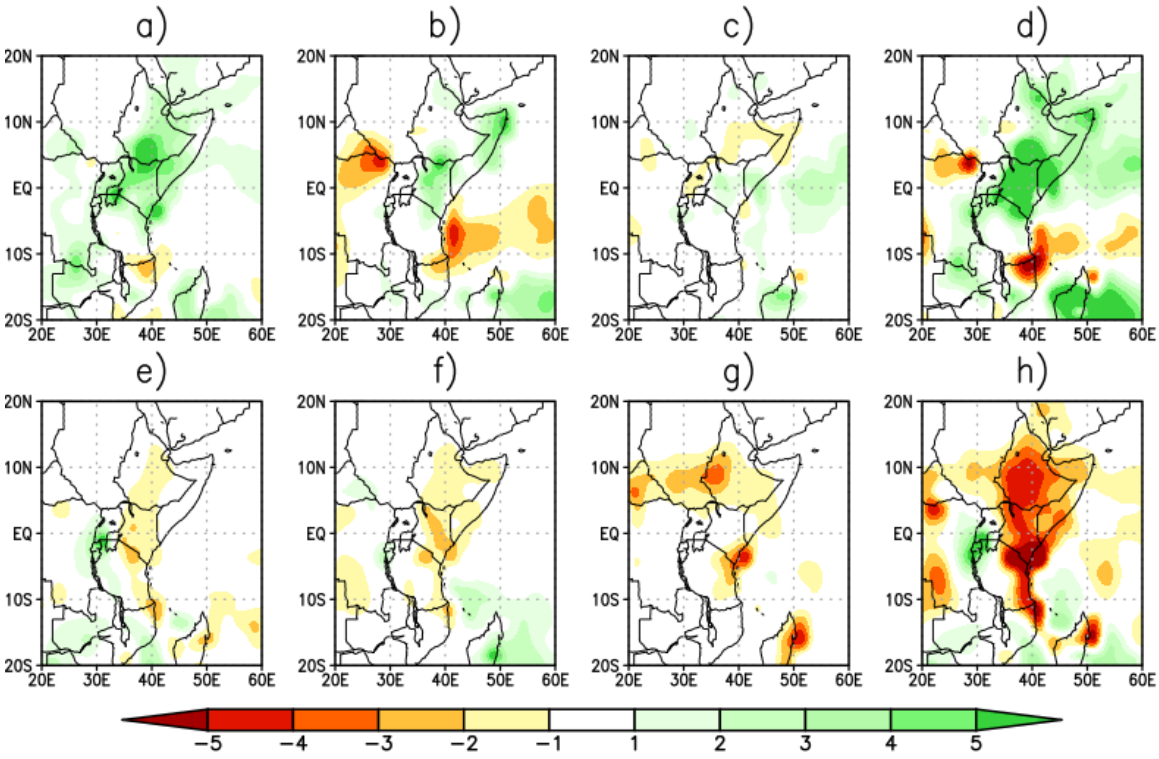

Figure 9: MAM rainfall anomalies for 1981 which was a wet case and 2009 which was a dry case using CAMS_OPI dataset. Top row is 1981 where a) is March, b) is April, c) is May and d) is the sum total of precipitation observed in a), b) and c). Bottom row is 2009 where e) is March, f) is April, g) is May and h) is the sum total of precipitation observed in e), f) and g).

Figure 9 displays rainfall anomalies for MAM 1981 which had extremely high rainfall and MAM 2009 with extremely low rainfall. In March 1981 displayed in Figure 9a), the highest rainfall anomalies were experienced over LVB and most parts of Kenya. Highest anomalies were also observed in Kenya in April as in Figure 9b) which decreased in May 1981 as in Figure 9c). Generally, for MAM 1981, rainfall concentration was highest in Kenya, extending into the LVB

in Uganda and in Northern Tanzania. This evidence is validated by the six selected stations in Figure 3.

In contrast, 2009 was dry. In March 2009, negative rainfall anomalies were greatest in Northern Tanzania. However, some parts of southwestern Uganda had higher than average rainfall as in Figure 9e). In April 2009 as in Figure 9f), negative rainfall anomalies were observed over most parts of Kenya and Tanzania. In May, negative rainfall anomalies were greatest in the coastal region, particularly the Kenyan coast. The 2009 MAM totals indicate that very dry conditions were observed particularly in the eastern portion of the East African region, especially around the Kenyan coast. This observation is validated in Figure 3 where the lowest rainfall for the six selected stations were observed in Mombasa on the Kenyan coast, followed by Marsabit and Garissa, in the eastern parts of Kenya.

Figure 10 displayed shows the 1986 MAM rainfall and 1998 MAM rainfall. In March 1986, positive rainfall anomalies were observed in some parts of coastal and Southern Tanzania. Yet, negative rainfall anomalies were observed over the LVB as in Figure 10a). In April 1986 displayed in Figure 10b), the positive rainfall anomalies were observed over LVB and some parts of Northern Tanzania, southern Uganda and Kenya. May 1986 was indicated in Figure 10c) where the highest positive rainfall anomalies were observed on the coast of Kenya. From the 1986 MAM totals indicated in Figure 10d), highest rainfall anomalies were observed at the coast and into the Indian Ocean. This is confirmed in Figure 3 where the time series indicated Mombasa station observing the highest rainfall in comparison to the other stations.

From Figure 10e), it is observed that March 1998 had negative rainfall anomalies in most parts of the region, the greatest in Uganda, LVB and Tanzania. In April 1998, negative rainfall anomalies were concentrated over Uganda as in Figure 10f), nevertheless coastal Kenya recorded positive rainfall anomalies. In May, although there were positive rainfall anomalies over some parts of western Kenya, the coastal Kenya into the Indian Ocean was particularly dry as in Figure 10g).

The 1998 MAM rainfall totals in Figure 10h), more negative rainfall anomalies were observed in most parts of Uganda and Tanzania while positive rainfall anomalies were observed in some parts of southern Kenya as observed in Dagoretti station in Figure 3, yet Kisumu station recorded low rainfall.

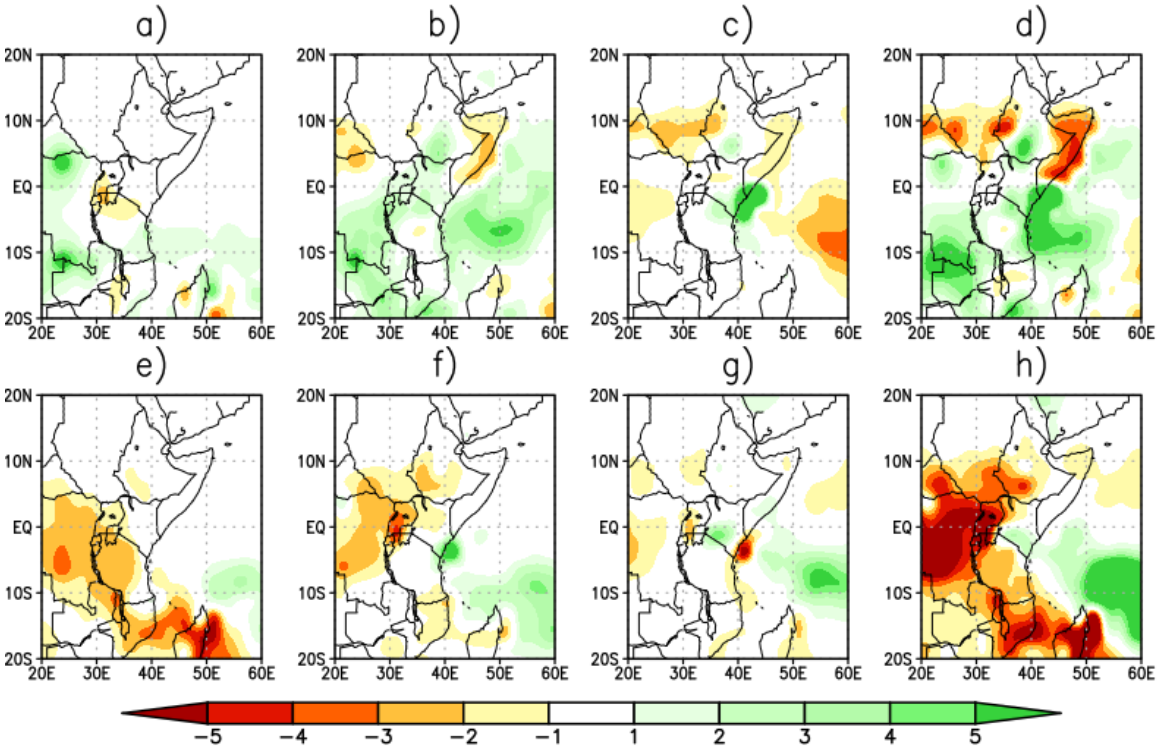

Figure 10: MAM rainfall anomalies for 1986 which was a wet case and 1998 which was a dry case using CAMS_OPI dataset. Top row is 1986 where a) is March, b) is April, c) is May and d) is the sum total of precipitation observed in a), b) and c). Bottom row is 1998 where e) is March, f) is April, g) is May and h) is the sum total of precipitation observed in e), f) and g).

4.3.3.2 Spatial Distribution for Years of Extreme Rainfall During OND Season

Figure 11 displays the OND rainfall anomalies for 1997 which had the highest rainfall recorded for the 40-year period and 2005 which had the lowest rainfall recorded. In October 1997, depicted in Figure 11a), the highest positive rainfall anomalies were recorded in most parts of Kenya. Similarly, highest rainfall anomalies were recorded in most of Kenya, as well as in parts of coastal Tanzania in November as seen in Figure 11b). In December, highest rainfall band was recorded southward, over central Tanzania. Positive rainfall anomalies were observed in most parts of Kenya as in Figure 11c). The OND totals for 1997 as seen in Figure 11d) show that most parts of the region received very high rainfall, which can be validated in Figure 4 which shows the six stations received very high rainfall, the highest being in Mombasa station.

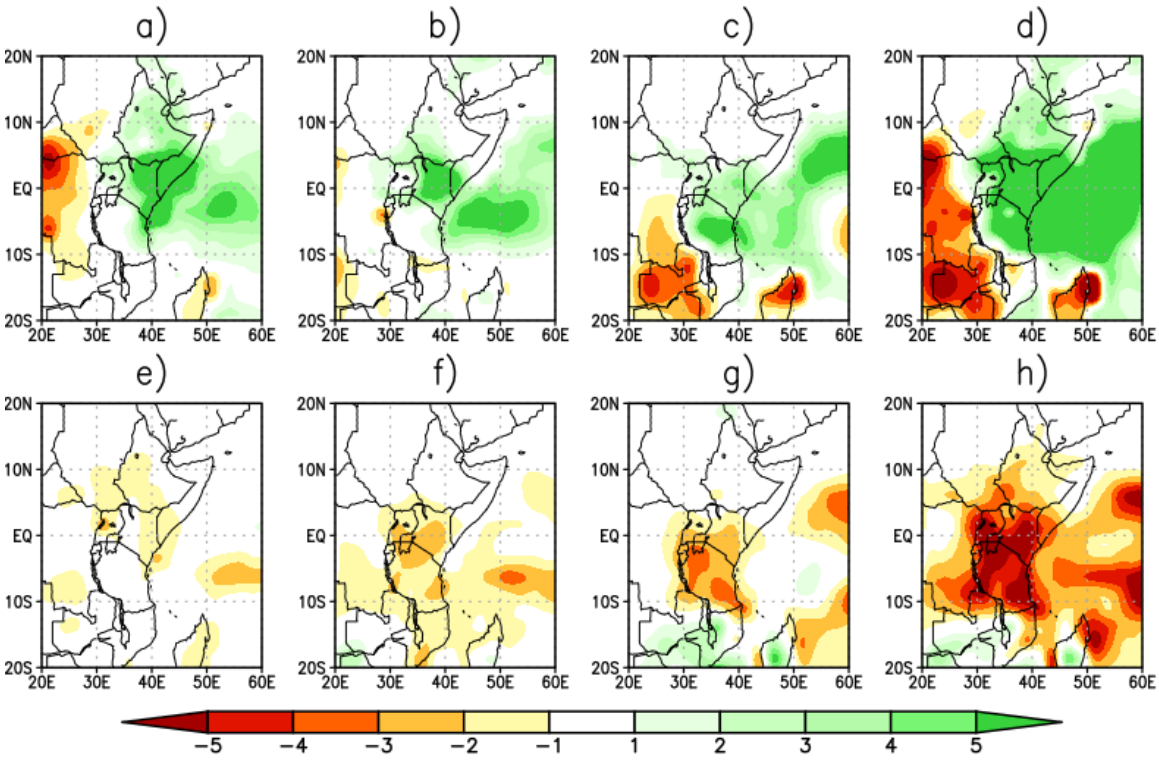

Figure 11: OND rainfall anomalies for highest rainfall of OND season (1997) and the lowest rainfall of the season (2005) using the CAMS_OPI dataset. Top row is 1997 where a) is October, b) is November, c) is December and d) is the sum total of precipitation observed in a), b) and c). Bottom row is 2005 where e) is October, f) is November, g) is December and h) is the sum total of precipitation observed in e), f) and g).

The OND season in 2005 was exceptionally dry especially in November and December as in Figures 11f) and 11g) respectively. Most of the region recorded highly negative rainfall anomalies as in Figure 11h) which is validated by the negative rainfall values recorded in the six selected rainfall stations in Figure 4.

Figure 12 shows the OND rainfall anomalies for 2019 and 1998. In October 2019, most parts of the region had higher than average rainfall as shown in Figure 12a). High rainfall anomalies were concentrated in the western part of the region in November 2019 as shown in Figure 12b), especially in western Uganda and LVB as well as central Tanzania. In December, positive rainfall anomalies were observed over most parts of the region as shown in Figure 12c). Generally, OND season of 2019 exhibited enhanced rainfall as in Figure 12d), confirming results in Figure 4 that showed Kisumu station recording the highest rainfall of the six selected stations, followed by Dagoretti, Narok and Mombasa.

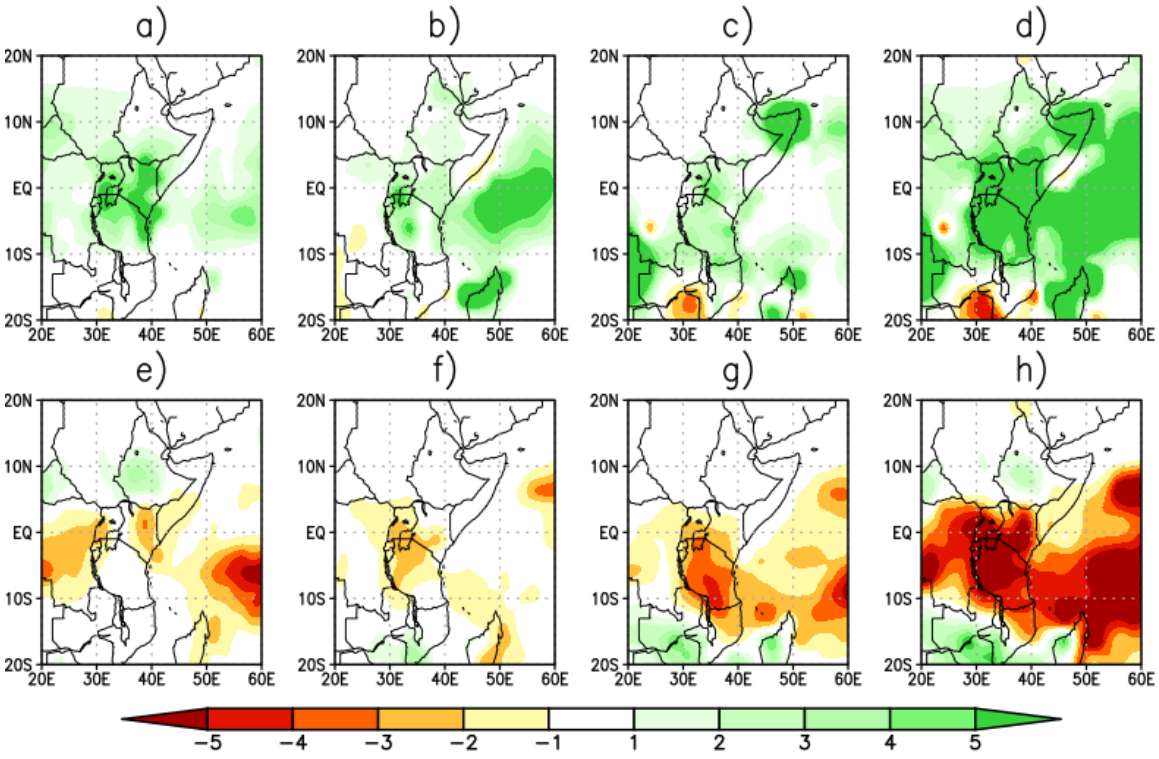

Figure 12: Rainfall anomalies for OND 2019 which was a wet case and OND 1998 which was a dry case using the CAMS_OPI dataset. Top row is 2019 where a) is October, b) is November, c) is December and d) is the sum total of precipitation observed in a), b) and c). Bottom row is 1998 where e) is October, f) is November, g) is December and h) is the sum total of precipitation observed in e), f) and g).

In October 1998, negative rainfall anomalies were concentrated in North-eastern Kenya and Western Uganda as in Figure 12e). In Figure 12f), November 1998 exhibited negative rainfall anomalies especially in Uganda and Tanzania. In December 1998, the negative rainfall anomalies were observed in most parts of the region with the greatest concentration over most parts of Tanzania. The OND season of 1998 was characterised by drier than average conditions as in Figure 12h), affirmed by very low rainfall values observed in the six selected stations in Figure 4.

Figure 13 shows the comparison of the wet OND season in 2006 and the dry OND season in 1993. 2006 recorded positive rainfall anomalies over most parts of East Africa especially in November and December as depicted in Figures 13b) and 13c) respectively. Most parts of the region recorded enhanced rainfall during the short rains of 2006 as observed in Figure 13d) and time series in Figure 4.

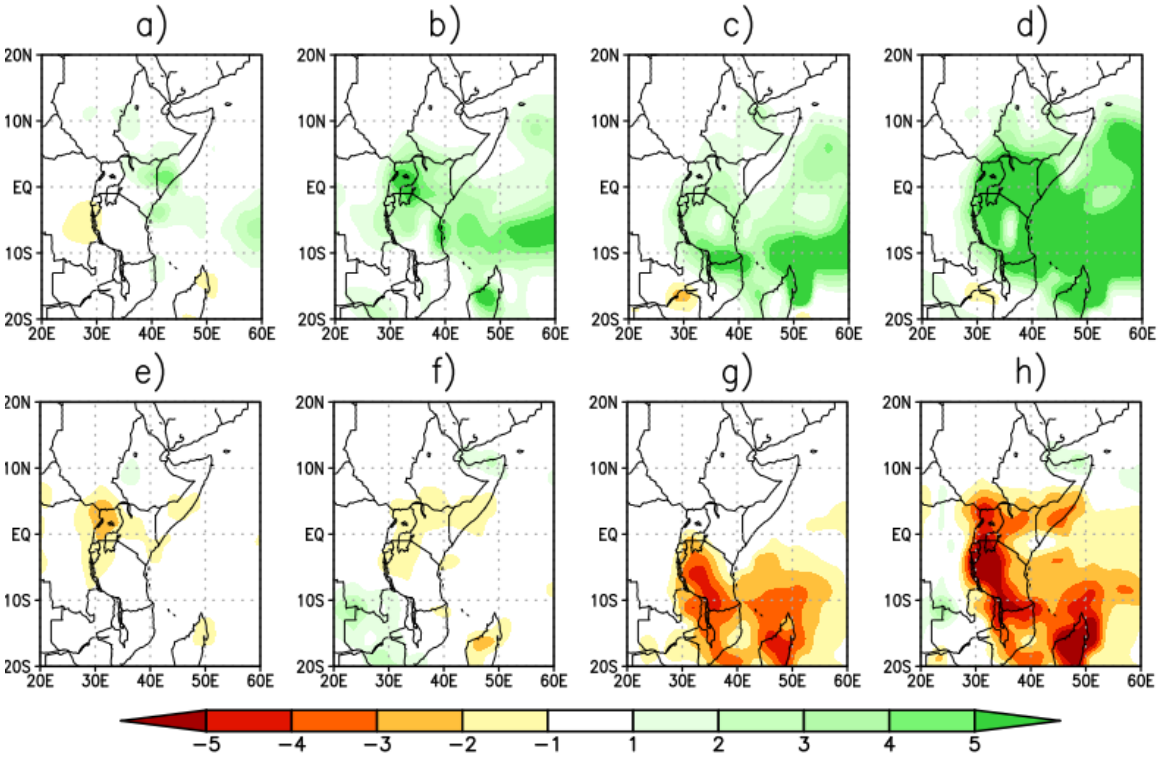

Figure 13: OND rainfall anomalies for 2006, a wet case and 1993, a dry case, using the CAMS_OPI dataset. Top row is 2006 where a) is October, b) is November, c) is December and d) is the sum total of precipitation observed in a), b) and c). Bottom row is 1993 where e) is October, f) is November, g) is December and h) is the sum total of precipitation observed in e), f) and g).

In contrast, October 1993 was characterised by negative rainfall anomalies particularly in Uganda and some parts of Kenya and Uganda as seen in Figure 13e). In Figure 13f), it is noted that November 1993 recorded negative rainfall anomalies in northern Kenya, most parts of Uganda, the LVB and western Tanzania. In December 1993, negative rainfall anomalies were concentrated in Tanzania. As seen in Figure 13h), most parts of the region were dry. In Kenya, the driest areas were in the western parts and north eastern, confirmed in Figure 4 where Kisumu had the lowest rainfall compared to the other stations, followed by Marsabit station.

Figure 14 represents the rainfall anomalies observed in OND 1982 and OND 2016. In October 1982, high rainfall anomalies were observed in the eastern parts of the region, particularly in Kenya and the coastal parts of East Africa as depicted in Figure 14a). In November, high rainfall anomalies were observed especially in Tanzania as in Figure 14b). Similarly, more positive anomalies were recorded in Tanzania in December 1982, as in Figure 14c). From Figure 14d), the

OND season of 1982 was characterised by enhanced rainfall throughout the region, which can be affirmed by the 6 selected stations in Figure 3.

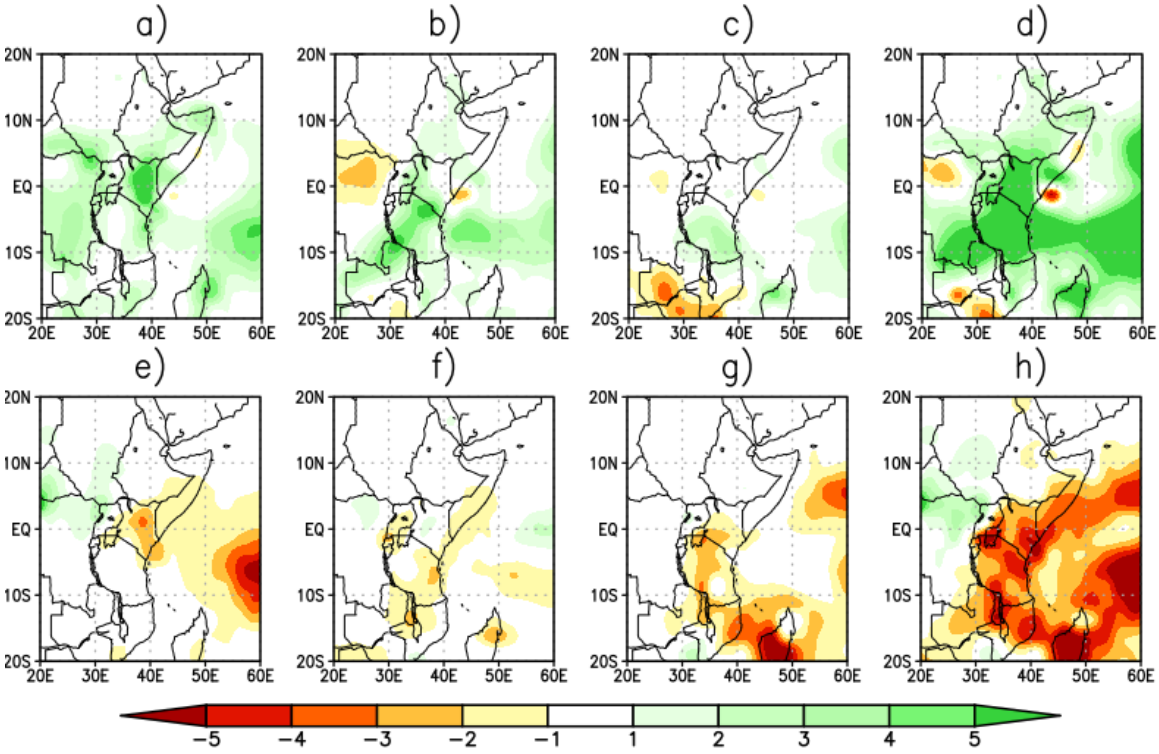

Figure 14: OND rainfall anomalies for 1982, a wet case, and 2016, a dry case, using the CAMS_OPI dataset. Top row is 1982 where a) is October, b) is November, c) is December and d) is the sum total of precipitation observed in a), b) and c). Bottom row is 2016 where e) is October, f) is November, g) is December and h) is the sum total of precipitation observed in e), f) and g).

Unlike 1982, October to December 2016 experienced depressed rainfall as depicted in Figures 14e) to 14g). Figure 14h) shows that the entire region exhibited drier conditions, noted by the six selected stations in Figure 4.

The distribution of rainfall anomalies during the MAM season differed for both the extremely high and extremely low rainfall cases. This may be due to the spatial incoherence of rainfall as was discussed by Camberlin and Philippon (2002). For the OND season, the rainfall anomalies, particularly the positive anomalies appeared to extend from the Indian Ocean. This may be attributed to the findings documented by Wainwright *et al.* (2021) that found that enhanced rainfall is consequential of moisture brought by low-level easterlies from the North Central Indian Ocean.

4.4 Location, Intensity and Orientation of the Anticyclones

The location of the anticyclones based on the position of the centre of the cells and their extent. The intensity involves the highest pressure at the centre of the cell and the orientation deals with the axis of the anticyclones, whether zonal or meridional.

4.4.1 Comparing the Years of Extreme Rainfall with Climatology of MAM Season

Comparison between individual years and the climatology exhibited observable changes in the anticyclones that occurred alluded to the extremely high rainfall (wet) or extremely low rainfall (dry) observed in the region during the MAM season.

4.4.1.1 Comparing the Wet Years with Climatology for the MAM Season

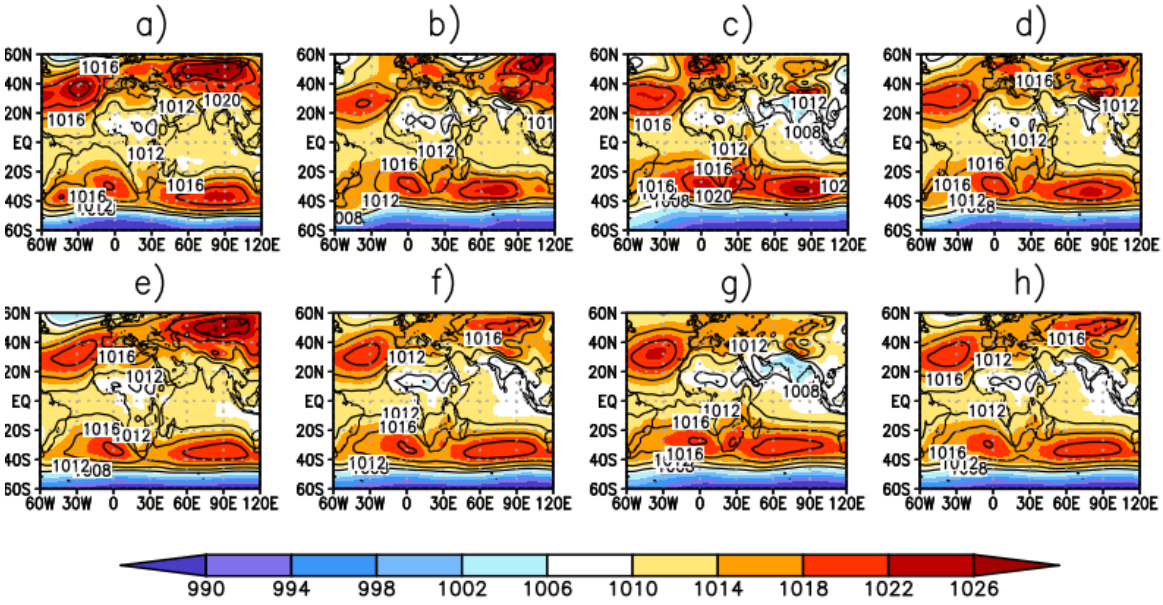

Figure 15: MSLP (in mb) of MAM 2020 (top) compared with climatology (bottom). a) represents March 2020, b) represents April 2020, c) represents May 2020 and d) represents the seasonal composite obtained by averaging pressure between March and May 2020. e) represents March climatology, f) represents April climatology, g) represents May climatology and h) represents seasonal composite obtained by averaging climatological pressure between March and May.

Figure 15 shows a comparison of MSLP for MAM 2020 which had extremely high rainfall with the climatological MSLP pattern. In March, the Azores high was more intense and poleward as in Figure 15a) as compared to the climatology in Figure 15e). The more intense Azores high pressure system contributed to a more equatorward 1012 mb isobar. The St. Helena high pressure cell exhibited similar intensity as the climatology although the centre was smaller. The Mascarene high was more intense and eastward as compared to the climatology. The 1012 mb isobar was quite

similar to the climatology, the trough in the Mozambique Channel was smaller. The Siberian high exhibited similar intensity as the climatology and it was more westward as compared to the climatology. It is observed that the 1012 mb isobar was more equatorward as compared to the climatology.

In April 2020, the Azores high displayed a similar position and orientation to the climatology, although its centre was smaller. Further, the 1012 mb contour was connected to that of the more equatorward St. Helena high which maintained a similar orientation to the climatology. The Mascarene high was more intense and westward as compared to the climatology and had a continental component. The Siberian high was eastward and more intense as compared to the climatology.

In May 2020 as in Figure 15c), the Azores high although with similar intensity to the climatology in Figure 15g) had a smaller centre. It was more equatorward as compared to the climatology. The St Helena high was more intense, meridional and equatorward.

The seasonal average in Figure 15d) when compared to the climatological average for the season in Figure 15h) revealed that the Azores high and the St. Helena high were equatorward and the 1012 mb contours of these highs were connected. The Mascarene high was more intense with a continental component and was westward. Although the Siberian high had similar orientation, it was more intense and eastward.

Figure 16 gives a comparison between the MSLP of the very wet MAM 2018 season and the climatological evidence. Comparing Figures 16a) and 16e) reveals that although the Azores high exhibited a similar intensity in March 2018, it was smaller. This can be attributed to the low pressure cells north of the Azores high, explaining why the 1012 mb isobar extended equatorward of the high. The St. Helena high was less intense, westward and equatorward with the 1012 mb isobar connecting with that of the Azores high. The Mascarene high was more intense and eastward whereas the Siberian high was less intense and eastward.

In April 2018, the Azores high was more intense and equatorward. The St. Helena high was less intense, zonal and westward. The 1012 mb contours of these two highs connected. The Mascarene high exhibited similar position and intensity as the climatology. The Siberian high was westward as compared to the climatology in Figure 16f).

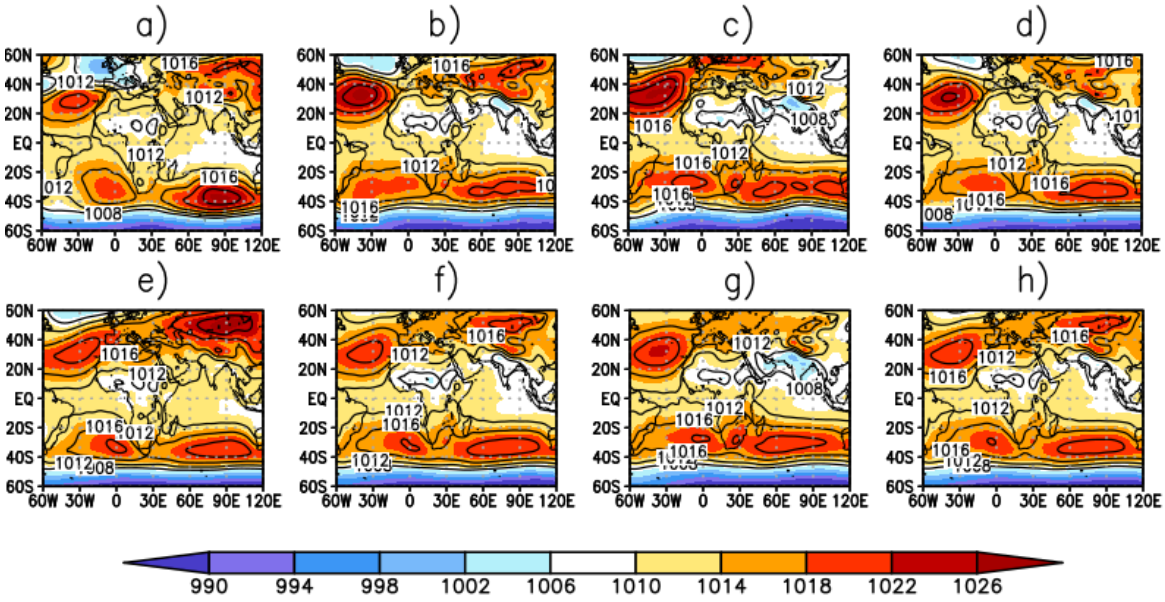

Figure 16: MSLP (in mb) of MAM 2018 (top) compared with climatology (bottom). a) represents March 2018, b) represents April 2018, c) represents May 2018 and d) represents the seasonal composite obtained by averaging pressure between March and May 2018. e) represents March climatology, f) represents April climatology, g) represents May climatology and h) represents seasonal composite obtained by averaging climatological pressure between March and May.

In May, the Azores high was more intense and equatorward. The St Helena high was equatorward as compared to the climatology and was westward. Although the St. Helena high exhibited similar intensity and zonal orientation, its centre was larger in 2018, and had continental component, unlike the climatological evidence in Figure 16g). The Mascarene high appeared similar to the climatology and the Siberian high was nearly dissipated.

Comparison of the seasonal composite in Figures 16d) and 16h) showed that the Azores high was more intense and equatorward. Its 1012 mb contour connected with that of the zonal, less intense, equatorward and westward St. Helena high. The Siberian high was less intense while the Mascarene high was quite similar to the climatology.

Figure 17 shows the MSLP of MAM 1981 compared to the climatological MSLP pattern. In March, the Azores high in Figure 17a) was less intense as compared to the climatology in Figure 17e), as influenced by the low pressure cell north of the high. Unlike in Figures 15a) and 16a), the 1012 mb contour maintained a similar position. The St. Helena high was equatorward and although it had similar intensity, it had a larger centre and its 1012 mb contour was equatorward. The Mascarene high was more intense and eastward. Notably, there was a smaller trough in the

Mozambique Channel as compared to the climatology. Finally, the Siberian high which had similar intensity to the climatology in Figure 17e) was eastward.

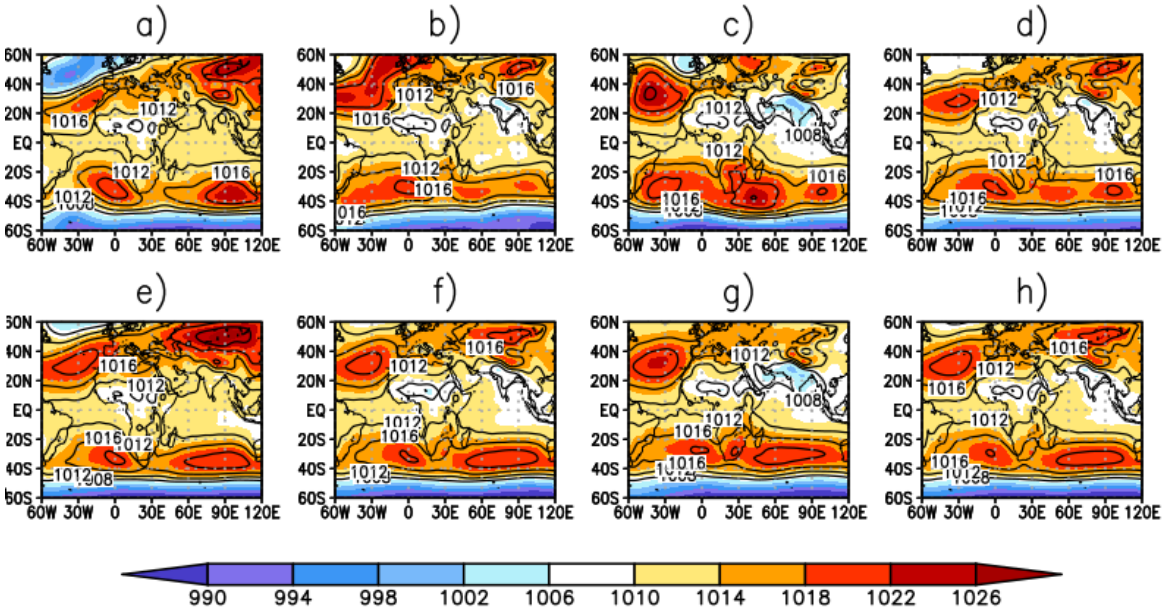

Figure 17: MSLP (in mb) of MAM 1981 (top) compared with climatology (bottom). a) represents March 1981, b) represents April 1981, c) represents May 1981 and d) represents the seasonal composite obtained by averaging pressure between March and May 1981. e) represents March climatology, f) represents April climatology, g) represents May climatology and h) represents seasonal composite obtained by averaging climatological pressure between March and May.

In April, the Azores high was more intense, eastward and meridional. The St. Helena was equatorward and zonal, with an equatorward 1012 mb isobar. The Mascarene high was less intense in Figure 17b) as compared to its climatology in Figure 17f). Although the Siberian high had similar intensity, it was smaller.

Comparing May 1981 in Figure 17c) with the climatology in Figure 17g), the Azores high was more intense but bore similar position, including that of the 1012 mb isobar. The St. Helena high was equatorward and further westward with the 1012 mb isobar further north of the equator. The Mascarene high was more intense and westward and its continental component extended further north. The Siberian high was very weak and almost dissipated.

Drawing comparison from the seasonal composites in Figures 17d) and 17h) revealed that the Azores high was quite similar to the climatology, the St. Helena high was more equatorward with an equatorward 1012 mb contour. The Mascarene and the Siberian highs were eastward.

Figure 18 exhibits the MSLP pattern in MAM 1986 compared with the MAM climatology. In March 1986, the Azores high was more intense and equatorward with an equatorward 1012 mb isobar. The St. Helena high in Figure 18a) was quite similar to the climatology in Figure 18e) but was more zonal. The Mascarene high was westward and more intense and there was no trough in the Mozambique Channel. The Siberian high was larger, more intense and was displaced westward.

In April, the Azores high was more intense as compared to climatology in Figure 18f). The St. Helena was less intense and westward. The Mascarene high was more intense. The Siberian high in Figure 18b) was more intense and westward compared to its climatology.

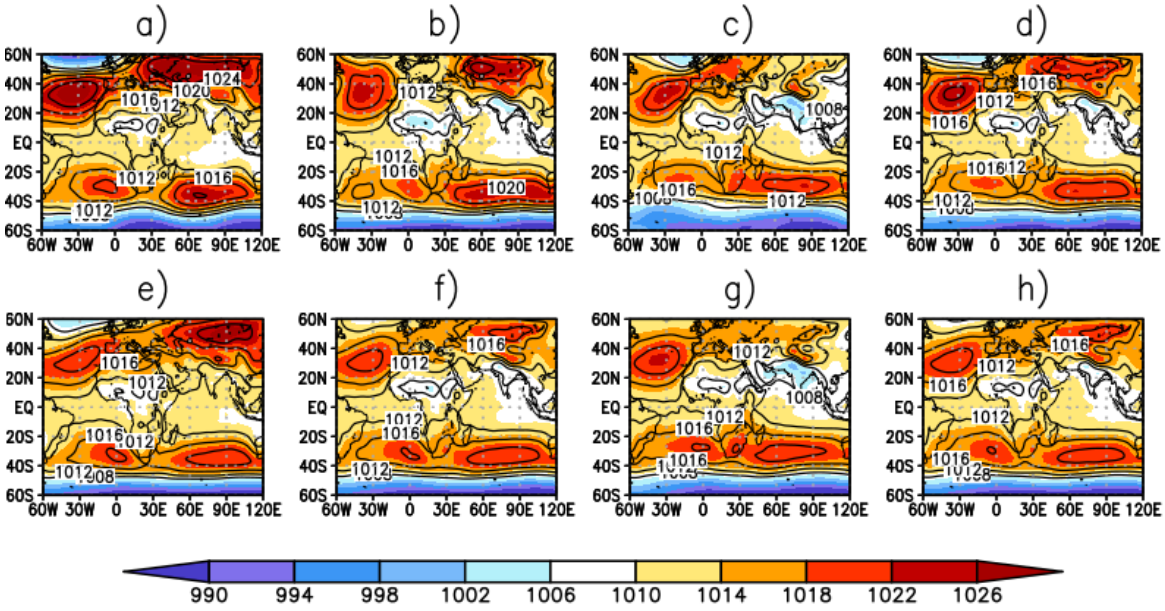

Figure 18: MSLP (in mb) of MAM 1986 (top) compared with climatology (bottom). a) represents March 1986, b) represents April 1986, c) represents May 1986 and d) represents the seasonal composite obtained by averaging pressure between March and May 1986. e) represents March climatology, f) represents April climatology, g) represents May climatology and h) represents seasonal composite obtained by averaging climatological pressure between March and May.

In May as in Figure 18c), the Azores high was meridional as compared to its climatology in Figure 18g) and was eastward. The St. Helena high was less intense and westward. The Mascarene high was more intense and the Siberian high dissipated.

Comparing the seasonal composites in Figures 18d) and 18h) revealed that on average, the Azores high was more intense than its climatology. The St. Helena in comparison to the climatology was

zonal, westward and had an equatorward 1012 mb isobar. The Mascarene high was slightly more intense. The Siberian high was more intense and westward compared to its climatology.

4.4.1.2 Comparing the Dry Years with Climatology for the MAM Season

Figure 19 shows the MSLP during MAM 2000 as compared to climatological MSLP for the MAM season. In March 2000, the Azores high was more intense, poleward and eastward, north of Africa. The St. Helena was more intense, poleward and although meridional, its orientation was Northeast to Southwest. The Mascarene high was more intense and westward. There was a deeper trough in the Mozambique Channel as evidenced by the 1012 mb isobar. The Siberian high maintained similarity with the climatology in Figure 19e).

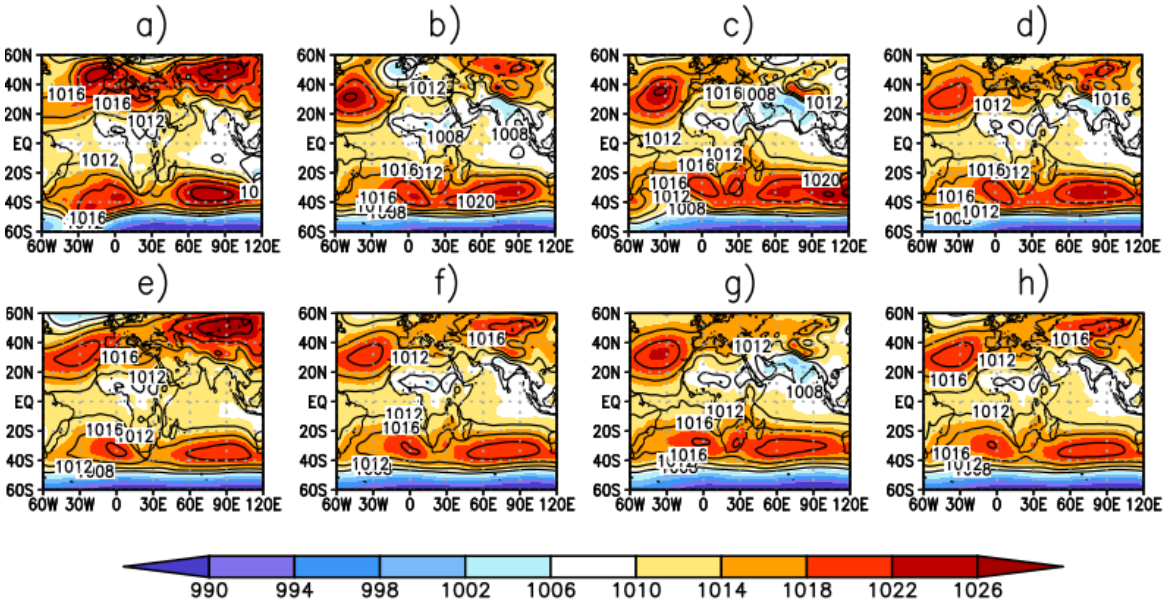

Figure 19: MSLP (in mb) of MAM 2000 (top) compared with climatology (bottom). a) represents March 2000, b) represents April 2000, c) represents May 2000 and d) represents the seasonal composite obtained by averaging pressure between March and May 2000. e) represents March climatology, f) represents April climatology, g) represents May climatology and h) represents seasonal composite obtained by averaging climatological pressure between March and May.

April 2000 in Figure 19b) when compared to the climatology in Figure 19f) revealed that the Azores high was more intense. The St. Helena was more intense, poleward and eastward. The Mascarene high was more intense, westward and had a continental component. Just like in March, the Siberian high was similar to its climatology.

In May, the Azores high was more intense. The St. Helena was eastward, meridional and was connected with the more intense (than the climatological evidence) Mascarene high. The Siberian high was almost dissipated in Figure 19c).

The seasonal composite in Figure 19d) when compared to the climatology in Figure 19h) showed that the Azores high was similar to the climatology, the St. Helena high was poleward and eastward. The Mascarene high was more intense and connected to the St. Helena high pressure system. The Siberian high was shrunken in comparison to the climatology.

Figure 20 displays a comparison between the MSLP during MAM 2004 and MAM climatology. Figure 20a) shows a more intense Azores high as compared to the climatology in Figure 20e) that was poleward and connected to the westward Siberian high which had a similar intensity to the climatology. The Mascarene high was more intense and had a significantly deep trough in the Mozambique Channel evidenced by the 1012 mb isobar.

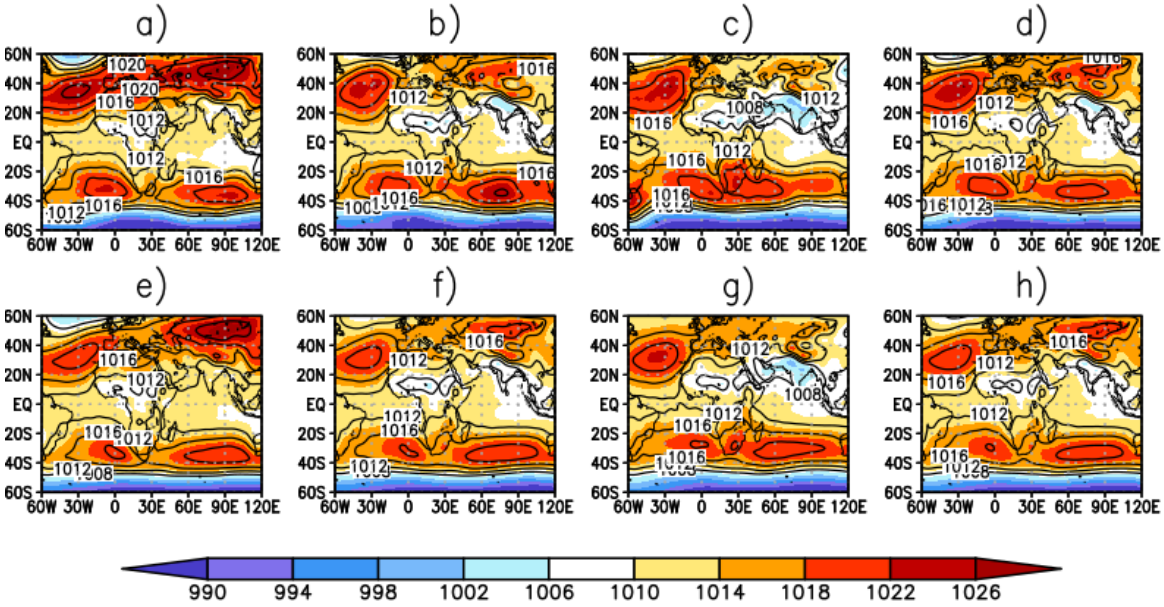

Figure 20: MSLP (in mb) of MAM 2004 (top) compared with climatology (bottom). a) represents March 2004, b) represents April 2004, c) represents May 2004 and d) represents the seasonal composite obtained by averaging pressure between March and May 2004. e) represents March climatology, f) represents April climatology, g) represents May climatology and h) represents seasonal composite obtained by averaging climatological pressure between March and May.

April 2004 in Figure 20b) as compared to climatology in Figure 20f) showed a more intense and poleward Azores high. The St. Helena high was zonal and although had similar intensity to the

climatology, it had a larger centre. The Mascarene high was westward, more intense and had a continental component. The Siberian high had dissipated.

In May, although the Azores high in Figure 20c) had a similar intensity to the climatology in Figure 20g), it was poleward. The St. Helena high was more intense, meridional and eastward. Further, the St. Helena high was connected to the Mascarene high which was westward, more intense and had an extensive and northward continental component.

Drawing comparison between the seasonal composite of MAM 2004 in Figure 20d) and that of the MAM climatology in Figure 20h) revealed that the Azores high was more intense and eastward. The St. Helena high was eastward. The Mascarene high had a continental component and the Siberian high appeared similar to the climatology.

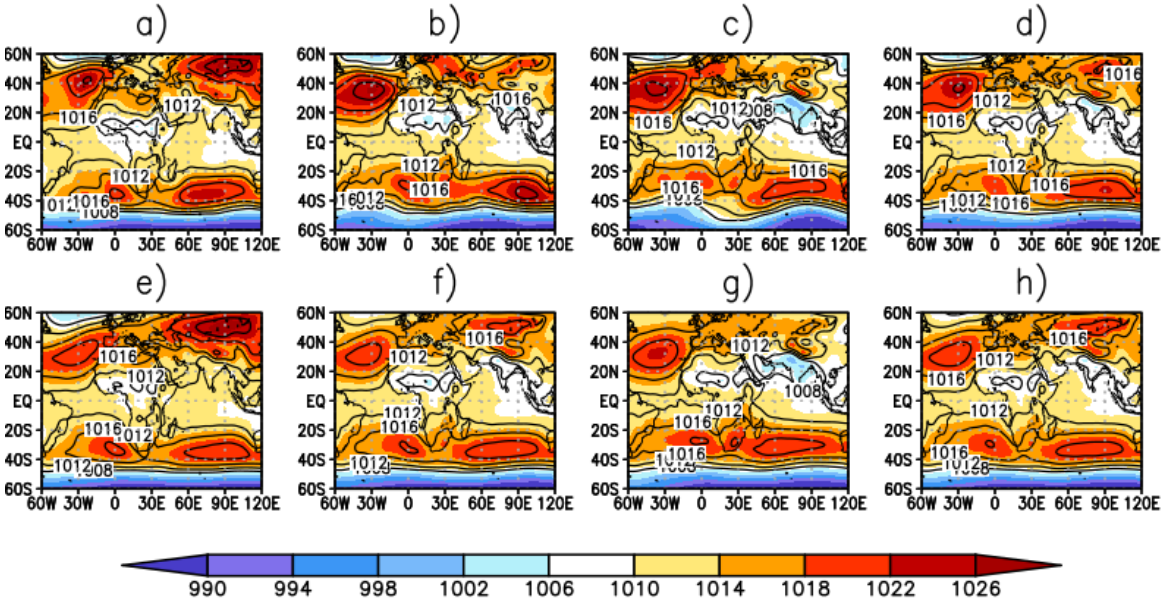

Figure 21: MSLP (in mb) of MAM 2009 (top) compared with climatology (bottom). a) represents March 2009, b) represents April 2009, c) represents May 2009 and d) represents the seasonal composite obtained by averaging pressure between March and May 2009. e) represents March climatology, f) represents April climatology, g) represents May climatology and h) represents seasonal composite obtained by averaging climatological pressure between March and May.

Figure 21 displays comparison between the MSLP during MAM 2009 and climatology of MAM. From Figure 21a) compared with Figure 21e), it is noted that in March 2009, the Azores high was poleward and more intense. Similarly, the St. Helena high was poleward. Therefore, the 1012 mb isobars were further from the equator. The Mascarene high was more intense and eastward and

there was a broad trough in the Mozambique Channel exhibited by the 1012 mb isobar. The Siberian high was eastward.

In April, the Azores high was more intense and equatorward with an equatorward 1012 mb isobar. The St. Helena high was eastward and poleward. The Mascarene high was more intense, eastward and had a continental component. The Siberian high was less intense and extended westward.

In May, the Azores high was more intense, poleward and had an eastward component as observed in Figure 21c) as compared to Figure 21g). The St. Helena was less intense and the 1012 mb isobar doesn't extend towards the equator. The Mascarene high had a similar intensity and the Siberian high had dissipated.

Comparison of the seasonal composite in Figures 21d) and 21h) showed that the Azores high was more intense and poleward. The St. Helena high was less intense and meridional. The Mascarene high was more intense and eastward. The Siberian high was shrunken as compared to the climatology.

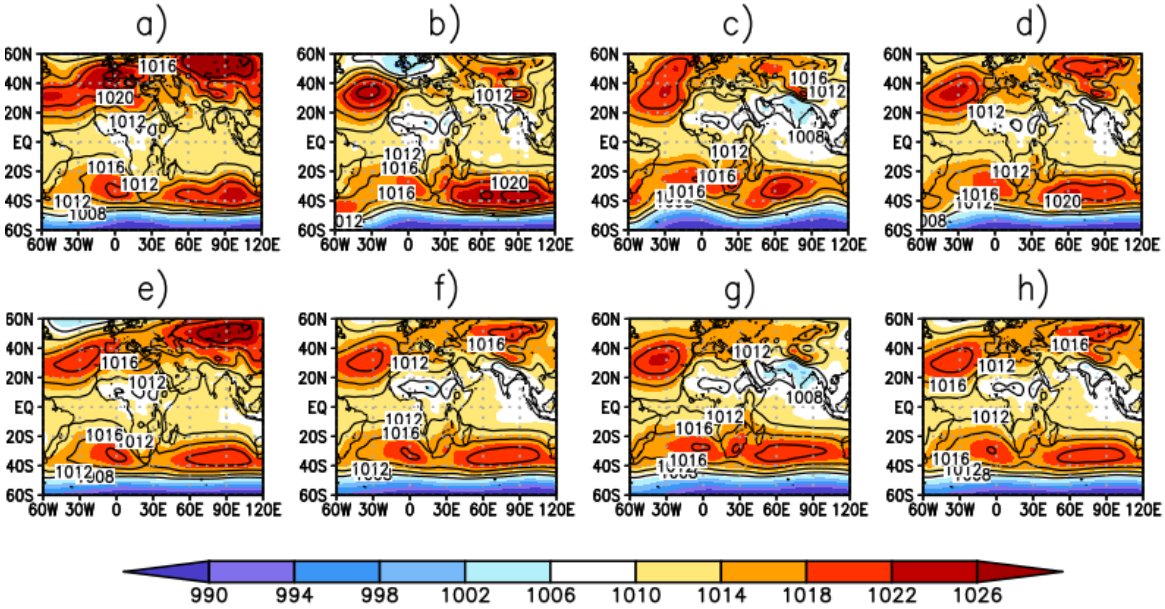

Figure 22: MSLP (in mb) of MAM 1998 (top) compared with climatology (bottom). a) represents March 1998, b) represents April 1998, c) represents May 1998 and d) represents the seasonal composite obtained by averaging pressure between March and May 1998. e) represents March climatology, f) represents April climatology, g) represents May climatology and h) represents seasonal composite obtained by averaging climatological pressure between March and May.

Figure 22 exhibits comparison of the MSLP for MAM 1998 with the MAM climatology. From Figure 22a) compared with Figure 22e), the Azores high was poleward and eastward. The St. Helena high was poleward. The Mascarene high was more intense. The Siberian high, although with similar intensity as the climatology, it had a larger centre and was westward.

In April 1998, the Azores high was poleward as compared to the climatology in Figure 22f). The St. Helena high was less intense. The Mascarene high was more intense, westward with a continental component. The Siberian high was shrunken.

In May, the Azores high was more intense, poleward and meridional. The St. Helena high was equatorward. The Mascarene high was more intense and meridional. The Siberian high was similar to the climatology.

The comparison of seasonal composites in Figures 22d) and 22h) revealed that the Azores high was more intense, poleward and eastward. The St. Helena was less intense. The Mascarene high was more intense and westward. The Siberian high was quite similar to the climatological average.

Given the results obtained and discussed in Section 4.3.1, some similarities were observed for the years with extremely high rainfall and for those with extremely low rainfall. They include:

The equatorward displacement of the Azores and St. Helena highs were associated with years with extremely high rainfall. This influenced equatorward 1012 mb isobars, and in some cases, the 1012 mb isobars were connected. The result would be effective pressure gradient force (PGF) from the Atlantic Ocean into the African continent. In the case of March 2020 in Figure 15a) where the Azores high was poleward, the 1012 mb isobar was still equatorward causing the extremely high rainfall observed. On the other hand, the poleward and eastward Azores high as well as the poleward St. Helena high were associated with the dry years. As such, the extent of the 1012 mb isobars were further from the equator. The PGF towards the African continent was not as effective as was in the years with extremely high MAM rainfall.

During March of the dry years, there was a trough in the Mozambique Channel, evident by the 1012 mb isobar due to the Mascarene high. According to Barimalala *et al.* (2020), this trough causes high negative precipitation anomalies over LVB and northern Tanzania, which was evident in Figures 7e), 8e),9e) and 10e). However, during the wet years, there was no trough in the Mozambique Channel, except for the 2020 case. Barimalala *et al.* (2020) noted that this trough

occurs when the Mascarene high is further eastwards in the Indian Ocean. However, from the observation of the dry years, two cases had an eastward Mascarene high and two cases had a westward Mascarene high. Nevertheless, the presence or absence of a trough in the Mozambique channel may offer good contribution to the outlook of rainfall for the other months of the MAM season.

In April of the wet years, St. Helena high was more zonal while in dry years, it maintained its orientation as the climatology or was meridional. For the dry years, the Mascarene high had significant continental component in April. This was contributed to by its higher intensity and westward migration observed in all dry years except 2009 when the Mascarene high was eastward, yet with a significant continental component.

For the MAM season, Siberian high is significant in March when it was intense and its 1012 mb isobar stretched equatorward. During the other months, the Siberian high shrunk and in some cases dissipated.

4.4.2 Comparing the Years of Extreme Rainfall with Climatology of OND Season

Comparing individual years with extreme rainfall during the short rainy season and the OND climatology allowed the observation of changes from the mean patterns of the anticyclones, alluding to the extreme conditions that occurred.

4.4.2.1 Comparing the Wet Years with Climatology for the OND Season

Figure 23 shows the comparison between the OND climatological pressure pattern and the MSLP of OND 1997. In October 1997, The Azores high in Figure 23a) was very weak as compared to the climatology in Figure 23e). The St. Helena high, although with similar intensity had a shrunken centre. The Mascarene high was more intense with its centre further east. The Siberian high had similar intensity but was smaller than the climatology and further to the east.

In November 1997 in Figure 23b) compared to the November climatology in Figure 23f) revealed that although The Azores high had similar position and intensity, it had a smaller centre. The St. Helena high was less intense and equatorward and its 1012 mb isobar reached the equator. The Mascarene high had the same intensity but had retracted further east. Although The Siberian high had similar intensity, it was still eastward as compared to the climatology.

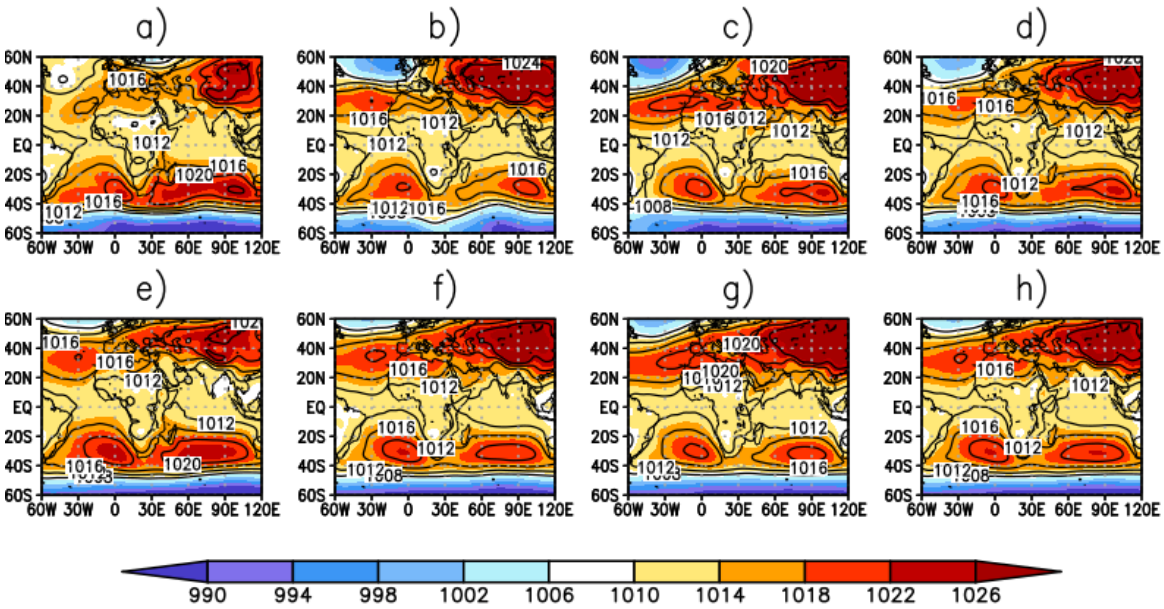

Figure 23: MSLP (in mb) of OND 1997 (top) compared with climatology (bottom). a) represents October 1997, b) represents November 1997, c) represents December 1997 and d) represents the seasonal composite obtained by averaging pressure between October and December 1997. e) represents October climatology, f) represents November climatology, g) represents December climatology and h) represents seasonal composite obtained by averaging climatological pressure for OND season.

The seasonal composite in Figure 23d) upon comparison with the climatological average in Figure 23h) showed that The Azores high was less intense. The St. Helena high was less intense and had similar position to the climatology yet its 1012 mb isobar extended north of the equator. The Mascarene and the Siberian highs were eastward.

Figure 24 displays the comparison of the MSLP for OND 2019 with that of OND climatology. In October 2019 in Figure 24a) in comparison to the October climatology in Figure 24e) revealed that the Azores high was less intense. The St. Helena high was less intense. The Mascarene high had the same intensity but was eastward. The Siberian high was eastward.

November 2019 in Figure 24b) when compared to the climatology in Figure 24f) showed that the Azores high was more intense. The St. Helena high was less intense. The Mascarene high was more intense and further east. The Siberian high was the same intensity but larger.

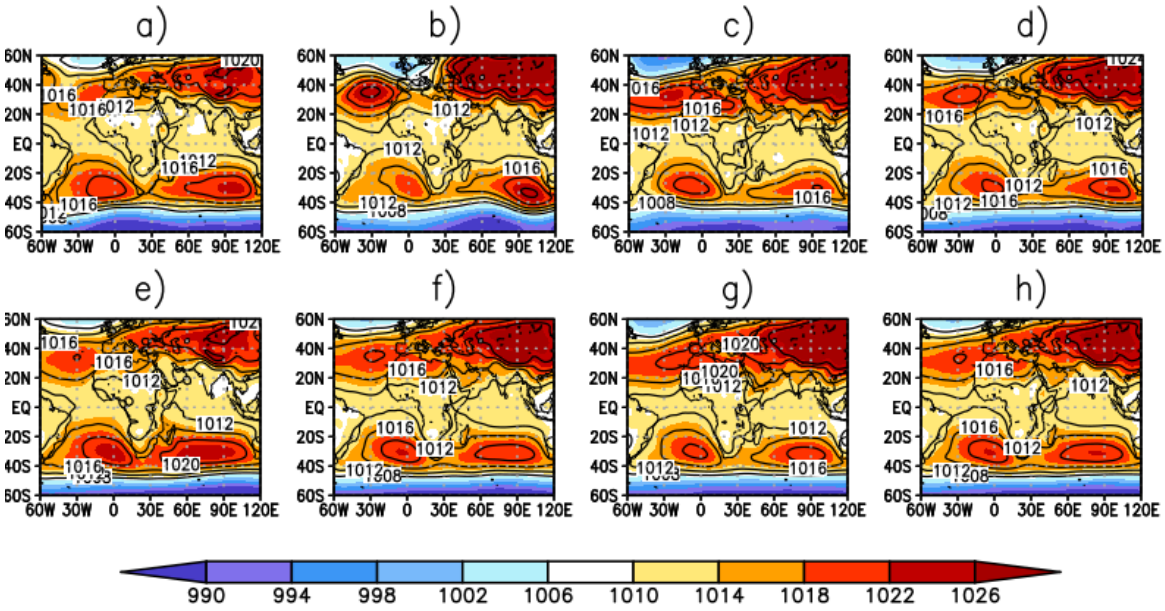

Figure 24: MSLP (in mb) of OND 2019 (top) compared with climatology (bottom). a) represents October 2019, b) represents November 2019, c) represents December 2019 and d) represents the seasonal composite obtained by averaging pressure between October and December 2019. e) represents October climatology, f) represents November climatology, g) represents December climatology and h) represents seasonal composite obtained by averaging climatological pressure for OND season.

In December 2019, the Azores high was more intense and poleward. The St. Helena high was more zonal. However, the connection of the 1012 mb isobar could be attributed to the intense Azores high. The Mascarene and the Siberian highs were eastward.

Given the above, the seasonal composite comparison from Figures 24d) and 24h) showed that on average, the Azores high had similar intensity but with a larger centre. The St. Helena high was less intense. The Mascarene high and the Siberian high were eastward.

Figure 25 shows the comparison between the OND climatological distribution of pressure and the MSLP during OND 2006.Comparing October 2006 in Figure 25a) to the climatology in Figure 25e) displays that the Azores high was less intense and westward, yet it was equatorward with its 1012 mb isobar extending towards the equator. The St. Helena high was more intense than the climatology and its 1012 mb isobar reached the equator. The Mascarene high was more intense as compared to the climatology with a similar position. The Siberian high was less intense and eastward.

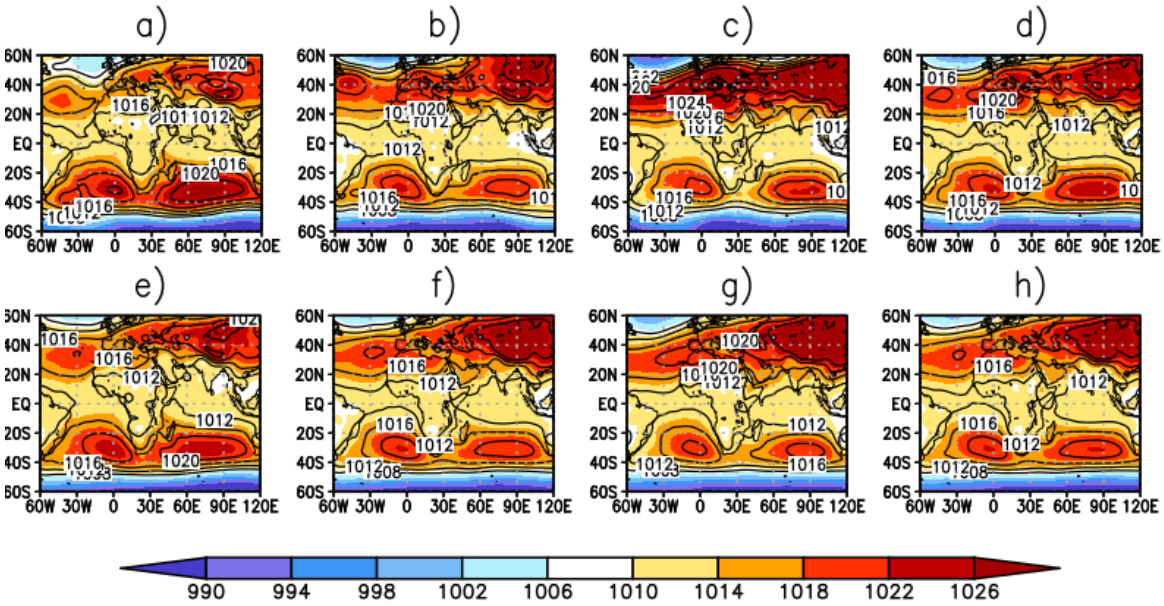

Figure 25: MSLP (in mb) of OND 2006 (top) compared with climatology (bottom). a) represents October 2006, b) represents November 2006, c) represents December 2006 and d) represents the seasonal composite obtained by averaging pressure between October and December 2006. e) represents October climatology, f) represents November climatology, g) represents December climatology and h) represents seasonal composite obtained by averaging climatological pressure for OND season.

In November 2006, the Azores high was more intense, poleward and westward. The St. Helena was quite similar to the climatology, with a larger centre, yet its 1012 mb isobar did not extend as further north as the climatology. The Mascarene high was similar in intensity to the climatology but eastward. The Siberian high was similar in intensity to the climatology with an eastward centre, yet it still connected to the Azores high.

In December, just like in November, the Azores high which was more intense connected to the equally intense Siberian high. The St. Helena high maintained a similar intensity and position as the climatology but its 1012 mb isobar was connected with that of the Azores high due to the very intense Azores high. The Mascarene high was more intense and eastward.

Comparison of the seasonal composite revealed that the Azores high was westward though and connected to the Siberian high. The St. Helena high was quite similar to the climatology. The Mascarene high was more intense than the climatology.

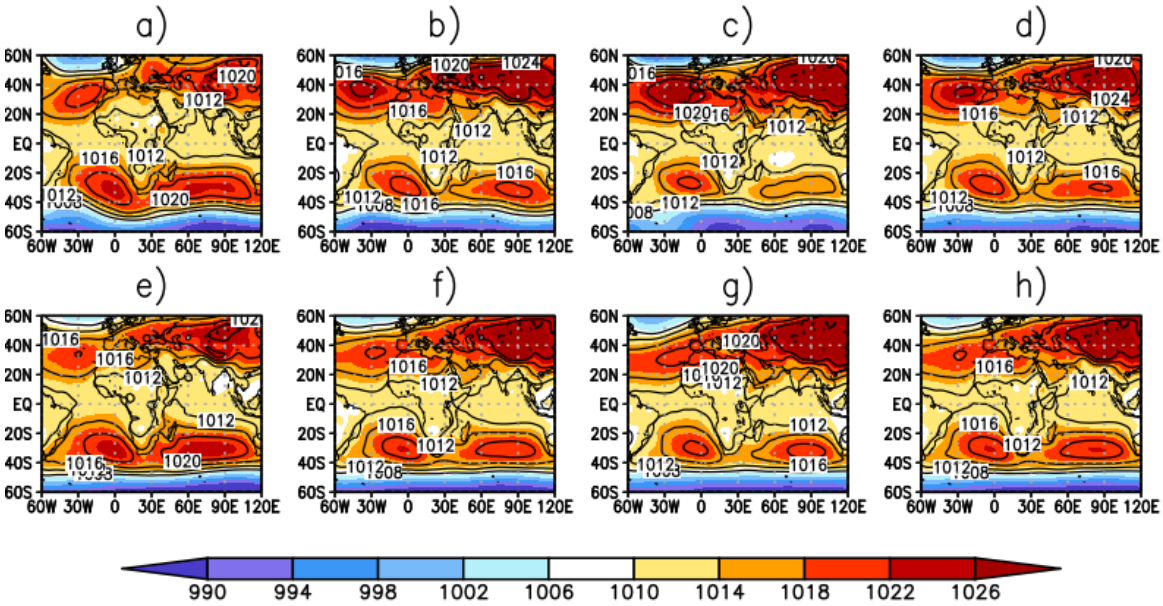

Figure 26: MSLP (in mb) of OND 1982 (top) compared with climatology (bottom). a) represents October 1982, b) represents November 1982, c) represents December 1982 and d) represents the seasonal composite obtained by averaging pressure between October and December 1982. e) represents October climatology, f) represents November climatology, g) represents December climatology and h) represents seasonal composite obtained by averaging climatological pressure for OND season.

Figure 26 draws comparison between the MSLP observed in OND 1982 and the OND climatological evidence. In October, the Azores high was westward and with a smaller centre. The St. Helena high was more meridional. The Mascarene high was quite similar to the climatology in Figure 26e) but with a slimmer centre. The Siberian high was less intense than the climatology.

In November, the Azores high became more intense and maintained a westward position in comparison to the climatology. The St. Helena high was less intense. The Mascarene high was eastward. The Siberian high with similar intensity was larger and connected to the Azores high.

In December, the Azores high was very intense. The St. Helena was equatorward. The Mascarene high was very weak and the Siberian high was similar to its climatology.

Drawing comparison of the seasonal composite of OND 1982 in Figure 26d) with the climatology in Figure 26h) revealed that the Azores high was more intense and eastward. The St. Helena high was less intense. The Mascarene high was less intense and eastward. The Siberian high was similar to its climatology.

4.4.2.2 Comparing the Dry Years with Climatology for the OND Season

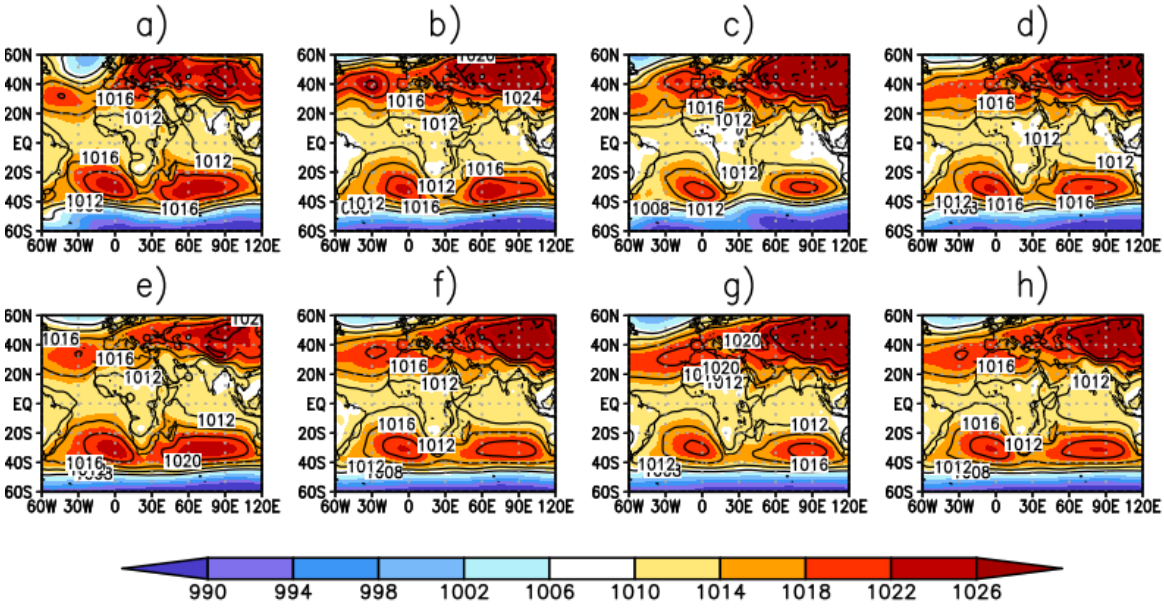

Figure 27: MSLP (in mb) of OND 2005 (top) compared with climatology (bottom). a) represents October 2005, b) represents November 2005, c) represents December 2005 and d) represents the seasonal composite obtained by averaging pressure between October and December 2005. e) represents October climatology, f) represents November climatology, g) represents December climatology and h) represents seasonal composite obtained by averaging climatological pressure for OND season.

Figure 27 shows comparison between the climatology and 2005 which was the driest year for the OND season. From Figure 27a) compared to Figure 27e), the Azores high in October was westward. The St. Helena high was similar to the climatology. The Mascarene high was similar to the climatology. The Siberian high was westward.

In November, the Azores high was more intense and poleward. The St. Helena high had similar intensity but had a larger centre. The Mascarene high was more intense and westward. The Siberian high was westward and connected with the Azores high.

In December as in Figure 27c) compared with Figure 27g), the Azores high was more intense, poleward and eastward. The St. Helena high which had similar intensity was poleward. The Mascarene high although with similar intensity was shrunken. The Siberian high was as intense as the climatology.

From the comparison of seasonal composites in Figures 27d) and 27h), the Azores high was less intense, the St. Helena high was similar intensity but was tending poleward. The Mascarene high was westward. The Siberian high westward.

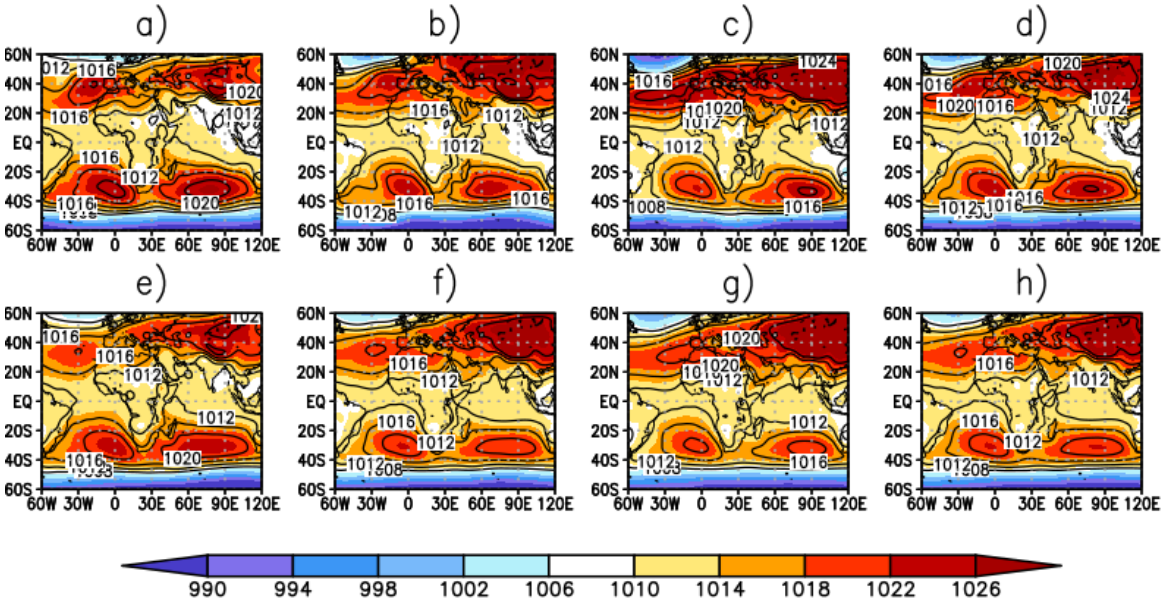

Figure 28: MSLP (in mb) of OND 1998 (top) compared with climatology (bottom). a) represents October 1998, b) represents November 1998, c) represents December 1998 and d) represents the seasonal composite obtained by averaging pressure between October and December 1998. e) represents October climatology, f) represents November climatology, g) represents December climatology and h) represents seasonal composite obtained by averaging climatological pressure for OND season.

Figure 28 draws comparison between OND 1998 which was a La Niña season and the OND climatology. Figure 28a) compared to Figure 28e) showed that in October, the Azores high was more intense, eastward and poleward. The St. Helena high was more intense, tending poleward. The Mascarene high was more intense and westward. The Siberian high was shrunken.

In November, the Azores high was more intense, poleward and eastward, connecting with the intense and westward Siberian high. The St. Helena high was more intense and poleward. The Mascarene high was more intense and westward.

The comparison of December 1998 in Figure 28c) with the climatology in Figure 28g) exhibited the Azores high as more intense and connected to the equally intense Siberian high. The St. Helena high was more intense and poleward. The Mascarene high was more intense and eastward.

The seasonal composite comparison revealed that the Azores high was more intense, poleward and eastward and was connected to the Siberian high. The St. Helena high was more intense and poleward. The Mascarene high was more intense and westward.

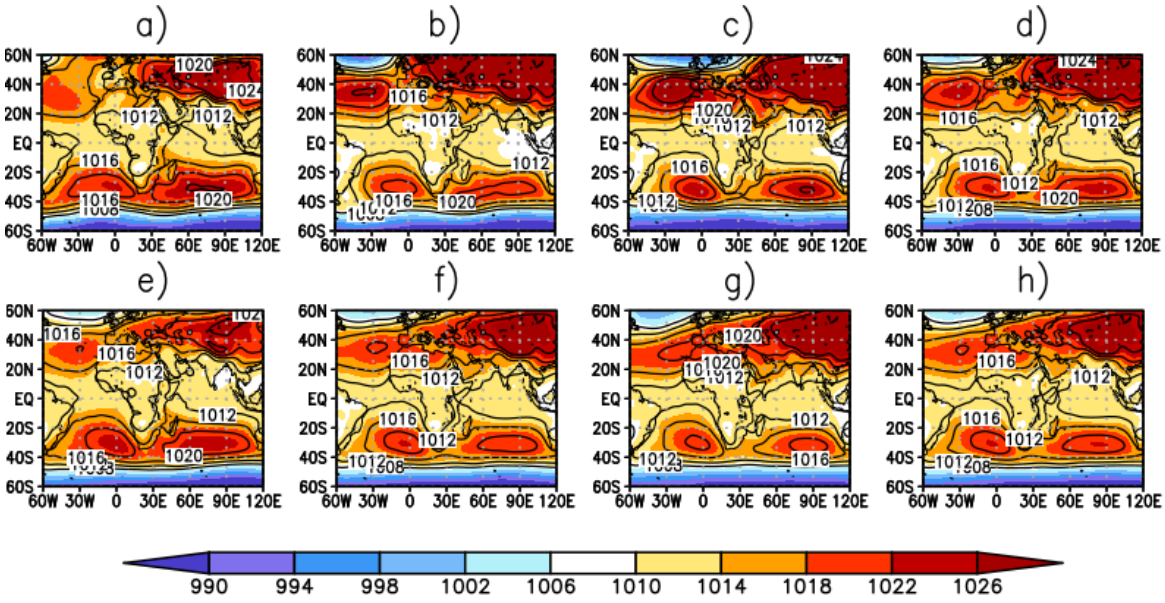

Figure 29: MSLP (in mb) of OND 1993 (top) compared with climatology (bottom). a) represents October 1993, b) represents November 1993, c) represents December 1993 and d) represents the seasonal composite obtained by averaging pressure between October and December 1993. e) represents October climatology, f) represents November climatology, g) represents December climatology and h) represents seasonal composite obtained by averaging climatological pressure for OND season.

Figure 29 displays MSLP for individual months and seasonal average of OND 1993 and the climatology which was utilized for comparison to determine changes in the anticyclones in 1993 that led to extremely low rainfall. In October as in Figure 29a) compared to Figure 29e), the Azores high was westward, equatorward and less intense. The St. Helena high was zonal with a smaller centre. The Mascarene high was more intense and westward. The Siberian high was similarly intense (to the climatology) and westward.

In November, the Azores high was more intense and westward. The St. Helena high was less intense and zonal. The Mascarene and the Siberian highs were westward as in Figure 29b).

In December, the Azores high and the St. Helena high were more intense as compared to their climatology in Figure 29g). The Mascarene high was more intense and westward. The Siberian high was as intense as its climatology and was connected to the Azores high.

Comparison of the seasonal composites in Figures 29d) and 29h) showed that the Azores high was more intense. The St. Helena high was similar to the climatology. The Mascarene high was more intense and westward. The Siberian high was westward.

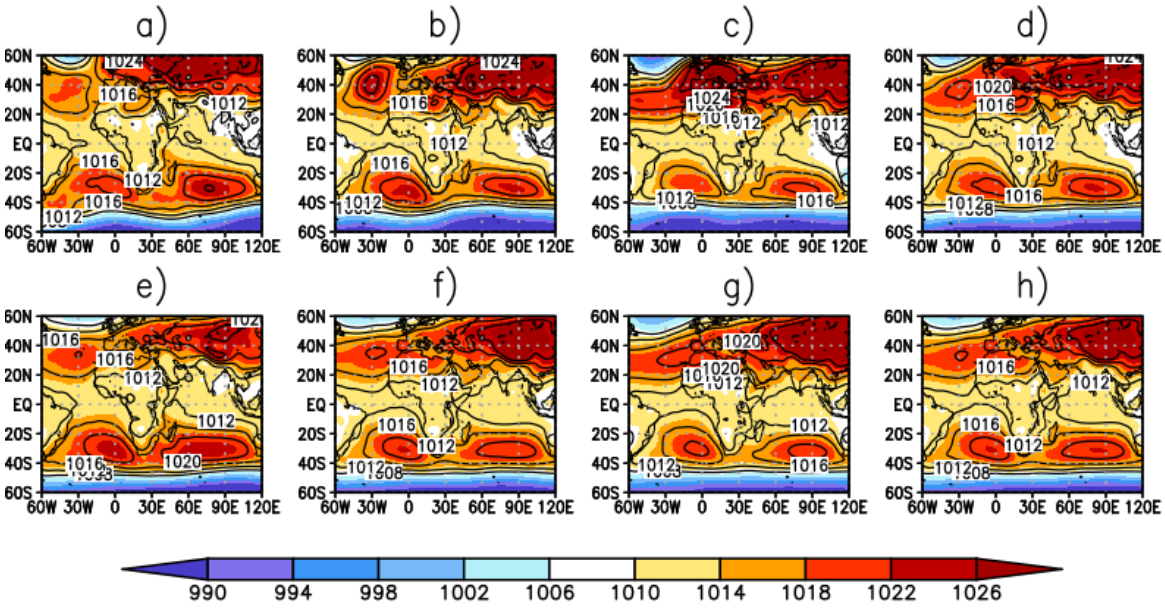

Figure 30: MSLP (in mb) of OND 2016 (top) compared with climatology (bottom). a) represents October 2016, b) represents November 2016, c) represents December 2016 and d) represents the seasonal composite obtained by averaging pressure between October and December 2016. e) represents October climatology, f) represents November climatology, g) represents December climatology and h) represents seasonal composite obtained by averaging climatological pressure for OND season.

Figure 30 displays the comparison between the OND climatological pressure pattern and the MSLP for OND 2016. In October, the Azores high was less intense as compared to the climatology in Figure 30e) and was meridional compared to the zonal orientation in the climatology. The St. Helena high was less intense. The Mascarene high was more intense and eastward. The Siberian high was larger and westward.

In November, the Azores high was more intense, poleward and meridional. The St. Helena high was poleward and more intense. The Mascarene high was more intense. The Siberian high was westward.

In December, the Azores high was more intense, eastward and poleward, connected to the Siberian high. The St. Helena high was less intense and zonal. The Mascarene high was quite similar to the climatology as in Figures 30c) and 30g).

Comparing the seasonal composites in Figures 30d) and 30h) displayed that the Azores high was poleward and connected to the westward Siberian high. The St. Helena high was less intense and poleward. The centre of the Mascarene high was westward.

Comparing the results of the extreme OND rainfall years with the climatology in Section 4.3.2 yielded some similarities for the extremely high rainfall years and for the extremely low rainfall years. These include:

The Mascarene high was eastward during the wet years, consistent with findings by Ongoma *et al.* (2015) and was westward during the dry years. The Siberian high was eastward during the wet years and westward during the dry years. The Azores high was poleward during the dry years. This would lessen its influence on PGF effective into the Africa continent and the East Africa region.
The St Helena was less intense during the wet years and more intense during the dry years. Colberg *et al.* (2004) noted that during El Niño years (which are most of the wet years), the St. Helena high was weaker and more intense during La Niña years, represented by most of the dry years discussed.
The St. Helena high was equatorward during the wet years, consistent with findings by Sun *et al.* (2017) that stipulated an equatorward St. Helena high was observed during El Niño.
A notable observation was that during the dry years in Figures 27 to 30, the Angola low was established in October and was vast in November. The Angola low as stated by Xulu *et al.* (2020) which is a dominant feature during the dry years is usually weaker during El Niño, explaining why it was not observable during most of the wet years.

4.5 Moisture Characteristics of the Wet and Dry Cases

The moisture characteristics in this section were determined by assessing the divergent moisture transport.

4.5.1 MAM Season

Figure 31 shows the divergent moisture transport vectors superposed on MSLP for wet case of MAM 2020 and dry case of MAM 2000. From Figure 31a) there was effective entry of northeasterlies especially at the Kenyan coast, from the north Indian Ocean, emanating from the ridging of the 1012mb contour. Similarly, southeasterlies entered the region.

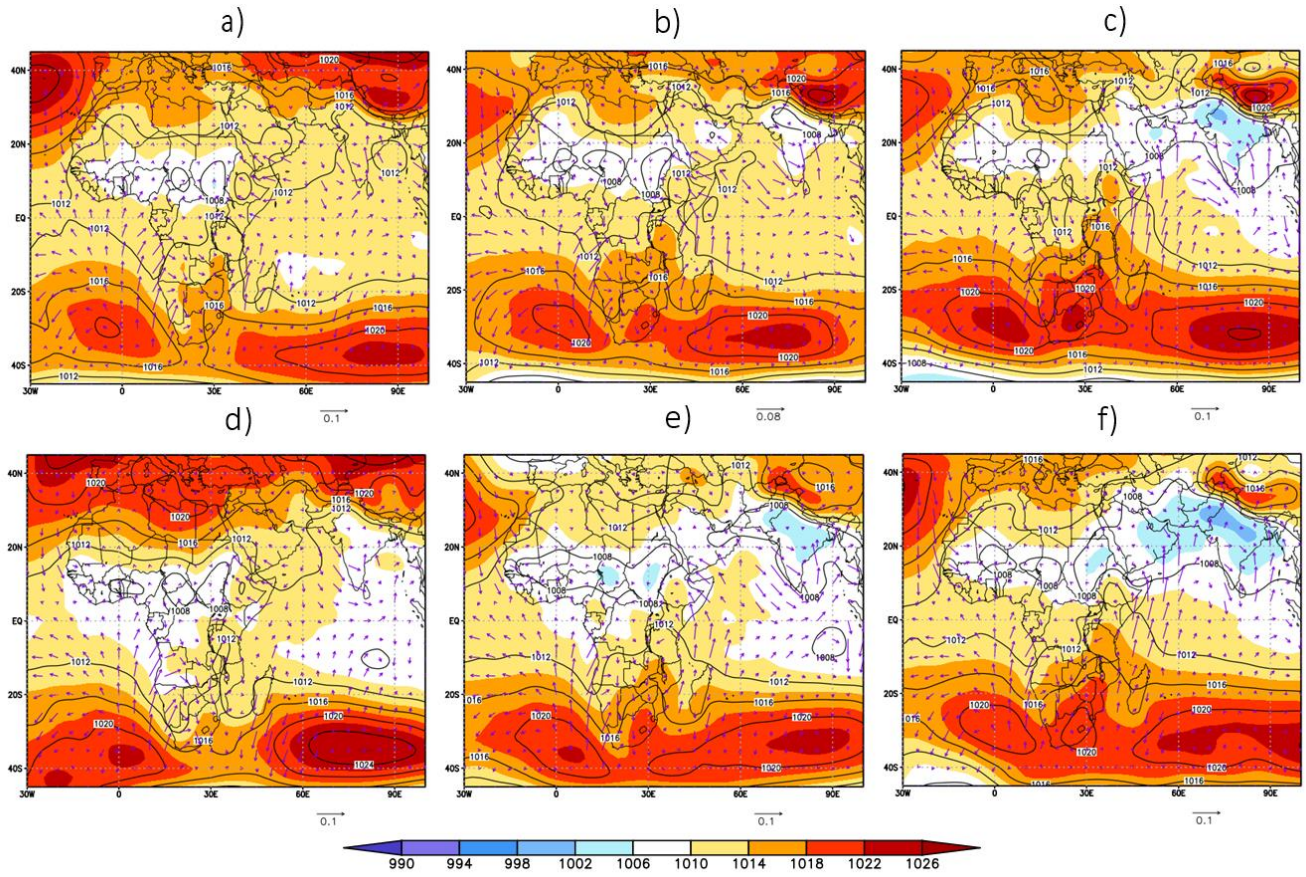

Figure 31: Divergent moisture flux superposed on MSLP (in mb) for 2020 (top) with extremely high rainfall and 2000 (bottom) which had the lowest rainfall during the MAM season, where a) is March 2020, b) is April 2020 and c) is May 2020. d), e) and f) represent March 2000, April 2000 and May 2000 respectively.

In Figure 31a), there was convergence between westerlies and easterlies in the western part of the region, especially in Uganda and the LVB, explaining the observed positive anomalies in March 2020 as shown in Figure 7a). The westerlies were a consequence of recurving of southerlies due to the St. Helena high. In Figure 31d) representing March 2000, although northeasterlies effectively reached the region, there was no influx of moist southeasterlies into the region. This can be attributed to the trough observed in the Mozambique Channel. The easterlies (both from the north and the south) veered further east in the Indian Ocean depriving the region of moisture. Divergence was observed in most parts of the region, an attribution to concentrated negative anomalies in Tanzania in Figure 7e). However, some convergence was observed over the LVB.

In April as in Figures 31b) and 31e), there was southeasterly flow of moisture into the region due to the Mascarene high, which converged with westerlies for the 2020 case. In April 2000, although

there was entry of some southeasterlies, there was no convergence with the westerlies. In fact, divergence was observed in parts of the region. The fewer westerlies reaching the region may be attributed to the recurving of westerlies into northerlies, west of the East African region.

In May when rainfall should be ceasing, the moisture fluxes were faster owing to the increased intensity of the southern hemisphere high pressure cells. However, there was observed divergence in Figure 31f) leading to dry conditions in May 2000.

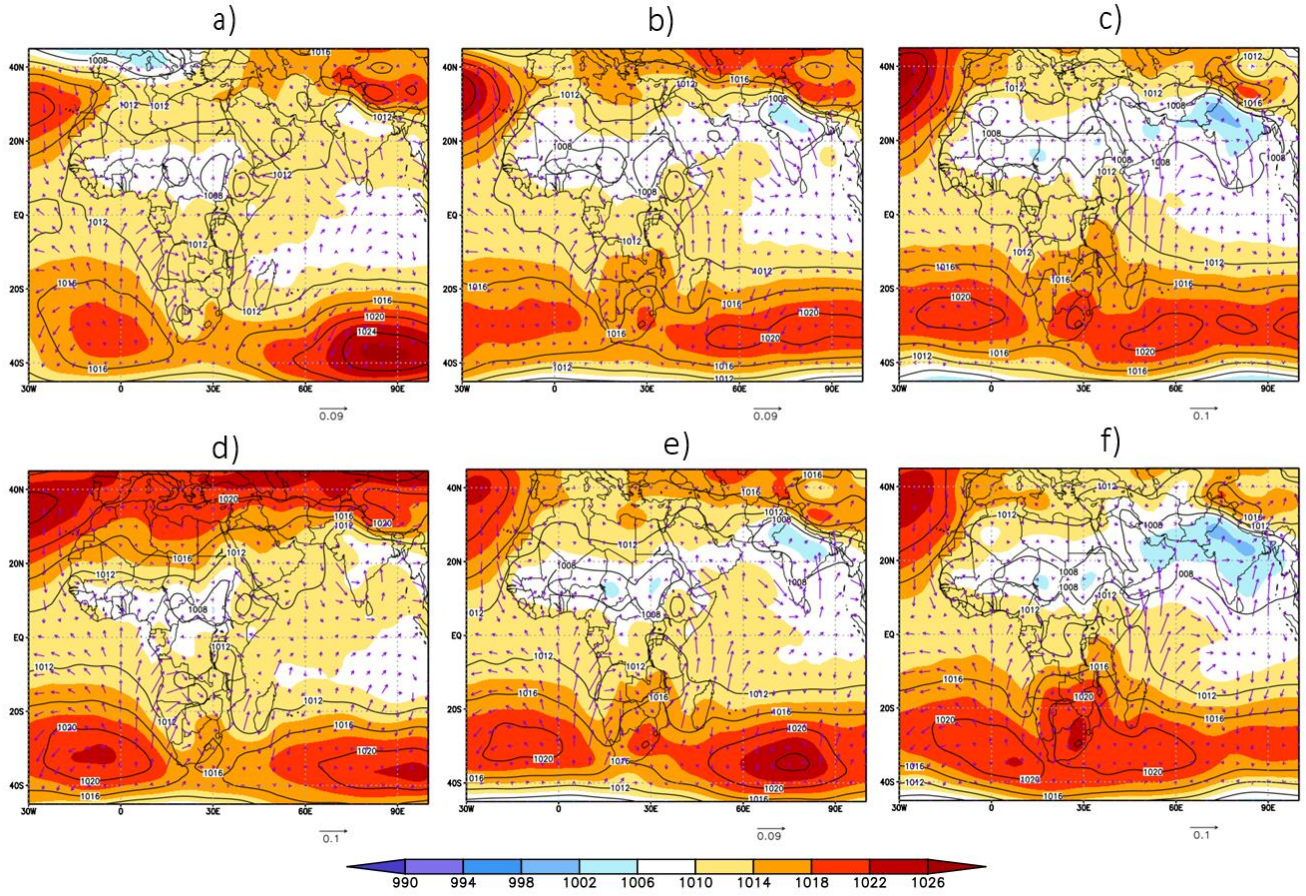

Figure 32: Divergent moisture flux superposed on MSLP (in mb) for 2018 (top) with extremely high rainfall and 2004 (bottom) which had extremely low rainfall during the MAM season, where a) is March 2018, b) is April 2018 and c) is May 2018. d), e) and f) represent March 2004, April 2004 and May 2004 respectively.

Figure 32 depicts divergent moisture transport vectors superposed on MSLP for cases 2018 (wet) and 2004 (dry). From Figures 32a) and 32d) it was observed that March 2018 was extremely wet as in Figure 8a) due to convergence of northeasterlies from the 1012 mb isobar of the Siberian

high and southeasterlies due to the Mascarene high at the coastal regions, as well as convergence of these easterlies and westerlies. On the other hand, there was divergence between the northeasterlies and southeasterlies at the coast in March 2004, which can be attributed to the veering of easterlies further east of the equatorial Indian Ocean. Although easterlies entered the region, there was divergence. However, there was convergence over the LVB with the positive anomalies observed over the LVB in Figure 8e) in an otherwise dry month.

In April 2018 as in Figure 32b), there was convergence of southeasterlies and westerlies. Notably, some southeasterlies curved over central parts of Kenya, which may have caused rain formation as shown by the positive anomalies observed over the same region in Figure 8b). Figure 32e) showed divergence within the region causing dry conditions as in Figure 8f).

In May 2018 and 2004 as observed in Figures 32c) and 32f) show that in 2018, the positive anomalies in Figure 8c) was due to moist southeasterly flow parallel to the Kenyan coast as well as convergence between northwesterlies from Central Africa and DRC due to both the St. Helena high and the Azores high and northeasterlies (due to the curving of southeasterlies). In 2004, there was divergence of southeasterlies at the coast, confirming the observation in Figure 8g). In the north-western part of the region, northerlies were observed that contributed to the dry conditions observed in Figure 8g).

Figure 33 displays the divergent moisture flux superposed on MSLP for extreme MAM cases 1981 (wet) and 2009 (dry). In Figure 33a), it is evident that easterlies due to the Mascarene high and the Siberian high entered the region through the coast. Hence the positive anomalies observed at the Kenyan coast in Figure 9a). There was convergence between the said easterlies and westerlies from the Congo basin due to action of the St. Helena high. The dry conditions in March 2009 were attributed to the divergence of moisture vectors at the East African coast as seen in Figure 33d). The westerlies recurved southwards especially west of Tanzania resulting in minimal convergence with easterlies leading to the dry conditions observed in Figure 9e).

In April 1981 as in Figure 33b), there was convergence between the southeasterlies and the westerlies. Further, the southeasterlies appeared to be curving in central Kenya. In Figure 33e) there was no convergence between easterlies and westerlies.

In May 1981, owing to the westward Mascarene high with an intense continental component as in Figure 33c), the southeasterlies became southerlies which converged with westerlies in the northern part of the region. There was convergence with westerlies in the LVB leading to rainfall confirmed by the positive anomalies observed in Figure 9c). From Figure 33f), westerlies curved southwards ridding East Africa of moisture. There was divergence in the eastern part of the region, which was subject to the influence of southerlies and southeasterlies due to the Mascarene high.

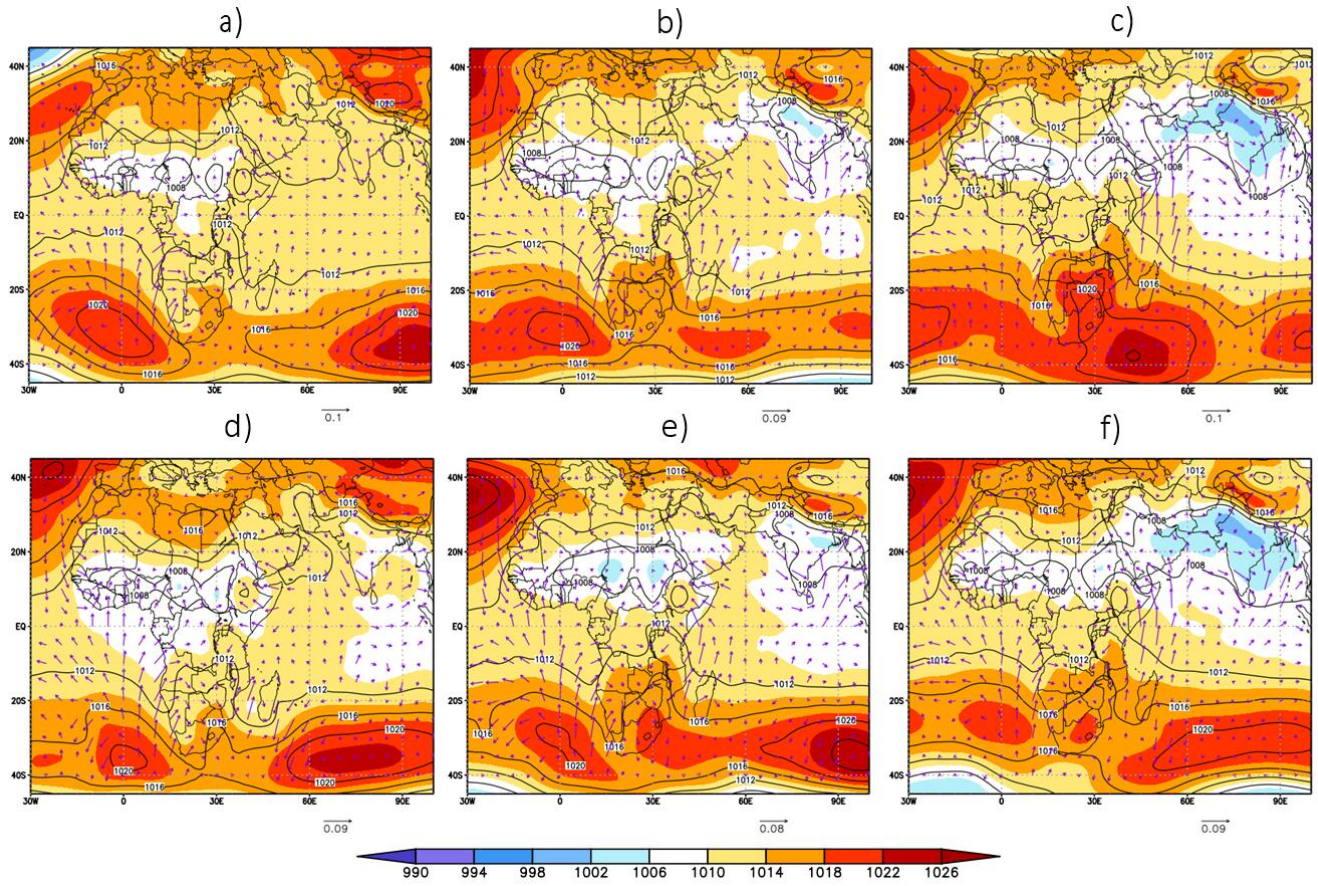

Figure 33: Divergent moisture flux superposed on MSLP (in mb) for 1981 (top) with extremely high rainfall and 2009 (bottom) which had extremely low rainfall during the MAM season, where a) is March 1981, b) is April 1981 and c) is May 1981. d), e) and f) represent March 2009, April 2009 and May 2009 respectively.

Figure 34 represents the divergent moisture flux superposed on MSLP for MAM 1986 which had extremely high rainfall and MAM 1998 which had extremely low rainfall. In March 1986 as in Figure 34a) had some effective westerlies entering the region and converging with easterlies in Kenya and Tanzania. Because of no convergence over Uganda, the said country and the LVB recorded negative rainfall anomalies as in Figure 10a). In March 1998, there was divergence of

southeasterlies from the Mascarene high at the coastal region with fewer northeasterlies reaching the region, making the region devoid of moist easterlies. Similarly, there were fewer westerlies entering the region due to the curving into northwesterlies and heading into south eastern countries like Zambia.

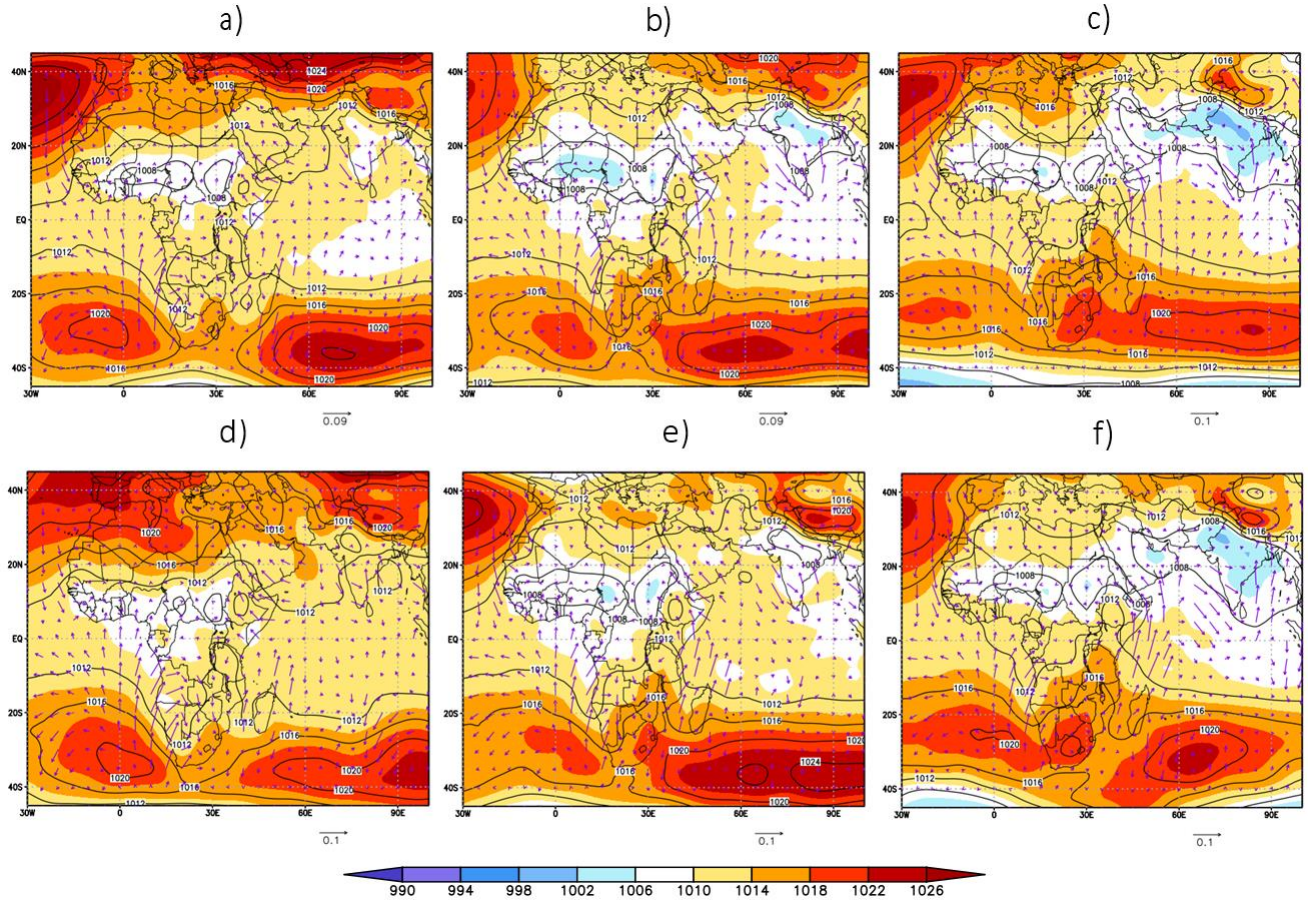

Figure 34: Divergent moisture flux superposed on MSLP (in mb) for 1986 (top) with extremely high rainfall and 1998 (bottom) which had extremely low rainfall during the MAM season, where a) is March 1986, b) is April 1986 and c) is May 1986. d), e) and f) represent March 1998, April 1998 and May 1998 respectively.

In April 1986 as in Figure 34b), the convergence between the easterlies and westerlies led to the observed positive anomalies over Kenya-Tanzania border and northern Tanzania in Figure 10b). In contrast, the dry conditions observed in April 1998 as in Figure 34e) was due to divergence of easterlies over Kenya and Tanzania as well as few westerlies reaching the region. Hence, as in Figure 10f) recorded very dry conditions especially in Kenya and some parts of Tanzania.

Based on the results observed and discussed in Figures 31 to 34, the following similarities for the wet years and for the dry years were noted as follows:

In March, the characteristics of the wet years included convergence of the northeasterlies due to the 1012 mb isobar of the Siberian high and southeasterlies driven by the Mascarene high, especially at the coast. Further, there was effective convergence with the westerlies as described by Johnson and Morth (1960) as good contributors to enhanced rainfall, flowing due to effective PGF caused by the equatorward Azores high and St. Helena high. The dry years were characterized by divergence of the easterlies, either due to the presence of the Mozambique Channel brought about by the Mascarene high, and/or veering of the easterlies further into the Indian Ocean.
In April where moist northeasterlies are fewer due to the shrinking of the Siberian high, there was effective influx of southeasterlies into the region which converged with westerlies due to effective PGF from the Atlantic Ocean into the Congo basin and the East African region due to the equatorward Azores high as well as the equatorward and zonal St. Helena high. On the other hand, the dry years were characterized by less convergence of moist southeasterlies and westerlies and/or divergence of moisture vectors in the region, mainly due to the intense continental component of the Mascarene high as well as the poleward St. Helena high.
In May the month where rainfall ceases, moist southeasterlies were a primary source of moisture for rain formation as well as convergence between the southeasterlies and westerlies. On the other hand, the dry years were characterized by divergence in the region.

4.5.2 OND Season

Figure 35 shows divergent moisture flux superposed on MSLP for the most extreme cases observed for the OND season. From Figure 35a) it is evident that convergence of southeasterlies and northeasterlies began in the Indian Ocean, which then may have been pushed into East Africa leading to the high positive anomalies observed in October 1997 in the eastern part of the region as shown in Figure 11a). In the western sector of the East African region experienced convergence between easterlies and westerlies. In contrast, October 2005 was dry owing to both southeasterlies and northeasterlies veering eastward into the Indian Ocean as in Figure 35d). There was divergence of southeasterlies at the East African coast.

In November 1997 as in Figure 35b), there was convergence of easterlies from the north and south in equatorial Indian Ocean and the East African coast. Further, the westerlies effective in reaching

East Africa converged with easterlies, leading to the very highly positive anomalies observed in Figure 11b).

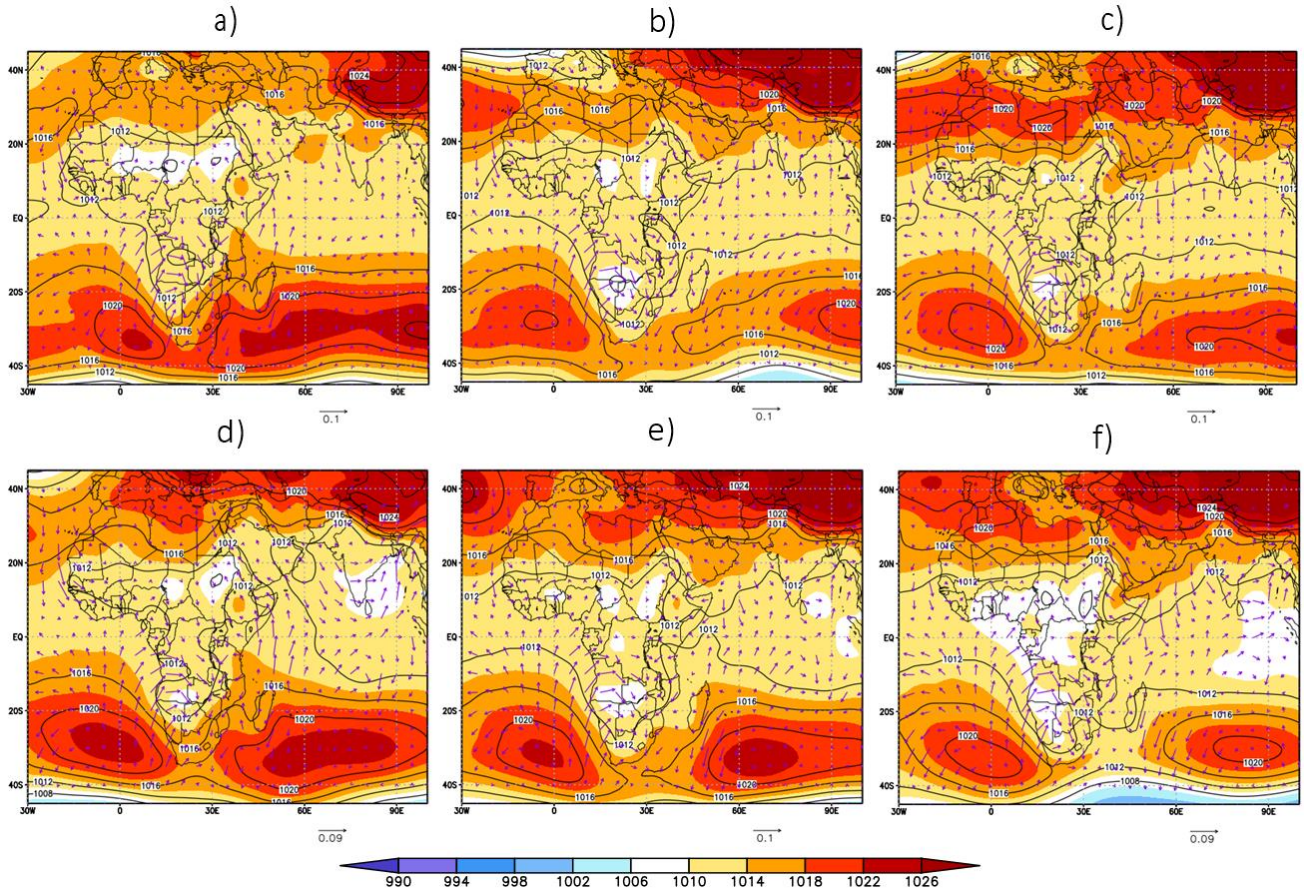

Figure 35: Divergent moisture flux superposed on MSLP (in mb) for 1997 (top) with extremely high rainfall and 2005 (bottom) which had the lowest rainfall during the OND season, where a) is October 1997, b) is November 1997 and c) is December 1997. d), e) and f) represent October 2005, November 2005 and December 2005 respectively.

In December 1997 as in Figure 35c), there was convergence of the easterlies in Indian Ocean, close to East Africa. There was convergence of easterlies and westerlies especially in Tanzania, an implication to the highly positive rainfall anomalies in Figure 11f). December 2005 was exceptionally dry due to divergence of northeasterlies at the East African coast and inland East Africa.

Figure 36 depicts divergent moisture flux superposed on MSLP for cases OND 2019 which had extremely high rainfall and OND 1998 which had extremely low rainfall. In Figure 36a), there were slow southeasterlies entering the region from the coast as well as convergence of easterlies

and westerlies in the western sector of the region, causing the high rainfall as observed in Figure 12a). On the other hand, the dry conditions in October 1998 may be alluded to divergence of southeasterlies at the coast as they veered off eastward, further from the region.

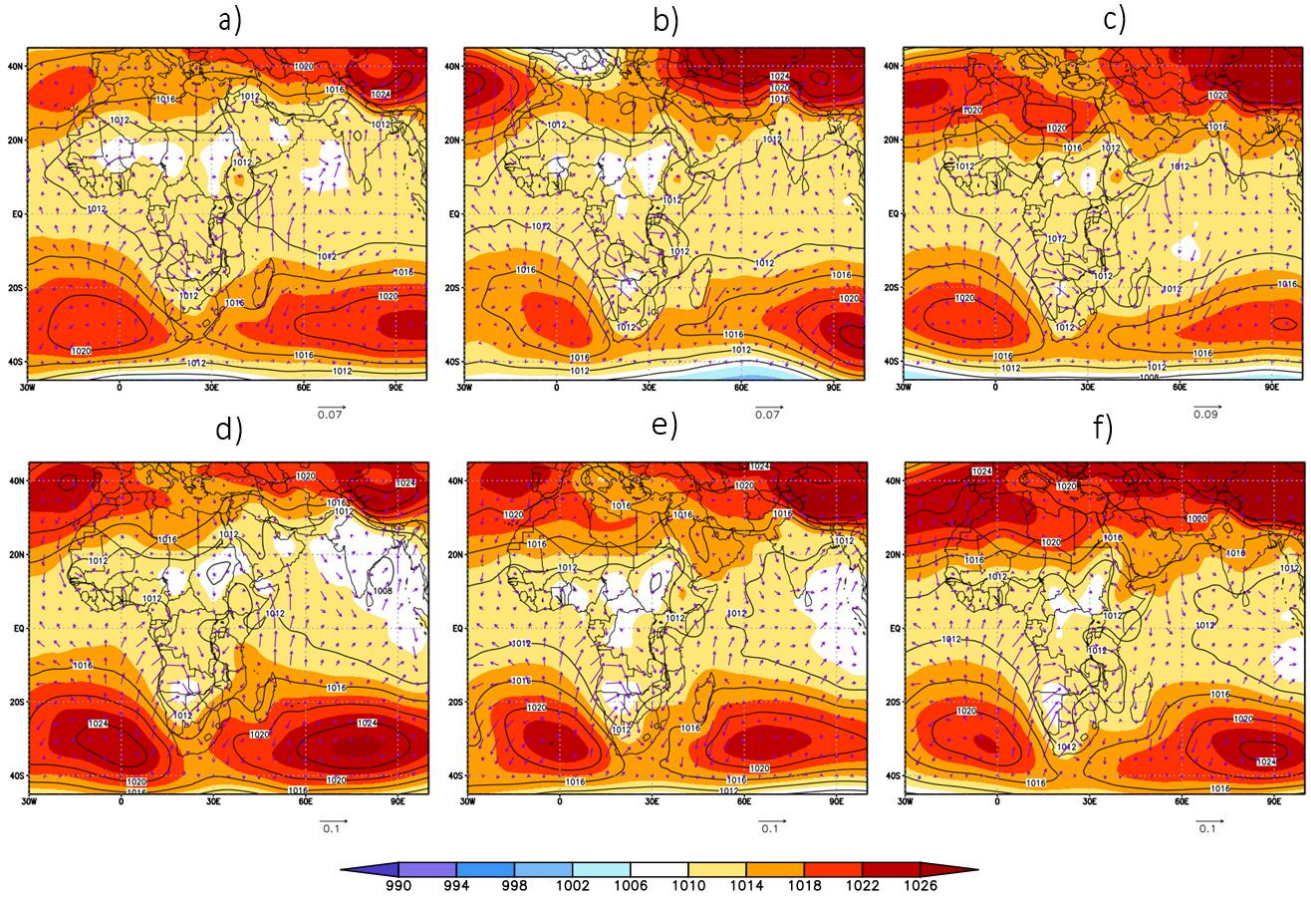

Figure 36: Divergent moisture flux superposed on MSLP (in mb) for 2019 (top) with extremely high rainfall and 1998 (bottom) which had extremely low rainfall during the OND season, where a) is October 2019, b) is November 2019 and c) is December 2019. d), e) and f) represent October 1998, November 1998 and December 1998 respectively.

In November 2019, there was convergence of northeasterlies and southeasterlies off the East African coast and entry of these easterlies into the region. The westerlies were effective in reaching the region as in Figure 36b). on the contrary, November 1998 in Figure 36e) was dry due to divergence of the southeasterlies at the East African coast as they veered further east in the Indian Ocean. There were fewer westerlies converging with easterlies inland of East Africa.

In December 2019 as in Figure 36c), there was convergence of the southeasterlies and northeasterlies at the East African coast and the Indian Ocean near the East African coast. The

westerlies pushed further inland of East Africa converging with the easterlies leading to the observation in Figure 12c). In December 1998 as in Figure 36f), East Africa was devoid of moisture from the Indian Ocean due to southeasterlies and northeasterlies veering eastward.

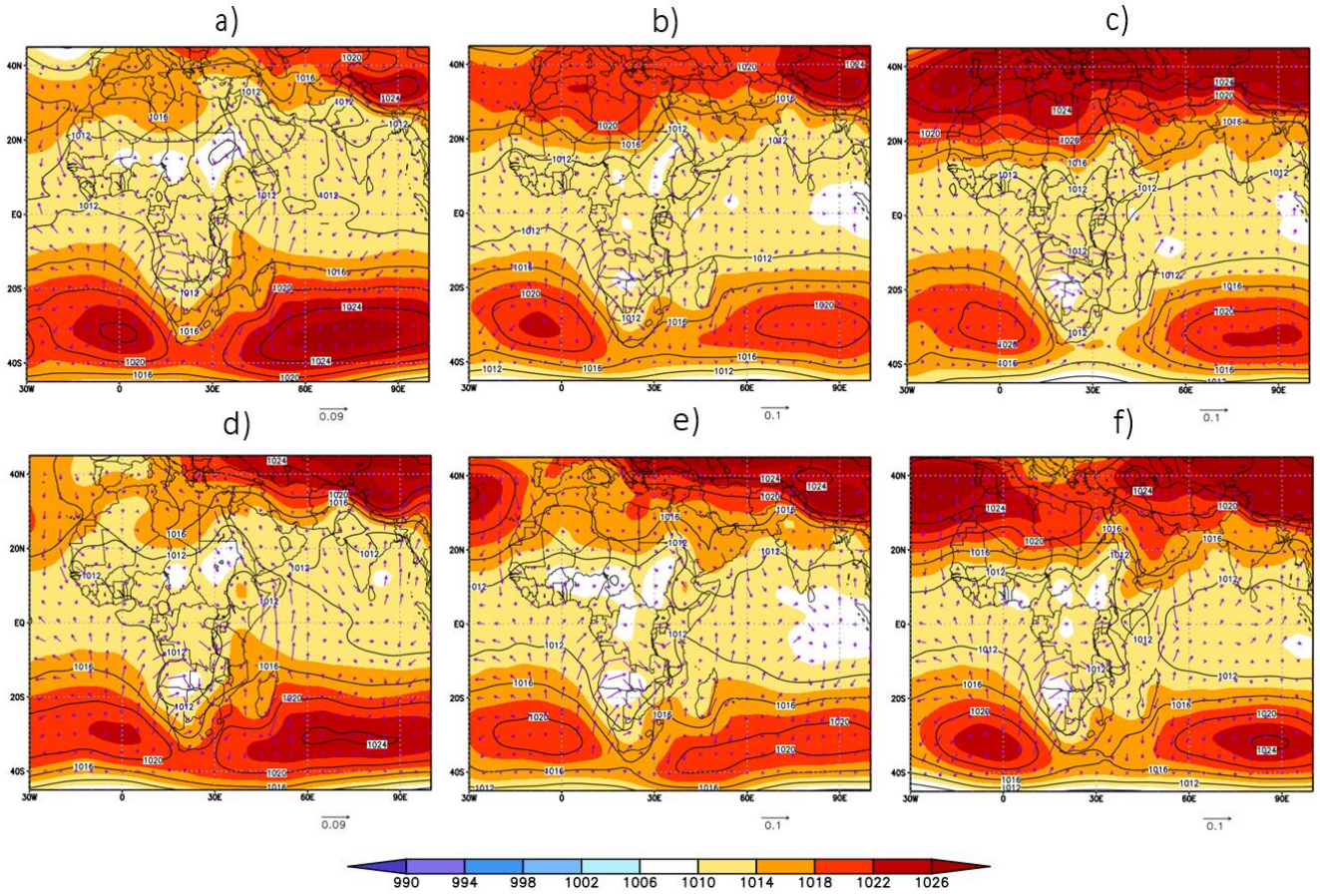

Figure 37: Divergent moisture flux superposed on MSLP (in mb) for 2006 (top) with extremely high rainfall and 1993 (bottom) which had extremely low rainfall during the OND season, where a) is October 2006, b) is November 2006 and c) is December 2006. d), e) and f) represent October 1993, November 1993 and December 1993 respectively.

Figure 37 displays divergent moisture flux superposed on MSLP for the OND extreme cases of 2006 and 1993. In October 2006 as in Figure 37a), there was divergence of southeasterlies at the coast due to high pressure at the coast. Nevertheless, there was effective easterlies in northern part of Kenya that contributed to the rainfall observed in Figure 13a). In October 1993 as in Figure 37e), there was greater divergence of southeasterlies at the East African coast and inland due to higher pressure of the westward Mascarene high. There was convergence of some of the easterlies with dry northwesterlies leading to minimal rainfall and dry conditions as observed in Figure 13e).

In November 2006, there was convergence of the easterlies at the equator near the coast, which would have contributed to rainfall observed in Figure 13b). There was convergence of easterlies with the westerlies. In 1993 as in Figure 37e), there was divergence of southeasterlies in the Indian Ocean near the East African coast as the moisture vectors curved eastwards.

In December 2006, there were faster westerlies entering East Africa and they converged with southeasterlies in southern Tanzania and with northeasterlies at the equator. Further, the easterlies converged in the Indian Ocean near the East African coast. In contrast, December 1993 was dry due to great divergence of the easterlies inland and off the coast as these easterlies veered eastward, far from the region.

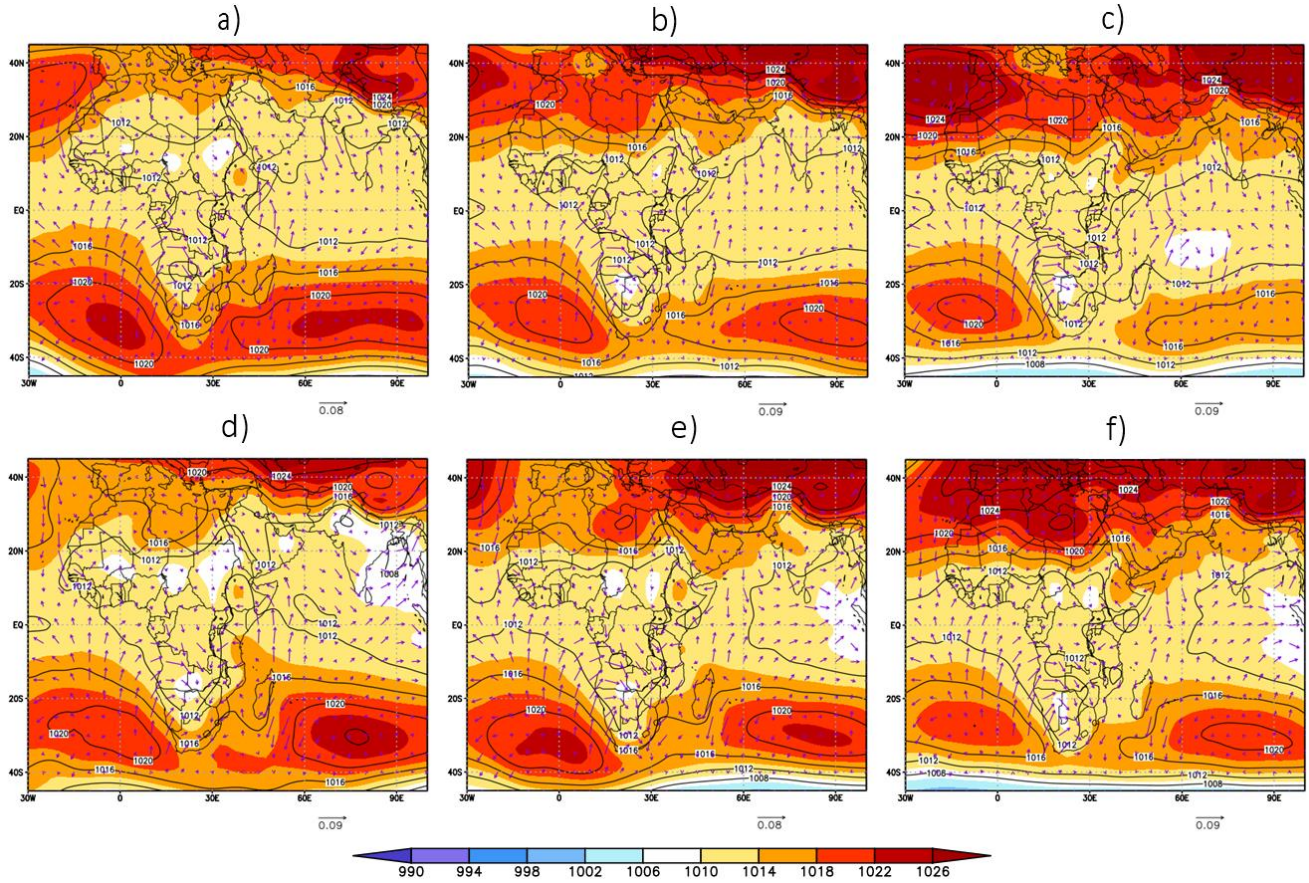

Figure 38: Divergent moisture flux superposed on MSLP (in mb) for 1982 (top) with extremely high rainfall and 2016 (bottom) which had extremely low rainfall during the OND season, where a) is October 1982, b) is November 1982 and c) is December 1982. d), e) and f) represent October 2016, November 2016 and December 2016 respectively.

Figure 38 exhibits the divergent moisture flux superposed on MSLP for the OND extreme cases of 1982 and 2016. In October 1982 as in Figure 38a), slow southeasterlies entered the Kenyan

coast into the north eastern parts of Kenya leading to rainfall observed in Figure 14a). October 2016 in Figure 38d) had divergence of fast southeasterlies near the East African coast, leading to dry conditions as observed in Figure 14e).

In November 1982 in Figure 38b), there was convergence of easterlies near the East African coast. Further, slow southeasterlies entered the region leading to rain formation. Some southeasterlies converged with the westerlies contributing to rainfall observed in Figure 14b). In contrast, November 2016 in Figure 38e) was dry due to divergence of the southeasterlies near the coast of East Africa as they veered eastward.

In December, moist northeasterlies effectively reached East Africa and converged with westerlies leading to rain formation. On the other hand, dry conditions in December 2016 were due to a lot of divergence at and near the East African coast as well as fewer westerlies entering the region leading to minimal convergence with easterlies inland.

Based on results obtained and discussed as the moisture characteristics during the extreme years of the OND season in Figures 35 to 38, the following similarities were drawn out:

In October of the wet years, there was convergence of northeasterlies and southeasterlies at the East African coast and in the Indian Ocean near the coast due to the eastward Siberian and Mascarene highs. In October of the dry years, there was divergence of easterlies as they veered further east into the equatorial Indian Ocean, as had been described by Hastenrath *et al.* (2006) and Johnson and Morth (1960). This was due to the westward Mascarene high, consistent with observations by Manatsa *et al.* (2014) and Ongoma *et al.* (2015) and the westward Siberian high. During the dry years with the Angola low present, the recurved southeasterlies flowed southward leading to weaker westerly flow, similar to stipulation by Xulu *et al.* (2020).

In November, there was convergence of northeasterlies and southeasterlies off the coast of East Africa as well as convergence of easterlies and some westerlies inland for the wet years due to the eastward Mascarene high and Siberian high and the less intense St. Helena high (Colberg *et al*., 2004). Nevertheless, during the dry years, there was divergence of easterlies off the coast of the region as they veered eastward in the Indian Ocean. This could be attributed to the westward Mascarene and Siberian highs that would encourage westerly flow, away from EA, as described by Wainwright *et al.* (2021). Of importance, the Angola low was vast during the dry years so the flows from the Atlantic Ocean curved southward (Xulu *et al.*, 2020).

In December, the wet years were characterized by convergence of northeasterlies and southeasterlies at the coastal areas as well as convergence of easterlies and some westerlies inland EA. In contrast, there was divergence of easterlies at the East African coast as they veered further east in the Indian Ocean ridding the region of moisture.

Although westerlies are weaker during OND as described by Xulu *et al.* (2020), they were more effective in reaching East Africa during the wet years as compared to the dry years. This observation of weaker westerlies during OND validates the stipulation by Howard and Washington (2019) that the CAB disintegrates during OND season.

CHAPTER FIVE

CONCLUSIONS AND RECOMMENDATIONS

5.1 CONCLUSIONS

This study aimed to investigate how anticyclones adjacent to Africa influence seasonal rainfall extremes over East Africa, during the March to May (MAM) and October to December (OND) rainy seasons. The research achieved its specific objectives by identifying years with extreme seasonal rainfall, determining spatial rainfall distribution, comparing the pressure characteristics of extreme years from that of the climatology, and investigating moisture transport and circulation patterns in the years with seasonal rainfall extremes.

The findings reveal that the migration of subtropical anticyclones significantly influences the distribution of moisture into East Africa, consequently controlling seasonal rainfall extremes in the region. During the wet years for the long rainy season (MAM), equatorward displacement from the mean of the Azores high and St. Helena high led to enhanced rainfall, with westerlies effectively entering the region and contributing to intense rainfall. Conversely, during dry years, the poleward displacement of these anticyclones from their mean relaxed the pressure gradient into East Africa, leading to limited moisture influx and reduced rainfall.

For the short rainy season (OND), wet years were associated with eastward-located Mascarene and Siberian highs when compared to the climatology, leading to an influx of moist easterlies from the Indian Ocean and increased convergence with westerlies. On the other hand, dry years experienced westward displacement from the mean of these anticyclones, leading to easterlies veering into the Indian Ocean, leaving East Africa devoid of moisture for rain formation.

The study highlighted the importance of the position and intensity of anticyclones in influencing rainfall extremes, with the location of the 1012 mb isobars in the Atlantic Ocean and North Indian Ocean being. Moreover, the presence of the trough in the Mozambique Channel significantly impacted the flow of westerlies and divergence of easterlies during dry MAM years. Similarly, during the OND season, the positions of the Azores high, Mascarene high, Siberian high, and the presence of the Angola low in October proved vital in determining rainfall extremes.

It has been established that changes in the mean pattern, location, intensity and orientation of the Subtropical anticyclones adjacent to the continent of Africa, particularly the Azores high, St. Helena high, Mascarene high and Siberian high, drive the wind flow over the region which determines the transport of moisture into the region. Modification of the influx of moisture into the region arising from changes in the characteristics of the subtropical anticyclones play an important role in the distribution of the observed rainfall over the region and act as synoptic controls of extremely high and extremely low rainfall on seasonal timescales in East Africa, alongside other large-scale systems and local forcing.

5.2 RECOMMENDATIONS

The results presented in this study demonstrate the significance of the anticyclones as synoptic controls of seasonal rainfall extremes in East Africa. Therefore, the following recommendations are suggested:

5.2.1 Recommendation to Scientists

Further research on the behaviour of anticyclones is recommended for shorter time scales like daily and sub-seasonal to seasonal (S2S) in order to understand the contribution of the 1012 mb isobar on the influx of moist northeasterlies as well as the characteristics of the Mascarene high that encourage the development and sustenance of the trough in the Mozambique Channel that influences rainfall over East Africa.

For meteorologists and researchers, this study is important in developing and improving the GCMs for the region in order to produce more accurate and comprehensive forecasts and to expand the scope of understanding of controls of rainfall and their teleconnections.

5.2.2 Recommendation to Policy Makers

For policy makes, more comprehensive forecasts would be fundamental in planning and allocating funds important for planning and mitigating the effects of drought and floods that are consequential to extremely high and extremely low rainfall respectively. Policy makers can also encourage multi-disciplinary co-production amongst institutions in order to meet the needs as well as safeguard lives and livelihoods of the users and general population.

5.2.3 Recommendation to Users

With improved forecast output that determines whether seasonal rainfall will be normal, extremely high or extremely low, users will be able to make decisions in their various socioeconomic sectors including agriculture, tourism, energy production, especially hydroelectric power, among others.

REFERENCES

Adler, R. F., Sapiano, M., Huffman, G. J., Wang, J., Gu, G., Bolvin, D., Chiu, L., Schneider, U., Becker, A., Nelkin, E., Xie, P., Ferraro, R., Shin, D. B. (2018) The Global Precipitation Climatology Project (GPCP) Monthly Analysis (New Version 2.3) and a Review of 2017 Global Precipitation. *Atmosphere*, *9*(4), 138. https://doi.org/10.3390/atmos9040138

African Union Commission (2015) Agenda 2063: The Africa we want (popular version), Addis Ababa, Ethiopia.

Asnani, G.C (1993) Tropical Meteorology. Vol. 1, Pune Indian Institute of Tropical Meteorology. ISBN:8190040006

Barimalala, R., Blamey, R. C., Desbiolles, F., & Reason, C. J. C. (2020). Variability in the Mozambique Channel Trough and Impacts on Southeast African Rainfall, *Journal of Climate*, 33(2), 749-765. https://doi.org/10.1175/JCLI-D-19-0267.1

Behera, S. K., Luo, J., Masson, S., Delecluse, P., Gualdi, S., Navarra, A., Yamagata, T. (2005) Paramount Impact of the Indian Ocean Dipole on the East African Short Rains: A CGCM Study, *Journal of Climate*, 18(21), 4514-4530. https://doi.org/10.1175/JCLI3541.1

Black E. (2005) The Relationship Between Indian Ocean Sea–Surface Temperature and East African Rainfall. *Philos. Trans. R. Soc. A Math. Phys. Eng. Sci*. 363(1826): 43–47.

Camberlin, P., Philippon, N. (2002) The East African March–May Rainy Season: Associated Atmospheric Dynamics and Predictability over the 1968–97 Period, *Journal of Climate*, 15(9), 1002-1019. https://doi.org/10.1175/1520-0442(2002)015%3C1002:TEAMMR%3E2.0.CO;2

Chang'a, L.B., Kijazi, A.L., Mafuru, K.B., Nying'uro, P.A., Ssemujju, M., Deus, B., Kondowe, A.L., Yonah, I.B., Ngwali, M., Kisama, S.Y., Aimable, G., Sebaziga, J.N., Mukamana, B. (2020) Understanding the Evolution and Socio-Economic Impacts of the Extreme Rainfall Events in March-May 2017 to 2020 in East Africa. *Atmospheric and Climate Sciences*, 10, 553-572. https://doi.org/10.4236/acs.2020.104029

Cherchi, A., Ambrizzi, T., Behera, S., Freitas, V., Morioka, Y., Zhou, T. (2018) The Response of Subtropical Highs to Climate Change. *Curr Clim Change Rep* 4, 371–382 (2018). https://doi.org/10.1007/s40641-018-0114-1

Climate Prediction Centre (CPC) Historical El Niño / La Niña episodes (1950-present) https://origin.cpc.ncep.noaa.gov/products/analysis_monitoring/ensostuff/ONI_v5.php

Colberg, F., Reason, C. J. C., Rodgers, K. (2004) South Atlantic Response to El Niño–Southern Oscillation Induced Climate Variability in an Ocean General Circulation Model, *J. Geophys. Res.*, 109, C12015. doi:10.1029/2004JC002301.

Dunning, C. M., Black, E., Allan, R. P. (2018). Later Wet Seasons with More Intense Rainfall over Africa under Future Climate Change, *Journal of Climate*, 31(23), 9719-9738. https://doi.org/10.1175/JCLI-D-18-0102.1

FAO, ECA, AUC (2021) Africa – Regional Overview of Food Security and Nutrition 2021: Statistics and trends. Accra, FAO. https://doi.org/10.4060/cb7496en

Finney, D.L., Marsham, J.H., Walker, D.P., Birch, C.E., Woodhams, B.J., Jackson, L.S., Hardy, S. (2020) The effect of westerlies on East African rainfall and the associated role of tropical cyclones and the Madden–Julian Oscillation. *Q J R Meteorol Soc*.2020; 146: 647– 664. https://doi.org/10.1002/qj.3698

Gacheru, J., Kiptum, C., Koros, D., Wainwright, C.M., Marsham, J.H. (2020) Kenyan Lakes Reach Record Levels, GCRF African SWIFT, Retrieved Sep 30, 2022, from https://africanswift.org/2020/09/16/kenyan-lakes-reach-record-levels/

Gebremeskel, H.G., Tang, Q., Leng, G., Jia, G., Wang, J., Cai, D., Sun, S., Baniya, B., Zhang, Q. (2020). Long-term spatiotemporal variation of drought patterns over the Greater Horn of Africa. *Sci. Total Environ*. 704, 135299. https://doi.org/10.1016/j.scitotenv.2019.135299

Gudoshava, M., Wainwright, C., Hirons, L., Endris, H. S., Segele, Z. T., Woolnough, S., Atheru, Z., Artan, G. (2022) Atmospheric and Oceanic Conditions Associated with Early and Late Onset for Eastern Africa Short Rains. *International Journal of Climatology*, 1– 17. https://doi.org/10.1002/joc.7627

Hammond, M., Lewis, N.T. (2021) The Rotational and Divergent Components of Atmospheric Circulation on Tidally Locked Planets, Proceedings of the National Academy of Sciences. https://doi.org/10.1073/pnas.2022705118

Hastenrath, S. (1991). Climate Dynamics of the Tropics. Berlin: Springer. ISBN 978-0-7923-1346-5

Hastenrath, S., Nicklis, A., Greischar, L. (1993) Atmospheric–Hydrospheric Mechanisms of Climate Anomalies in the Western Equatorial Indian Ocean. *J. Geophys. Res.*, 98, 20219–20235.

Hastenrath, S., Polzin, D., Mutai, C. (2006) Diagnosing the 2005 Drought in Equatorial East Africa. *Journal of Climate*, 20, 4628-4637. https://doi.org/10.1175/JCLI4238.1

Hermes, J. C., Reason, C. J. C. (2009) Variability in Sea-Surface Temperature and Winds in the Tropical South-East Atlantic Ocean and Regional Rainfall Relationships. *Int. J. Climatol.*, 29, 11–21.

Hirons, L., Turner, A. (2018). The Impact of Indian Ocean Mean-State Biases in Climate Models on the Representation of the East African Short Rains, *Journal of Climate*, 31(16), 6611-6631. https://doi.org/10.1175/JCLI-D-17-0804.1

Hogan, E., Shelly, A., Xavier, P. (2015) The Observed and Modelled Influence of the Madden–Julian Oscillation on East African Rainfall. *Met. Apps*, 22: 459-469. https://doi.org/10.1002/met.1475

Howard, E., Washington, R. (2019). Drylines in Southern Africa: Rediscovering the Congo Air Boundary, *Journal of Climate*, 32(23), 8223-8242. https://doi.org/10.1175/JCLI-D-19-0437.1

James, R., Washington, R., Abiodun, B., Kay, G., Mutemi, J., Pokam, W., Hart, N., Artan, G., Senior, C. (2018) Evaluating Climate Models with an African Lens, *Bulletin of the American Meteorological Society*, 99(2), 313-336. https://doi.org/10.1175/BAMS-D-16-0090.1

Janowiak, J. E., Xie, P. (1999) CAMS–OPI: A Global Satellite–Rain Gauge Merged Product for Real-Time Precipitation Monitoring Applications, *Journal of Climate*, *12*(11), 3335-3342. https://doi.org/10.1175/1520-0442(1999)012%3C3335:COAGSR%3E2.0.CO;2

Johnson, D. H., Morth, H. T. (1960) Forecasting Research in East Africa, in Bargman D. J. (ed.), Tropical Meteorology in Africa, Nairobi: Munitalp Foundation, pp. 56–137.

Kalnay, E., Kanamitsu, M., Kistler, R., Collins, W., Deaven, D., Gandin, L., Iredell, M., Saha, S., White, G., Woollen, J., Zhu, Y., Chelliah, M., Ebisuzaki, W., Higgins, W., Janowiak, J., Mo, K. C., Ropelewski, C., Wang, J., Leetmaa, A., Reynolds, R., Jenne, R., Joseph, D. (1996). The NCEP/NCAR 40-Year Reanalysis Project, *Bulletin of the American Meteorological Society*, *77*(3), 437-472. https://doi.org/10.1175/1520-0477(1996)077%3C0437:TNYRP%3E2.0.CO;2

KMD (Kenya Meteorological Department). (2019) The Forecast for January 2020, Weather Review for December 2019 and the Performance of October-December 2019 Short-Rains, Issued 30 December 2019.

KMD (Kenya Meteorological Department). (2021) State of the Climate in Kenya 2020, Kenya Meteorological Department, Kenya. Retrieved Oct 3, 2022, from https://meteo.go.ke/sites/default/files/downloads/STATE%20OF%20THE%20%20CLIMATE%202020_14042021.pdf

Kilavi, M., MacLeod, D., Ambani, M., Robbins, J., Dankers, R., Graham, R., Helen, T., Salih, A., Todd, M. (2018) Extreme Rainfall and Flooding over Central Kenya Including Nairobi City during the Long-Rains Season 2018: Causes, Predictability, and Potential for Early Warning and Actions. *Atmosphere*, 9(12), 472. https://doi.org/10.3390/atmos9120472

Kinuthia, J. H., Asnani, G. C. (1982). A Newly Found Jet in North Kenya (Turkana Channel), Monthly Weather Review, 110(11), 1722-1728. https://doi.org/10.1175/1520-0493(1982)110%3C1722:ANFJIN%3E2.0.CO;2

Li, Z., Chao, Y., McWilliams, J. C. (2006) Computation of the Streamfunction and Velocity Potential for Limited and Irregular Domains, *Mon. Wea. Rev.*, 134, 3384–3394. https://doi:10.1175/MWR3249.1.

Lindsey, R (2009) In Climate Variability: Oceanic Niño Index, Understanding Climate, Accessed on Feb 15, 2023, from https://www.climate.gov/news-features/understanding-climate/climate-variability-oceanic-ni%C3%B1o-index#:~:text=The%20Oceanic%20Ni%C3%B1o%20Index%20(ONI,Pacific%2C%20near%20the%20International%20Dateline.

Lyon, B., D. G. Dewitt (2012) A Recent and Abrupt Decline in The East African Long Rains, *Geophys. Res. Lett.*, 39, L02702, https://doi:10.1029/2011GL050337

MacLeod, D. A., Dankers, R., Graham, R., Guigma, K., Jenkins, L., Todd, M. C., Kiptum, A., Kilavi, M., Njogu, A., Mwangi, E. (2021). Drivers and Subseasonal Predictability of Heavy Rainfall in Equatorial East Africa and Relationship with Flood Risk, *Journal of Hydrometeorology*, 22(4), 887-903. https://doi.org/10.1175/JHM-D-20-0211.1

Manatsa, D., Morioka, Y., Behera, S.K., Matarira, C.H., Yamagata, T. (2014) Impact of Mascarene High Variability on the East African 'Short Rains'. *Climate Dynamics* 42, 1259 - 1274. https://doi.org/10.1007/s00382-013-1848-z

McHugh, M. J., Rogers, J. C. (2001). North Atlantic Oscillation Influence on Precipitation Variability around the Southeast African Convergence Zone, *Journal of Climate*, 14(17), 3631-3642. https://doi.org/10.1175/1520-0442(2001)014%3C3631:NAOIOP%3E2.0.CO;2

Morioka, Y., Engelbrecht, F., Behera, S.K. (2017) Role of Weddell Sea Ice in South Atlantic Atmospheric Variability. *Clim Res*, 74:171-184. https://doi.org/10.3354/cr01495

Morioka, Y., Takaya, K., Behera, S. K., & Masumoto, Y. (2015). Local SST Impacts on the Summertime Mascarene High Variability, *Journal of Climate*, 28(2), 678-694. https://doi.org/10.1175/JCLI-D-14-00133.1

Mutemi J.N. (2003) Climate Anomalies over Eastern Africa Associated with Various ENSO Evolution Phases, PhD. Thesis, University of Nairobi, Kenya.

Mutemi, J.N., Ogallo L.A., Krishnamurti T.N., Mishra A.K., Kumar V.T.S.V. (2006). Multi-Model Based Superensemble Forecasts for Short and Medium Range NWP Over Various Regions of Africa. *Meteorology and Atmospheric Physics*, 95:1-2, 87-113.

Ngoma, H., Wen, W., Ayugi, B., Karim, R. and Makula, E.K. (2021) Mechanisms Associated with September to November (SON) Rainfall Over Uganda During the Recent Decades. *Geographica Pannonica*, 25, 10– 23. https://doi.org/10.5937/gp25-29932.

Nicholson, S. E. (1996) A Review of Climate Dynamics and Climate Variability in Eastern Africa, in The Limnology, Climatology, and Paleoclimatology of the East African Lakes, edited by T. C. Johnson and E. O. Odada, pp. 25–56, Gordon and Breach Publ., Amsterdam.

Nicholson, S. E. (2014) A Detailed Look at the Recent Drought Situation in the Greater Horn of Africa, *J. Arid Environ.*, 103, 71–79, https://doi:10.1016/j.jaridenv.2013.12.003.

Nicholson, S. E. (2014b) The Predictability of Rainfall over the Greater Horn of Africa.: Part I: Prediction of Seasonal Rainfall. *Journal of Hydrometeorology*, 15(3), 1011–1027. http://www.jstor.org/stable/24914496

Nicholson, S. E. (2015). The Predictability of Rainfall over the Greater Horn of Africa. Part II: Prediction of Monthly Rainfall during the Long Rains, *Journal of Hydrometeorology*, 16(5), 2001-2012. https://doi.org/10.1175/JHM-D-14-0138.1

Nicholson, S.E. (2016) An Analysis of Recent Rainfall Conditions in Eastern Africa. *Int. J. Climatol.*, 36: 526-532. https://doi.org/10.1002/joc.4358

Nicholson, S.E. (2017) Climate and Climatic Variability of Rainfall over Eastern Africa. *Reviews of Geophysics*, 55(3), 590–635. https://doi:10.1002/2016RG000544

Nicholson, S. E. (2018) The ITCZ and the Seasonal Cycle over Equatorial Africa, *Bulletin of the American Meteorological Society*, *99*(2), 337-348. https://doi.org/10.1175/BAMS-D-16-0287.1

Nkurunziza, I.F., Guirong, T., Ngarukiyimana, J.P., Sindikubwabo, C. (2019) Influence of the Mascarene High on October-December Rainfall and Their Associated Atmospheric Circulation Anomalies over Rwanda. *Journal of Environmental & Agricultural Sciences*. 20:1-20.

Nyakwada W., Laban A., Ogallo L.A., Okoola, R.E. (2009) The Atlantic-Indian Ocean Dipole and its Influence on East African Seasonal Rainfall. *Journal of Meteorology and related Sciences*. 2009; 3:21-35.

Ogallo, L.J. (1988) Relationships between Seasonal Rainfall in East Africa and the Southern Oscillation. *Journal of Climatology*, 8, 31-43. https://doi.org/10.1002/joc.3370080104

Omeny P.A., Ogallo L., Okoola R., Hendon H., Wheeler M. (2008) East African Rainfall Variability Associated with the Madden-Julian Oscillation. *J. Kenya Meteorol. Soc*. 2(2): 105–114.

Omondi, O.A., Lin, Z. (2023) Trend and Spatial-temporal Variation of Drought Characteristics Over Equatorial East Africa During the Last 120 Years. *Front. Earth Sci.* 10:1064940. https://doi.org/10.3389/feart.2022.1064940

Ongoma, V., Ogwang, B.A., Xing, L., Ogou, F.K. (2015) Influence of Mascarene High and Indian Ocean Dipole on East African Extreme Weather Events. https://doi.org/10.5937/geopan1502064o

Owiti Z, Ogallo L, Mutemi J. (2008) Linkages between the Indian Ocean Dipole and East African Rainfall Anomalies. *Journal of Kenya Meteorological Society*. Vol2. 3 - 17.

Pokam, W. M., Bain, C. L., Chadwick, R. S., Graham, R., Sonwa, D. J., Kamga, F. M. (2014). Identification of Processes Driving Low-Level Westerlies in West Equatorial Africa, *Journal of Climate*, 27(11), 4245-4262. https://doi.org/10.1175/JCLI-D-13-00490.1

Seager, R., Murtugudde, R., Naik, N., Clement, A., Gordon, N., Miller, J. (2003). Air–Sea Interaction and the Seasonal Cycle of the Subtropical Anticyclones, *Journal of Climate*, 16(12), 1948-1966. https://doi.org/10.1175/1520-0442(2003)016%3C1948:AIATSC%3E2.0.CO;2

Serrat-Capdevila, A., Merino, M., Valdes, J., Durcik, M. (2016). Evaluation of the Performance of Three Satellite Precipitation Products over Africa. *Remote Sensing*, 8(10), 836. https://doi.org/10.3390/rs8100836

Shilenje, Z.W., Ongoma, V., Ogwang, B.A. (2015) Relationship between the North Atlantic Oscillation Index and October- December Rainfall Variability Over Kenya. *J Geol Geophys.*, 4:207. https://doi:10.4172/2329-6755.1000207.

Souza, P., Cavalcanti, I.F.A. (2009) Atmospheric Centres of Action Associated with the Atlantic ITCZ Position. *Int. J. Climatol.*, 29: 2091-2105. https://doi.org/10.1002/joc.1823

Sun, L., Semazzi, F. H. M., Giorgi, F., Ogallo, L. (1999), Application of the NCAR Regional Climate Model to eastern Africa: 2. Simulation of interannual variability of short rains, *J. Geophys. Res.*, 104(D6), 6549– 6562, https://doi:10.1029/1998JD200050.

Sun, X., Cook, K. H., Vizy, E. K. (2017). The South Atlantic Subtropical High: Climatology and Interannual Variability, *Journal of Climate*, 30(9), 3279-3296. https://doi.org/10.1175/JCLI-D-16-0705.1

Sun, Q., Miao, C., Duan, Q., Ashouri, H., Sorooshian, S., Hsu, K.-L. (2018) A Review of Global Precipitation Data Sets: Data Sources, Estimation, and Intercomparisons, *Reviews of Geophysics*, 56,79–107. https://doi.org/10.1002/2017RG000574

TMA (Tanzania Meteorological Authority). (2021) Statement on the Status of Tanzania Climate in 2020, Tanzania Meteorological Authority. Retrieved Oct 3, 2022, from https://www.meteo.go.tz/uploads/publications/sw1628770614-TMA%20BOOK%202020%20-2021%20UPDATE.pdf

Uhe, P., Philip, S., Kew, S., Shah, K., Kimutai, J., Mwangi, E., van Oldenborgh, G.J., Singh, R., Arrighi, J., Jjemba, E., Cullen, H. and Otto, F. (2018), Attributing drivers of the 2016 Kenyan drought. *Int. J. Climatol*, 38: e554-e568. https://doi.org/10.1002/joc.5389

Wainwright, C.M., Marsham, J.H., Keane, R.J., Rowell, D.P., Finney, D.L., Black, E., Allan, R.P. (2019a) 'Eastern African Paradox' Rainfall Decline Due to Shorter Not Less Intense Long Rains. *NpjClimate and Atmospheric Science*, 2(1), 1–9. https://doi.org/10.1038/s41612-019-0091-7

Wainwright, C., Finney D., Marsham, J., Koros, D., Hirons, L. (2019b) Heavy Rainfall and Tropical Cyclones Affect East Africa, GCRF Africa SWIFT, Published December 2019. https://africanswift.org/2019/12/13/heavy-rainfall-and-tropical-cyclones-affect-east-africa/

Wainwright, C.M., Finney, D.L., Kilavi, M., Black, E., Marsham, J.H. (2021) Extreme Rainfall in East Africa, October 2019–January 2020 and Context Under Future Climate Change. *Weather*, 76: 26-31. https://doi.org/10.1002/wea.3824

Webster, P. J., Moore, A. M., Loschnigg, J. P., Leben, R. R. (1999). Coupled Ocean–Atmosphere Dynamics in the Indian Ocean During 1997–98. *Nature*, 401(6751), 356. https://doi.org/10.1038/43848

Xulu, N. G., Chikoore, H., Bopape, M.-J. M., & Nethengwe, N. S. (2020). Climatology of the Mascarene High and Its Influence on Weather and Climate over Southern Africa. *Climate*, 8(7), 86. https://doi.org/10.3390/cli8070086

Yang, W., Seager, R., Cane, M. A., & Lyon, B. (2015). The Annual Cycle of East African Precipitation, *Journal of Climate*, 28(6), 2385-2404. https://doi.org/10.1175/JCLI-D-14-00484.1

Yengoh, G. T., Ardö, J. (2020). Climate Change and the Future Heat Stress Challenges among Smallholder Farmers in East Africa. *Atmosphere*, 11(7), 753. https://doi.org/10.3390/atmos11070753

Zhang, C. (2005). Madden-Julian Oscillation. *Reviews of Geophysics*, 43, RG2003. https://doi.org/10.1029/2004RG000158